

DEVELOPING TECHNIQUES IN ELECTROMYOGRAPHY TO FACILITATE
TRANSLATION TO HEALTHCARE

by STEPHEN LUKE TOEPP, M.Sc.

A Thesis Submitted to the School of Graduate Studies in Partial Fulfillment of the
Requirements for the Degree Doctor of Philosophy

McMaster University, April 2024

Descriptive Note

DOCTOR OF PHILOSOPHY (2024)
(Kinesiology)

McMaster University, Hamilton, Ontario

TITLE: Developing Techniques in Electromyography to Facilitate Translation to
Healthcare

AUTHOR: Stephen Luke Toepp, M.Sc.

SUPERVISOR: Dr. A. J. Nelson

NUMBER OF PAGES: xiii, 143

Lay Abstract

Surface electromyography (EMG) is the recording of electrical potentials within the muscle that drive muscle contraction, and ultimately movement. There are many surface EMG techniques that provide insightful glimpses of the processes governing movement, and they have long been used to study movement impairments caused by traumatic injuries, neurodevelopmental disorders, and neurodegenerative diseases. Use of surface EMG to inform treatment decisions and optimize therapeutic interventions may significantly improve health outcomes. However, clinicians across the various healthcare fields have been slow to take advantage of surface EMG, and it remains underutilized despite significant efforts promote its use. The goal of this thesis is to develop accessible surface EMG techniques that can be applied in therapy and assessment scenarios. Ultimately, beyond the thesis, this work is intended to advance the clinical adoption of surface EMG so that its benefits may be accessed by a greater portion of practicing clinicians and their patients.

Abstract

Voluntary or involuntary muscle activation can be captured by surface electromyography (EMG), which detects muscle action potentials via sensors on the surface of the skin. The technique has been prominent in the study of physiological underpinnings of movement for over 80 years and continues to be an essential tool in scientific research. Its research topic applications include motor disorders caused by stroke, spinal cord injury, cerebral palsy, multiple sclerosis, and many others. Benefits of integrating surface EMG into healthcare have been extensively argued and supported by scientific research, but adoption in clinical settings has been frustratingly slow. The overall goal of this thesis is to advance the clinical adoption of surface EMG by developing techniques that emphasize accessibility and the needs of the end-user (i.e., clinicians). In the first chapter, this dissertation leverages theoretical and empirical literature concerning influencers of adoption, and published clinician perspectives, to determine an effective translation strategy. Developing enhanced therapeutic surface EMG techniques and complementary assessments techniques were identified as key strategic goals. In Chapter 2, I develop a new classification-based surface EMG biofeedback system designed to emphasize tailorability, flexibility, and accessibility. The system performed well during a single session in healthy participants and one individual with multiple sclerosis. In Chapter 3, tailored interventions were implemented across multiple sessions in a group of multiple sclerosis patients with severe motor impairment. Implementation was found to be feasible, and the classification record emerged as an efficient and intuitive means to monitor and assess characteristics of a training session. In Chapter 4, I develop and test an easy-to-replicate surface EMG

acquisition approach, and an analysis method using simple cursor placements. The analysis method was reliable between raters and sessions in healthy male and female participants. Overall, this thesis contributes to the translation of surface EMG methods into clinical practice.

Acknowledgments

This thesis is the product of more than five years of work that could never have been completed without the many mentors, colleagues, and loved ones who freely gave their time and energy to support my success.

Dr. Aimee Nelson has been my supervisor for seven years (MSc and PhD) and is almost entirely responsible for my scientific identity. Her confidence in my potential for growth has always been greater than my own and continues to inspire me. I am endlessly grateful for her reliable support and guidance throughout my PhD studies and during the writing of this dissertation. My committee members, Dr. Baraa Al-Khazraji, Dr. Michael Carter and Dr. Joshua Cashaback have been an invaluable source of support and insight throughout this PhD process. Their feedback and guidance were integral to success of the work contained in this dissertation.

My Neurophysiology and Imaging Lab colleagues, past and present, have made this journey a joyful one, and have contributed to my growth as a human and a scientist. Stevie Foglia, Karishma Ramdeo, Ravjot Rehsi, and Faith Adams made critical contributions for the success of this dissertation, and I thank them deeply.

My family has been the most reliable positive influence on my motivation and mood throughout a long post-secondary career. I thank my mother and father for their unconditional love and support and their unwavering belief in my success. Finally, to my

beautiful and loving wife – there is absolutely no chance that I could have finished this dissertation without you. Thank you for being my bedrock during this long and often uncertain process.

Declaration of Academic Achievement

This thesis was written entirely by Stephen Toepp. All experiments and analyse were conducted by Stephen Toepp.

Chapter 2 – published in IEEE Sensors Journal

Toepp SL, Mohrenschildt M v., Nelson AJ. An EMG-Based Biofeedback System for Tailored Interventions Involving Distributed Muscles. *IEEE Sensors Journal* (2023); 23: 28095–28109.11: 59-74.

Stephen L. Toepp was responsible for the design and programming of the biofeedback application, data collection, data analysis, data interpretation, and writing of the manuscript; Dr. Martin v. Mohrenschildt assisted with the machine learning aspects of biofeedback design and editing of the manuscript. Dr. Aimee J. Nelson assisted with conceptualization and editing of the manuscript.

Chapter 3

Contributors: Toepp SL, Menon S, Harris J, Nelson AJ.

Stephen L. Toepp was responsible for conceptualization, data collection, data analysis, data interpretation, and writing of the manuscript; Dr. Suresh Menon and Dr. Jocelyn Harris assisted with editing of the manuscript; Dr. Aimee J. Nelson assisted with conceptualization and editing of the manuscript.

Chapter 4

Contributors: Toepp SL, Rehsi RS, Syroid AS, Gurlal GS, Nelson AJ.

Stephen L. Toepp was responsible for conceptualization, data collection, data analysis, data interpretation, and writing of the manuscript; Ravjot S. Rehsi contributed to data analysis, conceptualization of the paper and editing of the manuscript; Anika L. Syroid contributed to the writing of scripts comprising the cursor placement user interface and edited the

manuscript. Gural S Gill contributed to the editing of the Manuscript; Dr. Aimee J. Nelson assisted with conceptualization and editing of the manuscript.

Table of Contents

Chapter 1: Introduction	1
1.1 <i>Theories of Diffusion</i>	2
1.2 <i>Current and Historical Perspectives</i>	8
1.3 <i>Literature Review: Perceptions and Use of Surface EMG Among Clinicians</i>	11
1.4 <i>Translational Strategy</i>	18
1.5 <i>Goals of the Thesis</i>	20
Chapter 2: Study 1	22
2.1 <i>Introduction</i>	23
2.2 <i>Design Objectives</i>	26
2.2.1 <i>Creating a Motivational Biofeedback Environment</i>	26
2.2.2 <i>Accommodate Variable Sensor Configurations and Flexible Number of Channels</i>	27
2.2.3 <i>Use Open-source Components that are Accessible to a Wide Range of Researchers</i>	29
2.3 <i>Background</i>	30
2.3.1 <i>Acquisition and Pre-processing</i>	31
2.3.2 <i>Machine Learning</i>	31
<i>Feature Extraction</i>	32
<i>Feature Reduction</i>	34
<i>Classification</i>	36
2.3.3 <i>EMG Controlled Video Gaming</i>	36
2.4 <i>The Biofeedback Algorithm</i>	40
2.4.1 <i>Sensors</i>	40
2.4.2 <i>Feature Extraction</i>	41
2.4.3 <i>Machine Learning</i>	42
2.4.4 <i>Game Control</i>	43
2.5 <i>Implementation</i>	44
2.5.1 <i>Acquisition Setup</i>	44
2.5.2 <i>Realization in Code</i>	45
2.6 <i>Validation in Healthy Volunteers</i>	49
2.6.1 <i>Participants</i>	49
2.6.2 <i>Movements and Sensors</i>	50
2.6.3 <i>Calibration Procedure</i>	52
2.6.4 <i>Performance Outcomes</i>	55
2.6.5 <i>Results</i>	57
2.7 <i>Discussion</i>	58
2.8 <i>Conclusion</i>	62
Chapter 3: Study 2	63
3.1 <i>Introduction</i>	64
3.2 <i>Methods</i>	69
3.2.1 <i>Participants</i>	69
3.2.2 <i>Classification-Based EMG Biofeedback</i>	69

<i>Instrumentation</i>	69
<i>Calibration</i>	70
<i>Game Control</i>	71
<i>Tailoring and Intervention Design</i>	71
3.2.3 Data Analysis.....	72
3.3 <i>Results</i>	74
3.3.1 Case 1.....	74
3.3.2 Case 2.....	76
3.3.3 Case 3.....	77
3.4 <i>Discussion</i>	80
3.5 <i>Conclusion</i>	87
Chapter 4: Study 3	88
4.1 <i>Introduction</i>	89
4.2 <i>Methods</i>	92
4.2.1 Assessment Protocol Template	92
4.2.2 Upper-Limb Movements in Healthy Males and Females	95
<i>Participants</i>	95
<i>Movements and Positioning</i>	96
<i>Electromyography</i>	97
<i>Cursor Placements</i>	98
<i>EMG Measurements</i>	101
<i>Statistical Analysis</i>	102
4.3 <i>Results</i>	102
4.3.1 Inter-Rater Reliability	102
4.3.2 Inter-Session Reliability	102
4.3 <i>Discussion</i>	104
Chapter 5: Conclusions and Impact	113
References	117

Figures

Figure 1.1: Respondent Details	17
Figure 2.1: Graphical User Interface	45
Figure 2.2: Game Control Schematic	47
Figure 2.3: Calibration Movements and Positions	51
Figure 2.4: Calibration Processing Pipeline	54
Figure 2.5: Calibration and Training Data	56
Figure 3.1: Case 1	75
Figure 3.2: Case 2	78
Figure 3.3: Case 3	81
Figure 3.4: Accuracy and Portion in Agreement	83
Figure 4.1: Acquisition Protocol Template, Sensor Placement and Positioning	94
Figure 4.2: Cursor Placement Application	100
Figure 4.3: Inter-Rater Cursor Placements	103
Figure 4.4: Smallest Detectible Change	105

Tables

Table 1.1: Respondent Details	11
Table 2.1: Accuracy and Precision Metrics	57
Table 3.1: Case Demographics	73
Table 4.1: Relative Reliability of Features and Cursor Placements	107

List of Abbreviations

AD: analog-to-digital	MAV: mean absolute value
ALS: amyotrophic lateral sclerosis	MNF: mean frequency
AN: anconeus	MOV: <i>movement</i> phase
ANT: anterior	MS: multiple sclerosis
BAL: <i>balance</i> training scheme	NDD: neurodevelopmental disorder
BB: biceps brachii	NLDA: non-linear discriminant analysis
BL: <i>baseline</i> phase	NN: neural network
CIMT: constraint-induced movement therapy	OT: occupational therapist
CP: cerebral palsy	PC: personal computer
DOI: diffusion of innovations theory	PCA: principal component analysis
ECRL: extensor carpi radialis longus	PIA: portion in agreement
EDS: extensor digitorum superficialis	PrT: pronator teres
EDSS: expanded disability status scale	PT: physiotherapist
EEG: electroencephalography	RMS: root mean square
EEG-BCI: EEG brain-computer interface	SCI: spinal cord injury
EF: elbow flexion	SDC: smallest detectible change
EHR: electronic health record	SENIAM: surface electromyography for non-invasive assessment of muscles
EL: <i>elbow</i> training scheme	SRLM: spectral regression extreme learning machine
EMG: electromyography	SSC: slope sign changes
FCR: flexor carpi radialis	SVM: support vector machine
GNB: gaussian naïve bayes	TB: triceps brachii
GUI: graphical user interface	t-SNE: t-distributed stochastic neighbor embedding
HA: <i>hand</i> training scheme	UL: <i>upper limb</i> training scheme
HCI: human-computer interface	USB: universal serial bus
HOP: hand opening	VL: vastus lateralis
ICC: interclass correlation coefficient	WEF: wrist extension and flexion
ICU: intensive care unit	WL: waveform length
IDE: integrated development environment	ZC: zero crossings
IHI: interhemispheric inhibition	
KNN: k-nearest neighbors	
LAT: lateral	
LDA: linear discriminant analysis	
LL: <i>lower limb</i> training scheme	
LPV: localized provoked vulvodynia	
MAS: modified Ashworth scale	

Chapter 1: Introduction

Surface electromyography (EMG) non-invasively captures electrical potentials in the muscle during voluntary or involuntary activation by recording from sensors on the surface of the skin. The technique has been used to study physiological processes governing movement since the 1940s (Cram 2003), with applications in stroke (Klein et al. 2018), spinal cord injury (SCI) (Balbinot et al. 2022), cerebral palsy (CP) (Cappellini et al. 2020), multiple sclerosis (MS) (Cofré Lizama et al. 2016), and many other diseases causing motor impairment. Despite a considerable body of literature describing the potential benefits of its use in healthcare, surface EMG adoption in clinical settings has been slow (Campanini et al. 2020, Manca et al. 2020).

The goal of this thesis is to advance the clinical adoption of surface EMG so that its benefits may be accessed by a greater portion of practicing clinicians and their patients. In this introductory chapter, I explore theoretical frameworks that are useful in understanding the propagation of practices and technologies in clinical communities. I also consider the history of translational efforts and conduct a review of published clinician perspectives on the topic of surface EMG. These sources of insight are then combined in an informed translational strategy. I take steps to execute this strategy in Chapters 2, 3 and 4. In Chapter 5, I reflect on the major findings and impact of the steps undertaken in the previous chapters.

1.1 Theories of Diffusion

The propagation of innovative practices, products, or technologies among populations of consumers, or adopters, is an entire field of study. To better understand drivers of surface EMG adoption or rejection, it is helpful to refer to established theories of innovation *diffusion*. These can provide a simple and intuitive framework that contextualizes the perspectives of practicing clinicians (Section 1.2), and the efforts and observations made by surface EMG advocates (see Section 1.3).

The primary theory discussed in this section is Diffusion of Innovations theory (DOI), which was developed by Everett Rogers (Rogers 2003). Classic DOI was designed for market research, e.g. (Nejad et al. 2014), but it has since demonstrated utility for explaining trends in the adoption new technologies and practices (i.e., innovations) in specific fields, including healthcare (Celik et al. 2014, Sharp and Miller 2016, Novikov et al. 2024). The main constructs in DOI are: stages of adoption, innovativeness level, innovation attributes, and decision type (Rogers 2003). Classic DOI was not developed specifically for healthcare, so additional context-specific perspectives and concepts are needed to supplement its main ideas (Balas and Chapman 2018). As such, I will discuss the above-listed DOI constructs as well as insights from healthcare-specific diffusion literature.

According to classic DOI theory, the process of adoption occurs in five ordered stages. In the initial *knowledge* stage, potential adopters gain awareness of the innovation and begin to understand its need. During *persuasion*, they develop positive or negative attitudes

towards the innovation. The *decision* stage is where individuals decide to adopt or reject an innovation. If it is adopted, *implementation* occurs when the innovation is initially adapted for use. Finally, *confirmation* is defined by continued or permanent use of the new practice or technology. These stages can describe the status of an individual at a discrete moment, but they say little about transitions from one stage to the next. Specifically, how long does movement from one stage to the next take in certain circumstances?

Many factors that determine the rate of progression through the stages in healthcare are specific characteristics of the field. For instance, a prominent influence is the high propensity of healthcare adoption decisions to have high stakes. In one example a clinical trial in 2001 suggested better outcomes for critical ICU patients when a specific glucose control approach is used (Van den Berghe et al. 2001), but eight years later a larger trial reported poorer outcomes with the new approach than the original (NICE-SUGAR Study Investigators et al. 2009). In that case, an estimated ~ 26,000 deaths may have resulted from adopting the innovation too early (Kavanagh and Nurok 2016). Clinicians are wary that the impact of their decisions can be exceptionally high and are encouraged to adhere to principles of evidence-based practice, requiring that treatment decisions to be made on the basis of scientific evidence (Herbert et al. 2001). The amount of accumulated evidence (and therefore time) required for clinicians to feel comfortable implementing a new surface EMG technique is thus probably associated with perceived risk of worse patient outcomes.

The seven-step model created by Balas and Boren (2000) estimated an absolute and relative timescale for the adoption process using the observable timeline for generation of scientific

evidence and its delivery to practicing clinicians. The steps include completion of original research, submission for publication, acceptance, publication, inclusion in bibliographic databases, incorporation into reviews and textbooks, and implementation. Based on available literature at the time, an average estimate of 1.4 years was estimated to elapse between completion of original research and inclusion in bibliographic databases. After inclusion in databases, the incorporation into reviews and textbooks requires an estimated 6 to 13 years, and practical implementation requires an additional 9.3 years (Balas and Boren 2000).

While DOI's stages emphasize experiences, attitudes, and perceptions of individual adopters, Balas and Boren scrutinized the ability of clinicians easily access scientific evidence as the major prerequisite of practical implementation in healthcare. Effectively, the perspective separates DOI's knowledge stage into six steps, while combining its persuasion, decision, implementation, and confirmation stages into one stage, i.e., implementation. It highlights the pivotal role of accessible knowledge resources in enabling the formation of positive or negative attitudes toward an innovation during the persuasion stage. Indeed, it has been argued that systematic reviews and other synthesized knowledge formats are the "basic unit of knowledge translation" (Grimshaw et al. 2012).

The challenge of consolidating evidence in reviews and textbooks for the positive impacts of a few specific surface EMG techniques has been acknowledged (Merletti et al. 2021), but other key factors cause implementation delays even when the evidence is clear, and the

risk of harm is low. One important influence is investment by industry stakeholders in the development and scaled manufacturing of new technologies required to make the innovation accessible to clinicians. Merletti et al. (2021) cites the almost exclusive focus by firms on providing surface EMG products to a niche researcher market as a major impediment to adoption. If the technology is available, innovations that are widely considered beneficial and low risk (i.e., with respect to health outcomes) may still require significant time to reach majority adoption. One such example is electronic health record (EHR) systems, which can improve workflow efficiency and improve quality of care, and are unlikely to directly or indirectly cause patient harm (Reis et al. 2017). After the advent of the first commercially available EHR system in Norway, it was 12 years until majority adoption was seen among general practitioners and 20 years before majority adoption was seen in hospitals (Heimly et al. 2011). This considerable delay probably reflects a reality in which motivating the adoption by healthcare professionals and institutions requires more than access to information and the availability of the necessary hardware/software components.

Although access to evidence and technology will play a significant key role in the decisions of all clinicians, DOI provides a useful structure for understanding varying sources of evidence and the contextual factors impacting adoption on an individual level. DOI categorizes adopters into five innovativeness levels defined by how early they tend to adopt innovations in cases where they ultimately do adopt (i.e., for successful innovations). The relative size of each category and its prototypical personality traits are described as well.

The earliest category, *innovators* comprise approximately 2.5% of adopters, are highly tolerant of risk, and value novelty more than others. Next are the *early adopters*, making up about 13.5%, who have sufficient resources to feel comfortable taking risks and trying new things. They are seen as leaders in their professional community, and frequently exchange ideas with innovators. The third category is the *early majority* who represent roughly 34% of all adopters. These are more likely to make decisions based on personal familiarity than on scientific research or evidence and are heavily influenced by familiar figures in their local community. Members of the early majority are less comfortable with risk than innovators or early adopters. The *late majority*, also comprising about 34%, is more conservative and requires proof before trying new innovations. This often corresponds with the practice or technology becoming the new standard. The latest adopters are the *laggards*, representing about 16% of adopters. Members of this group are traditionalists who make careful choices and tend toward tried-and-true approaches based on personal experience.

According to DOI, adopters at all innovativeness levels are influenced by five key innovation attributes. The *relative benefit* is the advantage of adoption relative to the cost in time, effort, and/or money. The innovation's *complexity* is its perceived sophistication or requirement for technical expertise, as opposed to intuitiveness or user-friendliness. Alignment of the innovation with the adopters' values, beliefs, past experiences, and potential needs describes its *compatibility*. The innovation's *trialability* is the opportunity to use it on a limited basis. Lastly, observability is the ability to observe the benefits others

adopting the innovation. Intuitively, this aspect of DOI translates well to healthcare since, with requisite knowledge, clinicians probably develop positive or negative attitudes towards an innovation similarly to adopters in other professional fields.

Although DOI integrates little of organisational structures present in healthcare, it does consider external influences by classifying adoption decisions into three types. Decisions made independently from the adopter's social community are called *optional*, decisions made by consensus among members of a community are termed *collective*, and decisions made under pressure from groups with power, expertise, or prestige are called *authority* decisions.

The adoption decision type, innovativeness level, and innovation attributes interact to determine whether the diffusion progresses from one stage to the next. Different stages require knowledge transformation efforts targeted to certain types of adopters to overcome specific barriers. Balas and Chapman (2018) considered these interactions in their “Road Map for Diffusion of Innovation in Health Care.” They specified four waves or stages of adoption and identified four key groups of potential adopters, which were derived from DOI's innovativeness levels. The first wave is *clinical study*, where innovators are the predominant adopters and must establish the innovation's feasibility before the next stage can occur. Outcome assessment, evaluation of cost effectiveness, integration into clinical practice, and development of businesses to support the integration are the keys to establishing feasibility. The second wave is *leading practice*, where early adopters should

be targeted by communicating the innovation's public health impact, producing consensus statements, offering training sessions and trials, and providing opportunities for educational reinforcement. Beyond initial adaptation, early adopters must effectively operationalize the innovation to support continued use (i.e., reach the confirmation stage), before the next wave can occur. The *majority adoption* wave occurs when the innovation spreads to early and late majority adopters. This wave can be facilitated by establishing clinical guidelines and mechanisms for decision support (e.g., computer algorithms), providing access to relevant patient information, and creating supportive policies and incentives. Failure to provide these types of support are the main barriers in this stage, which is also the most impactful by virtue of the relative portion of adopters in play. The *general access* wave is comprised of the laggards and requires the introduction of textbook content, compulsory accreditation, public awareness campaigns, and other pressures. This integrated conceptualization is important in suggesting translational priorities for innovations in certain scenarios. Thus, by describing the current scenario with respect to the diffusion of surface EMG methods in healthcare, it is possible to arrive at an appropriate translational strategy.

1.2 Current and Historical Perspectives

Several initiatives have been promoted to increase awareness (i.e., knowledge) of surface EMG methods. In 1999, the European campaign, "Surface Electromyography for Non-Invasive Assessment of Muscles" (SENIAM) provided a set of practical recommendations to standardize surface EMG use (Hermens et al. 2000), which are periodically updated and

available online (www.seniam.org). Other coordinated efforts have since been pursued, including projects to develop tutorials for audiences with minimal engineering background (Merletti and Muceli 2019, Del Vecchio et al. 2020, McManus et al. 2020, Merletti and Cerone 2020) and consensus papers on various topics relevant to the clinical implementation of surface EMG (Besomi et al. 2019, 2020, Hodges 2020, McManus et al. 2021, Gallina et al. 2022). Considerable effort has thus been made to make information about this technology available to potential adopters.

However, it seems unlikely that a unidirectional strategy where educational institutions drive adoption among practicing clinicians will be independently successful. While educational materials on the topic of surface EMG are more accessible than ever, practicing clinicians often lack the time and inclination to seek out educational resources (Feldner et al. 2019, Paci et al. 2021). Several authors have called for mandatory surface EMG training to be included in formal education of clinical practitioners (Campanini et al. 2020, Goffredo et al. 2020, Manzur-Valdivia and Alvarez-Ruf 2020, Merletti et al. 2021), or for the creation of new training programs to create dedicated clinical specialists (Merletti et al. 2023). The strategy aims to create professionals who begin their clinical career needing no additional training to make effective use of surface EMG. The approach leans heavily on obtaining favorable *authority* type adoption decisions that are driven by the influence of prestigious figures within educational institutions. However, as clinicians transition from their initial formal training, they are exposed to new strong influences. For example, practicing Australian physiotherapists consider their colleagues' treatment decisions, and patient

expectations to be important in their clinical decision making process (Gleadhill et al. 2022). Moreover, as clinicians gain experience, they begin to rely more heavily on their own experience working with patients than educational reference materials (Nilsson and Nordholm 1992, Carr et al. 1994), and the tendencies that they develop (evidence-based or not) can be expected influence the behaviors of impressionable colleagues. For an innovative surface EMG technique to be adopted widely, implementation feasibility must proven to individual and organizational decision-makers (Scurlock-Evans et al. 2014). These decision makers must be prepared to reinforce educational initiatives by devoting time and resources to training courses and affirmation of the technique as an appropriate use of clinical time. That is, efforts to convince educational institutions to adopt surface EMG training programs should be coordinated with the promotion of practical methods directly to practicing clinicians and clinical organizations.

Arguably, the most important item to coordinate is which of the many existing distinctive surface EMG applications to promote. A significant portion of techniques were developed to address niche hypotheses or technical issues that are not relevant in many clinical contexts. It is thus important to identify appropriate techniques that can be effectively promoted for both inclusion in formal training programs and immediate use by practicing clinicians. In the next section, likely surface EMG methods are discussed from the perspective of practicing clinicians.

1.3 Literature Review: Perceptions and Use of Surface EMG Among Clinicians

To identify likely surface EMG techniques, I conducted a review of published surveys and interviews. A PubMed search was performed using the terms “((surface EMG) OR (sEMG) OR (surface electromyography)) AND ((clinician) OR (doctor) OR (specialist) OR (therapist) OR (physiotherapist) OR (occupational therapist) OR (physiatrist)) AND ((perception) OR (survey) OR (interview) OR (questionnaire)).” The search returned 356 results, and 17 passed initial screening of titles and abstracts. The inclusion criteria were: 1) studies must include surveys or interviews of practicing clinicians, and 2) the topic of surveys and interviews must include the use or perceptions of surface EMG. One manuscript was not available in English. Each of the 16 included studies is listed in Table 1.1 with its general topic, the respondent region (s) of origin, and respondent occupation.

Table 1.1: Review Summary

<i>Study</i>	<i>Topic</i>	<i>Region(s)</i>	<i>Respondents</i>
(De Carvalho et al. 2017)	Amyotrophic Lateral Sclerosis	United Kingdom; Germany; Poland; Portugal; Italy; France; Sweden; North America; South America; Africa; Australia	ALS Experts (N=40) *

<i>Study</i>	<i>Topic</i>	<i>Region(s)</i>	<i>Respondents</i>
(Singh 2017)	Botox/Spasticity	United Kingdom	Physiotherapists (N=4); Psychiatrists (N=33); Neurologists (N=3)
(Picelli et al. 2017)	Botox/Spasticity	Italy	Physiatrists (N=24)
(Peters and Giuffre 2018)	Carpal Tunnel Syndrome	Canada	Plastic Surgeons (183)
(Li Pi Shan et al. 2015)	Carpal Tunnel Syndrome	Canada	Clinical Neurophysiologists (N=53); Psychiatrists (N=18)
(Okamura et al. 2018)	Carpal Tunnel Syndrome	Brazil	Plastic Surgeons (N=174)
(Cappellini et al. 2020)	Cerebral Palsy	Italy	Physiotherapists (N=16); Medical Doctors (N=7); NDD therapists (N=5)
(Yahya et al. 2018)	Cubital Tunnel Syndrome	United States	Plastic Surgeons (N=1,096)

<i>Study</i>	<i>Topic</i>	<i>Region(s)</i>	<i>Respondents</i>
(van Snippenburg et al. 2019)	Dysphagia	Netherlands	ICU Staff (N=67) *
(Chipchase et al. 2009)	Electrophysiological Agents	Australia	Physiotherapists (N=3,538)
(Hartmann et al. 2007)	Localized, Provoked Vulvodynia	United States	Physiotherapists (N=193)
(Johnsen et al. 1994)	Laboratory Exams	Italy; Belgium; France; Denmark; Portugal; Germany; United Kingdom	Clinical Neurophysiologists (N=9)
(Feldner et al. 2019)	Neurorehabilitation	United States	Physiotherapists (N=7); Occupational Therapists (N=13); Psychiatrists (N=2)
(Manca et al. 2020)	Neurorehabilitation	Australia; Austria; Belgium; Canada; France; Germany; Ireland; Italy; Netherlands; Switzerland; United;	Physiotherapists (N=37); Clinical Neurophysiologists (N=2); Psychiatrists (N=5); Kinesiologists (N=3); Biomedical Engineers (N=12)

<i>Study</i>	<i>Topic</i>	<i>Region(s)</i>	<i>Respondents</i>
		Kingdom; United States	
(Goffredo et al. 2020)	Stroke	United States	Physiotherapists (N=3); Biomedical Engineers (N=2)
(Lu et al. 2011)	Stroke	United Kingdom; United States; Canada; Switzerland; Australia; Ireland; Columbia; Israel	Physiotherapists (N=167); Occupational Therapists (N=62); Nurse (N=2); Recreational Therapist (N=1); Stroke Coordinator (N=1)

Details of the 16 manuscripts included in the literature review *are presented*. * Indicates an instance where the group of respondents was not defined by occupation or clinical role.

The contribution of different occupations to the reviewed studies is summarized in Figure 1.1. Physiotherapists (PT) were the most studied group by far, representing more than two thirds of all respondents (Figure 1.1A), followed by physicians at approximately 27%. The representation of clinicians from countries contributing more than 1% of respondents are shown in the Figure 1.1B. Almost two thirds of surveyed clinicians were working in Australia, followed by the ~24% working in United, and 6 and 3% contributions from Canada and Brazil, respectively. Clinicians practicing in Italy, Netherlands, and the United Kingdom each represented ~1% of all respondents. Physicians are separated by specialization in Figure 1.1C, which shows that the vast majority (94%) of surveyed

physicians were plastic surgeons with the only other significantly represented group being physiatrists. The remaining clinical figures, contributing less than 5%, are represented in the Figure 1.1D. Most prominent among this group were occupational therapists (OT), and clinical neurophysiologists. The ICU staff, and amyotrophic lateral sclerosis (ALS) experts are also represented significant portion of the respondents in Figure 1.1D, but specific occupations were not provided.

Several neurophysiology techniques that include surface EMG have been widely adopted by clinical neurophysiologists and referring physicians. More than 50% of the surveyed plastic surgeons and physiatrists routinely ordered (or performed themselves) nerve conduction studies to diagnose carpal tunnel syndrome (Li Pi Shan et al. 2015, Okamura et al. 2018, Peters and Giuffre 2018), and they rely on the insights obtained to make decisions regarding the appropriateness of surgical interventions (Yahya et al. 2018). Surface EMG is also a component of gait analysis protocols for guiding Botox injections for 30 to 40% of physicians treating spasticity in ambulatory patients following stroke (Picelli et al. 2017, Singh 2017). In addition, more than 50% of surveyed ALS experts indicated that EMG investigations, including nerve conduction studies and motor unit potentials, are essential for the detection and management of the disease (De Carvalho et al. 2017).

Cohorts comprised mostly of non-physicians and non-neurophysiologists (higher portion of PTs, OTs, etc.) reported lower rates of surface EMG adoption, probably related to a lack of specific formal education. Surface EMG experience was claimed by only 6 of 28 (~21%)

respondents from an Italian pediatric neurorehabilitation clinic (Cappellini et al. 2020) and only 3 of 22 (~13%) interviewees from pediatric or adult rehabilitation clinics in the United States (Feldner et al. 2019). Nonetheless, many of these clinicians were aware of surface EMG and its practical applications in rehabilitation. Only 56% of respondents to one survey agreed with the claim that surface EMG is rare in rehabilitation, and only 53% agreed that surface EMG is currently more relevant for researchers than clinicians (Manca et al. 2020). The same cohort also expressed high agreement on the utility of the surface EMG in the pursuit of several specific clinical aims, including monitoring changes in muscle activity with interventions (91% agreement) and delivering interventions in the form of biofeedback (86% agreement). They also rated surface EMG biofeedback, specifically, as very likely to be useful in increasing muscle selectivity (91% agreement), reducing excessive muscle tone (88% agreement), and engaging weak or hyperactive muscles (91% agreement). A thematic analysis of focus groups responses by Feldner (2019) also revealed a perception that surface EMG could improve standardization of assessments and provide early evidence of progress in the cases of very severe motor disability. There appears to be a disconnect between high perceived utility of surface EMG and low levels of adoption.

However, the disconnect seems to be more pronounced when considering surface EMG methods for assessment versus methods for intervention. No clinicians reported using a specific stand-alone surface EMG method to diagnose or assess a specific condition. It appears that, while many are enthusiastic about the prospect of using surface EMG assessments to plan or monitor intervention outcomes, the expertise required to interpret

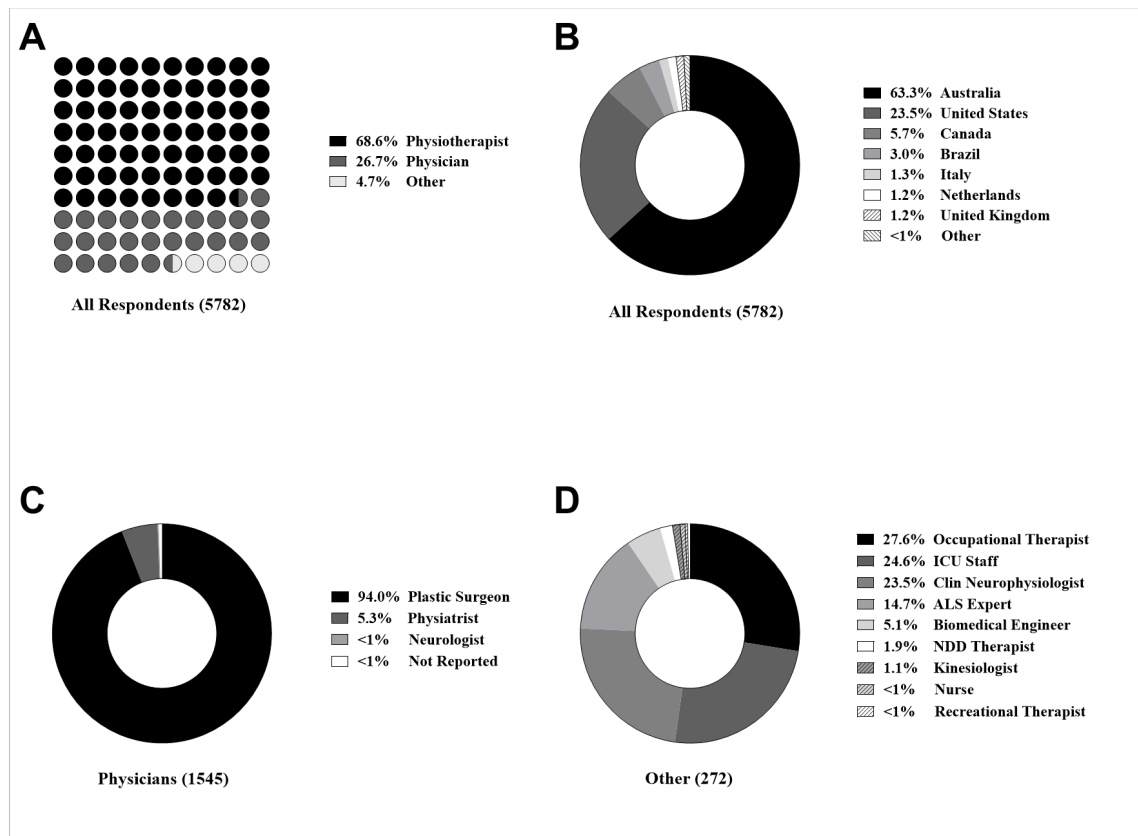


Figure 1.1: Respondent Details

Survey and interview respondents are separated by their occupation and country in which they practice. Panel A shows the percentage of all respondents who were physiotherapists, physicians, and other clinicians. Panel B shows the portion working in each represented country. Panel C shows specializations among physician respondents. Panel D shows the composition of the group of labelled ‘Other’ in Panel A. These groups include specific occupations and non-specific designations reported by the authors (e.g., ICU staff). NDD – neurodevelopmental disorders therapist; ALS – amyotrophic lateral sclerosis; ICU – intensive care unit

the data ultimately undermines adoption (Feldner et al. 2019, Manca et al. 2020). In contrast, use of surface EMG to deliver biofeedback intervention was reported by 10% of ICU staff to rehabilitate dysphagia (van Snippenburg et al. 2019), 9% of PTs and OTs to facilitate stroke recovery (Lu et al. 2011), and 66% of physiotherapists who treat localized provoked vulvodynia (LPV) (Hartmann et al. 2007). In addition, 42.5% of Australian

physiotherapists reported having used EMG biofeedback, and 57% indicated that they have access to the tool (Chipchase et al. 2009). During the focus groups conducted by Feldner (2019), biofeedback was also the most frequently mentioned surface EMG technique. Moreover, the participants who indicated having experience with the modality had used it in the context of intervention via robotic training, functional electrical stimulation, or biofeedback training (Feldner et al. 2019).

1.4 Translational Strategy

Choosing techniques that clinicians are likely to adopt is a central challenge in the promotion of surface EMG. The available literature describing use and perceptions of surface EMG revealed that surface EMG is most often used by physicians and neurophysiologists, and rarely in a stand-alone capacity. It is usually combined with nerve stimulation within nerve conduction studies or with other kinematic modalities during gait analysis.

Surface EMG biofeedback was striking as the predominant method that non-physician and non-neurophysiologist clinicians were aware of, perceived positively, and had used in their practice. It should be noted that this group of clinicians was mostly (~95%) PTs, who represent a large and influential block of rehabilitation professionals. Merletti and colleagues (2023) recently highlighted the leading role of this clinical figure in assessment, monitoring, and intervention, and their potential role in adoption of new techniques. They propose that PTs "...are at the pivot of creating basic knowledge about new technologies

in clinical contexts,” and that, with increasing awareness of new technologies, the PT “... is potentially placing itself at the most efficient lever to deliver evidence-based therapies in a rehabilitation team.” (Merletti et al. 2023). It appears as if surface EMG biofeedback methods may diffuse within this group more readily than other combined or stand-alone technique. If the reason for this pattern can be interpreted, translational strategies will almost certainly be improved.

As I mentioned in the previous section, stand-alone surface EMG assessment is rarely used by clinicians, despite expressed understanding of their value. Clinician concerns about the interpretations of surface EMG data indicate that complexity is a major contributor to this situation. In contrast, EMG biofeedback applications do not require complex data analysis. Outside of short calibration steps, the benefit is obtained in a completely automated manner via simple software that translates recorded signals into visual or auditory stimuli. In essence, EMG biofeedback is a rapid form of automated EMG assessment delivered directly to the patient and presenting very little technical challenge to the user. This has previously been suggested as an innovation that is likely to accelerate translation (Merletti et al. 2021).

EMG biofeedback may also diffuse more readily within large communities of PTs because, as a mode of therapeutic treatment, it is more *compatible* with the traditional role occupied by members of the profession. PTs tend to prefer quick, low-tech assessment options that do not soak up large amounts of time that could be used to deliver treatment, which is more

aligned with their perceived professional mandate (Snöljung et al. 2014, Braun et al. 2018). Surface EMG methods that are developed for assessment must therefore overcome the barrier of poor *trialability*. Surface EMG biofeedback applications may also partially address this challenge by offering clinicians an opportunity to try simple interpretation of data generated during the training. That is, without the need to invest additional time learning and implementing separate acquisition protocols with complex analysis methods.

1.5 Goals of the Thesis

As was stated at the beginning of this chapter, the overall goal of this thesis is to advance the clinical adoption of surface EMG and expand access to its benefits by clinicians and patients. In the previous sections, I have identified biofeedback as an appropriate focus for translational efforts. A wide variety of specific EMG biofeedback technologies exist with distinct advantages and disadvantages, and no individual system likely reflects the optimal version of this modality. As I discuss in Chapter 2, results in poor representation of the *relative benefit* of biofeedback by clinical research studies. Consolidating the most beneficial features of existing EMG biofeedback systems will therefore greatly benefit translational efforts.

The goals of this thesis are to develop and test 1) EMG biofeedback that integrates the most impactful features of existing methods, and 2) an EMG analysis framework for clinicians to easily assess and interpret the data types that are typically obtained during biofeedback

training. The first component is addressed in Chapters 2 and 3, and the second in Chapter 4.

Chapter 2: Study 1

In this chapter, I develop an optimized version of a surface EMG biofeedback system. I review relevant technical and empirical scientific literature to ensure that the product is adaptable and can deliver a potentially beneficial training interventions in a variety of contexts. During development, I ensure that my methods are reproducible by using commercially available hardware and open-source software. I test the system during a single training session in a group of healthy volunteers and one volunteer with primary progressive multiple sclerosis (MS). This work makes progress toward a “gold standard” in EMG biofeedback system design, which is necessary to develop a common language surrounding its implementation and its impact.

An EMG-based Biofeedback System for Tailored Interventions Involving Distributed Muscles

Toepp SL, Mohrenschildt M v., Nelson AJ. An EMG-Based Biofeedback System for Tailored Interventions Involving Distributed Muscles. *IEEE Sens. J.* (2023); 23: 28095–28109.

Abstract

Electromyography (EMG)-based biofeedback has considerable potential as a mode of therapeutic exercise for individuals with motor impairments. Advances in technology now allow the delivery of biofeedback with cheap, compact computers and sensors. Reliable machine learning classification of EMG signals in real-time, which is a core component of many biofeedback systems, is also now easily accessible through various open-source software libraries. Despite this progress and the attention garnered by EMG biofeedback

among researchers, broad clinical acceptance remains elusive. We aim to open this technology to a broader audience by proposing an accessible standard approach to the design and implementation of EMG-based biofeedback systems. We highlight important considerations when designing a system to deliver potent biofeedback, including maximizing motivation, minimizing constraints on sensor number or configuration, and maximizing replicability by other researchers. Based on relevant neuroscientific and technical literature, we recommend methods and procedures by which these goals can be achieved. Finally, we create and test a biofeedback system in a sample of both healthy and motor impaired volunteers. We found that the EMG biofeedback system supported accurate and stable control by healthy and impaired users and could be implemented with minimal access to coding expertise and an off-the-shelf EMG device. This work expands awareness of effective design principles for EMG biofeedback systems and will advance the state-of-the-art in this field.

2.1 Introduction

Surface electromyography (EMG) biofeedback, where feedback from electrical muscle signals is used to train muscle tone or coordination (Basmajian 1981), has been used since the 1950s (Mims 1956, Cram 2003). This technique involves using recorded muscle potentials to provide artificial proprioceptive feedback. Measures of activity in one muscle, or the relative activity in antagonist versus synergist muscles are computed and communicated to the user in an intuitive visual or audio format (Davis and Lee 1980, Cordo et al. 2013, Marin-Pardo et al. 2020, Cikajlo et al. 2021, Marin-pardo et al. 2021). In the

past seven decades, EMG biofeedback has been a topic of interest to researchers and clinicians who seek to improve motor recovery in a multitude of scenarios, including stroke (Marin-Pardo et al. 2020, Cikajlo et al. 2021, Marin-pardo et al. 2021, Munoz-Novoa et al. 2022), loss of bladder control in multiple sclerosis (MS) (McClurg et al. 2006, 2008, Lúcio et al. 2016), work or accident-related neck and shoulder disorders (Holtermann and Roeleveld 2006, Ehrenborg and Archenholtz 2010, Holtermann et al. 2010, Van Eerd et al. 2016), and pelvic pain (Wagner et al. 2022).

EMG biofeedback is generally understood to facilitate motor training and adaptation by providing supplemental proprioception (Basmajian 1973, Glanz et al. 1997), and its benefits are thus greatest when natural proprioception is severely limited. An illustrative example is the use of EMG biofeedback following nerve transfer. Nerve transfer surgery involves redirecting an intact nerve from a donor muscle to the distal undamaged portion of a completely severed or severely damaged nerve that innervates a paralyzed muscle (Liu et al. 2012). The procedure developed by Sturma and colleagues uses EMG to sense and reinforce volitional motor outputs that are present, but not strong enough to produce noticeable movement (Sturma et al. 2018). When volitional movement is possible, motor activity can be reinforced independently of movement amplitude, smoothness, coordination, or dexterity. That is, users need only produce changes in electrical activity in the muscle and, unless the motor pathway is completely severed, this is attainable for patients experiencing even very extreme paresis, hypertonia, or spasticity. Essentially,

EMG biofeedback provides an accessible mode of therapeutic exercise for patients along the entire continuum of care.

Despite the opportunities presented by EMG biofeedback methods, they have not been widely adopted in clinical practice (Manca et al. 2020). Recent clinician surveys suggested that contributing factors are lack of awareness, slow dissemination of research findings, time constraints, and restricted access to appropriate training in EMG methods (Feldner et al. 2019, Manca et al. 2020). In the current literature, consensus is lacking regarding the efficacy of EMG biofeedback compared to non-EMG interventions (Munoz-Novoa et al. 2022), and this also limits the willingness of institutions to spend on technologies that they consider “experimental”. This is probably because biofeedback delivery methods vary considerably from study-to-study with many unique systems using different numbers and types of sensors and integrating EMG signals into feedback differently (Anwer et al. 2011, 2013, Yoo et al. 2014, Garcia-Hernandez et al. 2019, MacIntosh et al. 2020, 2021, Marin-Pardo et al. 2020, Cikajlo et al. 2021, Dost Sürücü and Tezen 2021, Jian et al. 2021, Marin-pardo et al. 2021, Oña et al. 2022). There is presently no recognized state-of-the-art or gold standard for EMG biofeedback systems design, and it difficult to produce convincing evidence for the efficacy of a treatment modality that is so poorly defined.

Even so, it is encouraging that biofeedback applications were most mentioned by clinicians when asked to comment on the potential benefits of using EMG-based technologies in their practice (Feldner et al. 2019) . This suggests that EMG biofeedback may be closer to the proverbial “goal line” of acceptance than other EMG technologies. To cover the remaining

distance, best practices for designing EMG biofeedback systems must be developed. This will ensure that research investigating this type of technology reveals the benefits of the “gold standard” version, supporting a clearer and more convincing base of evidence.

Thus, to advance towards clinical viability, we identify several useful guiding principles for designing effective EMG biofeedback. We then review the relevant neuroscientific, behavioral, and technical background literature to identify appropriate methods and procedures by which to achieve the objectives. We subsequently apply the identified methods and procedures within the design and implementation of a biofeedback algorithm. Finally, to show that the product of this work is functional and flexible, we test its performance in a limited validation study including healthy and motor impaired volunteers.

2.2 Design Objectives

2.2.1 Creating a Motivational Biofeedback Environment

Many versions of EMG biofeedback involve auditory tones or graphical depictions that reflect the timing and magnitude of muscle activations in relation to explicitly set targets or thresholds (Anwer et al. 2011, 2013, Cikajlo et al. 2021). However, applications where users adjust their muscle activity to control avatars or objects within a game have recently become more popular (Yoo et al. 2014, Garcia-Hernandez et al. 2019, MacIntosh et al. 2020, 2021, Marin-Pardo et al. 2020, Jian et al. 2021, Marin-pardo et al. 2021, Oña et al. 2022). This trend follows growing support for the view that immersive virtual reality-like formats can enhance rehabilitation by increasing motivation and participation (Maggio et

al. 2019b, 2019a, Baeza-Barragán et al. 2020). Indeed, using gameplay-based rehabilitation results in more movement repetitions per session (Peters et al. 2013), and greater motivation (Lee and Bae 2022) than with traditional therapy following stroke. In a pediatric population, it was also shown that exercising in a virtual environment resulted in greater levels of muscle activity compared to normal training (Schuler et al. 2011). Considering this, delivering EMG biofeedback within a game scenario is preferred over more “bare bones” threshold matching or target tracking tasks.

2.2.2 Accommodate Variable Sensor Configurations and Flexible Number of Channels

Our second objective is to capture and integrate the activities of multiple muscle groups into biofeedback training. Many published EMG biofeedback schemes operate on data streams from individual sensors, or pairs of sensors. However, motor deficits result from discoordination or weakness in distributed muscles that require several EMG sensors to capture. Some of these deficits include motor overflow (Cleland and Madhavan 2022), and abnormal muscle synergies (Israely et al. 2018).

Muscle synergies are sets of muscles that are activated together as one unit. These units are modules that can be weighted and combined by the motor system to achieve behavior (D’Avella et al. 2006, Bizzi et al. 2008). After injury, these synergies can merge (Clark et al. 2010) or fractionate (Cheung et al. 2012), causing weakness or intrusive co-activation that contributes to dysfunction. It is especially important to address dysfunctional synergies because they can mask residual motor capacity (Beer et al. 2007, Hadjiosif et al. 2022) and

interfere with rehabilitative processes. When using EMG to reinforce muscle activation, it is important to avoid reinforcing inappropriate synergies. Biofeedback systems must therefore monitor both desired and undesired muscle activity, which requires several sensors.

Motor overflow is unintentional ipsilateral or contralateral muscle activation accompanying voluntary movements (Armatas et al. 1994). Mirror movements are a type of motor overflow characterized by activation in homonymous muscles contralateral to a volitional movement. This is regulated by transcallosal interhemispheric inhibition (IHI) in fully developed individuals, with the active hemisphere suppressing drive from the contralateral hemisphere during unilateral movements (Hübers et al. 2008). It is thought that IHI is critical for inter-limb coordination (Mayston et al. 1999) and the independent control of each limb (Fling and Seidler 2012). In many impaired populations IHI is unbalanced, and this often coincides with increased mirror movements (Pantano et al. 2002, Karandreas et al. 2007, Mackey et al. 2014, Takechi et al. 2014, Ternes et al. 2014, Kim et al. 2015, Chen et al. 2018, Cleland and Madhavan 2022, Simon-Martinez et al. 2022). On the other hand, re-balancing of IHI coincides with impressive functional improvements after constraint-induced movement therapy (CIMT) (Avanzino et al. 2011, Abdullahi et al. 2020). The ability to strategically place sensors across impaired and unimpaired limbs opens the possibility of using EMG pattern recognition to implement CIMT-like biofeedback wherein only selective activation on the target side is reinforced.

Accommodating many sensor channels will enable biofeedback to preferentially reinforce the execution of movements where muscle synergies and motor overflow are controlled. In addition, the configuration of these sensors should be chosen by the researcher or clinician. Restricting biofeedback input to a specific body segment because there are too few channels or because the sensors are fixed in a segment-specific arrangement, will limit clinical utility. For example, all seven physiotherapists interviewed on their impressions of the Myo Armband (Thalamic Labs) by Feldner asked if the device could be used in the lower extremity (Feldner et al. 2019). For a biofeedback system to be viable in a clinical setting, the answer to such questions should be an unequivocal “Yes”. In our view, the only acceptable application restrictions are those imposed by limitations in the musculoskeletal anatomy and physiology knowledge of the clinician, or by the severity of the neurological injury being addressed. That is, if muscles of interest can be identified, and some (even minimal) motor drive remains, the system should be usable.

2.2.3 Use Open-source Components that are Accessible to a Wide Range of Researchers

Our goal is not only to design a potent EMG biofeedback system, but also to present an approach and software architecture that is open and can easily be reproduced by non-software experts in other programming environments. There are many commercially available EMG devices with proprietary software and even programmer interfaces, but building a biofeedback system requires more than just data acquisition. The data must be processed and converted into a feedback signal, to be presented to the user, e.g., as a simplified signal or as an interactive game element, to close the loop.

The practical implementation of EMG videogame control can be complicated. Replicating existing approaches from literature often requires specific technical skills or access to proprietary software. For example, the innovative Tele-REINVENT system that was developed by Marin-Pardo and colleagues (Marin-pardo et al. 2021) features custom games created with the Unity game engine (Unity Technologies, San Francisco, CA, USA), signal processing scripts created in MATLAB (MathWorks, Natick, MA, USA), and a user interface written in C#.

Understandably, the focus of such development is to address an identified need, and not necessarily to make the resulting technology accessible to other researchers. However, reproducibility is important to encourage the independent validation of each approach by multiple research groups. Reproducibility benefits from avoiding (where possible) the use of proprietary software and preferentially using popular and open-source components. Adopting these tendencies will advance our objective of promoting wide community access to newly developed EMG biofeedback systems.

2.3 Background

At a high level, the EMG biofeedback system should translate potentials captured with the sensors from the muscle into a control stream that allows the user to interact with visual or auditory entities within a game environment. In this section, we review the literature relevant to various approaches for signal acquisition and pre-processing, feature extraction,

and machine learning. Each of these components play an important role in the realization of our design objectives.

2.3.1 Acquisition and Pre-processing

According to our objectives, it is important that clinicians or researchers are free to place sensors according to their expert judgment (see Section 2B). The configuration of the EMG sensor montage should thus only be constrained by established best practices for acquiring quality signal from the muscles of interest (Hermens et al. 2000). Since the highest frequency muscle-related signals oscillate at ~450-500Hz, the EMG system should have a sample rate of at least 1000 Hz. The raw data should also be pre-processed in accordance with standard procedures. Specifically, muscle-related signal contains the information in the 10 to 400 Hz frequency band (McManus et al. 2020), hence high and low-pass filtering is used.

2.3.2 Machine Learning

The object of machine learning in a biofeedback system is to create a classifier based on a statistical assumption, that predicts the user's intended game control inputs by processing the real-time EMG signals.

Classifiers are trained using sets of labeled class samples such that, when given an unlabeled sample, they can identify the corresponding class. A classifier usually works on already pre-processed data, in a feature space. The feature extraction is the process of

computing measurements of the time-domain signal that describe important signal characteristics. The literature also contains deep learning approaches, for example neural networks, that take the entire time domain signal as an input, essentially bypassing feature extraction. There are moderate advantages and disadvantages to these types of approaches (Anam and Al-Jumaily 2017, Batzianoulis et al. 2018). However, EMG signals are quite simple to classify, and the prediction of hand poses has a typical accuracy in the 80% range and higher, regardless of the feature extraction method (Khan et al. 2020). Feature reduction is a common procedure that attenuates redundant features and enhances those that are relevant to class discrimination. In our experience with time domain signals, a well-designed, often non-linear feature extraction step, followed by data reduction, supports the creation of efficient and stable real-time classification models. We therefore focused our development on this traditional machine learning approach, starting with feature extraction.

Feature Extraction. The purpose of feature extraction is to obtain information from EMG signals, information in the sense of quantifiable measurements like amplitude, frequency, energy, etc. EMG signals are time domain signals, which are usually processed by filters, or using windowing. Windowing means the signal is cut into smaller segments, the windows, over which quantities are computed from the data. We call this the extraction window, and it produces feature values that can be arranged into a feature vector.

The size of the extraction window determines the system control rate, which should be sufficiently high to prevent the perception of lag. For this reason, extraction windows

shorter than the typical visual reaction time of 300ms are recommended (Barbarotto et al. 1998). Using even shorter windows provides the opportunity to implement majority vote procedures that can increase the stability of the control stream. For example, Englehart et al used extraction windows as narrow as 16ms so that each value in the control stream could include information from the prior 18 feature vectors (Englehart and Hudgins 2003).

Selecting appropriate features is a widely studied topic, and there exist many papers and webpages listing many potential features. Khan and colleagues recently reviewed the merits of more than 30 different features, including time domain, frequency domain, and time-frequency domain features (Khan et al. 2020). Clearly the computational cost of different types of features varies widely. We consider computationally inexpensive features appealing, and as we have alluded to above, the literature shows that even simple features are sufficient for EMG classification.

The distinction between time domain and frequency domain features is noteworthy. Time domain features best fit our requirements because frequency and time-frequency features tend to be complex and more expensive in terms of computational resources (Khan et al. 2020). Among time domain features, the mean absolute value (MAV), root of the mean squared values (RMS) and waveform length (WL) are commonly applied in gesture recognition and fatigue estimation (Khan et al. 2020). Some other time domain features, such as the number of zero-crossings (ZC), number of slope sign changes (SSC) actually contain frequency information while retaining the simplicity and low computational load

as time-domain features (Ison and Artemiadis 2014). To preserve both amplitude and frequency information, we favor selecting at least one feature from RMS, MAV, and WL, and one from ZC and SSC.

Given the above, and confirmed by experiments, there is no need to compute complex transformations (e.g., wavelets), or to use deep neural networks to extract more sophisticated information.

Feature Reduction. Feature reduction is an entire topic of machine learning and is widely studied. Generally, feature reduction techniques are designed to attenuate redundant features by finding an uncorrelated lower-dimensional subspace that also preserves most of the important information, or variance. Choosing an appropriate reduction method is a key part in building a good classifier.

A common approach is to perform a class-naïve data reduction such as principal components analysis (Wold et al. 1987) or manifold learning (Saul and Roweis 2003, Pai et al. 2019) and then optimize class separation by testing the performance of a classifier model fitted to the transformed data (see Section 3B1). Since naïve approaches can produce as many dimensions as the input feature vector, the main optimization parameter is the number of lower dimensions that are used to fit the model. The first N dimensions, ordered by their explained variance, that produce a classifier model with maximized accuracy are used and the remaining dimensions are discarded as unimportant noise.

An alternative, and perhaps more direct, approach is to use a supervised data reduction method to project the feature data into a de-correlated subspace that also maximizes separation between the different movement classes. Supervised reduction methods use class-labeled feature vectors to determine which features change in-between classes and which are constant. Such methods include multi-class Linear Discriminant Analysis (LDA) (Yu and Yang 2001), Non-Linear Discriminant Analysis (NLDA) (Billings and Lee 2002), or the more recently developed Spectral Regression Extreme Learning Machine (SRLM) (Anam and Al-Jumaily 2015) technique. These methods produce a limited, predetermined number of output dimensions equal to the number of classes, less one. Compared to class-naïve feature reduction, low-dimensional feature projections obtained from supervised methods result in more stable accuracy across different classifier models. In a study comparing SRLM to unsupervised t-Distributed Stochastic Neighbor Embedding (t-SNE), Thiamchoo and Phukpattaranont reported that classification error of seven classifiers ranged from 1.50% to 2.65% for SRLM and 1.27% to 17.15% for t-SNE (Thiamchoo and Phukpattaranont 2022). A further advantage of the multiclass LDA specifically, is that it is computationally fast, with similar processing time to PCA, while supporting far better classification accuracy (Chu et al. 2006, Thiamchoo and Phukpattaranont 2022). Nonlinear supervised feature reduction may support slightly better classification, but they require much more processing time (e.g., (Chu et al. 2006)) than linear methods, especially when the input is high-dimensional and/or variable.

Classification. Now that we have a meaningful feature vector, we can build a classifier that decides if a sample belongs to some movement class. Many different approaches to classification are used for EMG signals, including neural networks (NN) (Pulliam 2011), k-nearest neighbors (KNN) (Kim et al. 2011), support vector machines (SVM) (Purushothaman and Vikas 2018), linear discriminant analysis (LDA) (Kim et al. 2011), Gaussian Naïve Bayes (GNB) (Domingos and Pazzani 1996), and many more (Khan et al. 2020). Any of these will result in acceptable accuracy in classifying the EMG signals. The use of the multi-class LDA for classification, as well as feature reduction, is the most popular method because of its simple implementation, low computational cost, and sufficient accuracy (Khan et al. 2020). The GNB approach is less often used but is also very simple to implement and is not computationally resource-intensive (Purushothaman and Vikas 2018).

2.3.3 EMG Controlled Video Gaming

Controlling video games by means other than keyboards or joysticks is an active subfield of Human-Computer Interface (HCI) research. The literature contains many articles reporting specifically on EMG-based HCI for video game control (Armiger and Vogelstein 2008, Stepp et al. 2011, Van Dijk et al. 2016, Prahm et al. 2018, Garcia-Hernandez et al. 2019, MacIntosh et al. 2020, Marin-pardo et al. 2021, Muguro et al. 2021, Kumar et al. 2022, Oña et al. 2022) [83]–[88]. Some studies use EMG HCI to investigate motor skill acquisition (Kumar et al. 2022), or develop accessible game controls for entertainment (Muguro et al. 2021), but most aim to enhance rehabilitation by using game control as

biofeedback (Stepp et al. 2011, Garcia-Hernandez et al. 2019, Marin-Pardo et al. 2020, Jian et al. 2021, Oña et al. 2022).

In the EMG video gaming literature, many focus on simplified applications that can be used independently at home, enabling exercise prescription monitoring, and increasing motivation in disabled individuals (Garcia-Hernandez et al. 2019, Enciso et al. 2021, Marin-pardo et al. 2021, MacIntosh et al. 2022). Most of these authors use a simple equation-based method that assumes a certain relationship between the signal detected by a particular sensor and user intention. For example, EMG from sensors over the left and right sternocleidomastoid are assigned to variables that scale left and right on-screen movements with neck rotation (Muguro et al. 2021). The same principle is applied for extensor-to-flexor ratios at the wrist (Marin-pardo et al. 2021, Donnelly et al. 2023), and single-sensors over the digit flexors (Garcia-Hernandez et al. 2019), biceps and triceps (Enciso et al. 2021, Jian et al. 2021), and even hyoid and masseter muscles (Stepp et al. 2011, Enciso et al. 2021, Muguro et al. 2021). These schemes control on-screen avatars that users manipulate on the screen to avoid obstacles or match targets. Equation-based approaches are appealing for home use because the opportunity for user error is small. The simple formulas only take one or two sensor inputs, and the placement is simple to replicate, especially when recording locations are standardized for all users. However, this easy implementation comes at the cost of flexibility and therapeutic impact in cases where additional sensors and individualized placement are beneficial (see Section 2.2.2). It is also not simple to modify equation-based schemes since each added sensor must be integrated

into the control formula for an existing or new degree of freedom within the game. This means each new sensor increases the complexity of the game control.

An alternative approach is to use machine learning for videogame control. As we explain in Section 2.3.2, machine learning assigns new EMG feature vectors to one of several previously learned movement classes. Thus, while EMG scales the game inputs continuously in equation-based approaches, machine learning makes class determinations corresponding to discrete control inputs. Studies have shown that this difference is associated with slower but more stable game control when using machine learning compared to equation-based estimates (Muguro et al. 2020, 2021). It should be noted that higher system control speed of is only beneficial for performance to a certain point. Control will be hampered when the position of user-controlled game elements updates faster than the human visual reaction time, which is usually no less than 300 milliseconds (Barbarotto et al. 1998). Indeed, naïve users were more effective in positioning their avatar to intercept falling objects with a slower machine learning versus the much faster equation-based EMG controller (Muguro et al. 2021).

A notable advantage of the machine learning approach is its scalability with respect to the number of EMG sensors. For example, the Myo Armband (Thalmic Labs, Kitchener, Canada) is a popular eight-sensor wearable device frequently used for videogame control with a neural network machine learning classifier (Côté-Allard et al. 2019, MacIntosh et al. 2020, Oña et al. 2022). While this hardware is inflexible (see Section 2B), the machine

learning approach is quite appealing. The number of in-game degrees of freedom determines how many EMG signatures the classifier must learn, but how many sensors contribute to the learning and where they are placed does not impact the game control mechanics. Adding more sensors and placing them appropriately in each case supports more effective control, and the machine learning approach permits this without re-engineering the control scheme.

We were also interested in literature concerning the creation of game environments. Ona et al., developed four different games with the Unity 3D game engine for control with the Myo Armband (Oña et al. 2022). Similarly, Armiger et al. (Armiger and Vogelstein 2008) modified a Guitar-Hero 3 controller (GH3; Activision, Santa Monica, CA) to take external inputs from a computer running EMG pattern classification on the forearm. Unlike the Myo Armband, six-to-eight unfixed EMG sensors were placed around the forearm to detect the finger movement patterns that controlled the game. Not only did these authors avoid restricting the number or configuration of the sensors, but they also made use of existing game software. Notably, many do not take advantage of pre-developed games, instead building custom games from scratch using game development software (Garcia-Hernandez et al. 2019, Enciso et al. 2021, Marin-pardo et al. 2021, Muguro et al. 2021, Oña et al. 2022). Of course, hacking a commercially available game controller may not be feasible for many researchers, but there are many open-source PC games available that are no less engaging and immersive than ones created from scratch by (even very talented) researchers. Games do not need to be complicated or have advanced graphics. Basic arcade-type games

are intuitive and often addicting, and they feature simple game logic, which is important when access to coding expertise is limited. There are many open-source GitHub repositories with scripts in C, Python, and JavaScript that create simple but engaging games like Pong, Space Invaders, Pacman, Tetris, or Snake. With a simple internet search, we were able to quickly find GitHub repositories with ready-made games written in Python (Bedi 2016, Kim 2017, Tated 2019, Biswas 2021, Sharma 2021).

2.4 The Biofeedback Algorithm

In the following, we describe our proposed design of a biofeedback system guided by our objectives from Section 2. As is common, we distinguish two phases, the initial training/calibration phase and then the actual gameplay phase. We decompose the system into several sub systems. The raw data from the EMG sensors is filtered and the features are extracted generating the feature stream. During training a feature reduction is learned that leads to a simple mean-based (Gaussian) classifier. Finally, during gameplay the classifier converts the control stream into game commands. In the following we describe these steps in detail.

2.4.1 Sensors

An EMG acquisition setup that can transmit digitized signal from at least four EMG sensors to a PC is required for our approach. Including more sensor channels enables multi-muscle recording that is more effective in identifying movement patterns. Appropriate sensor placement and type depends on the biofeedback scenario, but general best practices in this

area have been developed and should be considered (Hermens et al. 2000). To support biofeedback adaptability, sensors should not be fixed in a configuration that constrains their independent placement (see Section 2.2.1). Traditional laboratory EMG acquisition setups that include modules for differential amplification, analog low- and high-pass filtering, and analog-to-digital (AD) conversion, are generally acceptable. As is common, we band-pass filter between 20 and 400 Hz (2nd order Butterworth) and sample at a rate of $FS = 4$ kHz.

2.4.2 Feature Extraction

As described in Section 3B, we use a feature extraction approach. To generate the feature stream, we use a sliding window of size $N = 256$ samples (64 milliseconds) with a window hop of $N/2$ (128 samples; 32 milliseconds). For the features themselves, we choose a small set of features that results in the desired performance. For each window, and for each channel, we compute 4 features: root of the mean squared values (RMS), waveform length (WL), number of zero crossings (ZC), and slope sign changes (SSC). The exact formulas of these features are given below:

$$RMS = \sqrt{\sum_{k=1}^N x^2} \quad (1)$$

$$WL = \sum_{k=1}^{N-1} |x_{k+1} - x_k| \quad (2)$$

$$ZC = \sum_{k=1}^{N-1} f(x_k x_{k+1}) \quad (3)$$

$$SSC = \sum_{k=1}^{N-1} f(x_k - x_{k+1}) f(x_{k+1} - x_k) \quad (4)$$

where $f(x) = 1$ if $x \geq \epsilon$

The feature stream now has a dimension of 4 times the number of channels and $FS/(window\ size/2)$ data rate.

2.4.3 Machine Learning

The machine learning setup in the case of EMG signal from 4 sensor channels is depicted in Figure 2.4. Given our objectives, we aim to create a simple and reliable classifier. The feature stream captures the information we require; we need only to classify. During training, we collect a set of K feature vectors for each of the movement classes. These feature vectors are highly correlated within and across the different movement classes. We work with the assumption that the distributions are Gaussian. The objective is to project the feature vectors into a low-dimensional, de-correlated subspace that maximizes the separation between the movement classes. We chose to perform multi-class linear discriminant analysis for reasons discussed in Section 2.3.2 on *Feature Reduction*. LDA is a supervised dimensionality reduction method; we have labeled samples for each of the movement classes. Mathematically, LDA projects into a subspace maximizing the separation of the classes by maximizing the projected variances of the class means. This results in a matrix A of the most significant eigenvectors. This matrix is then used to project the feature vectors into a de-correlated subspace by computing $A:f_n$, where f_n is the n^{th} feature vector. The algorithmic details of LDA are beyond the scope of this publication, and not needed, we can use this algorithm as a black box (Yu and Yang 2001).

After de-correlation, the classification is simple. We assign each sample to the class whose mean is the closest in terms of the Mahalanobis distance (the distance to the mean of the class) (Mahalanobis 1936), often referred to as naïve Bayesian classification.

2.4.3 Game Control

To stabilize the classifier output, we perform a 5-1 voting reduction such that the vote over five consecutive values in $f(n)$ determines the control input to the feedback interface. Therefore, the resulting control stream $c(n)$ has a rate of $FS/[(N/2) * 5] = 6.25\text{Hz}$. The control stream $c(n)$ replaces game inputs usually provided by a controller such as a keyboard, allowing the user to interact with a videogame interface by mapping each of the movement classes to a controller event.

We acknowledge that the control rate for videogames is traditionally much higher than 6.25 Hz, typically on the order of 60 Hz. This could be improved by choosing a smaller window size, for example, by reducing the window size from 64ms ($N=256$) to 16ms ($N=64$) for a control rate of 25Hz. However, this will likely not make a very perceivable difference because 64ms is already well below the typical human visual response time. At the same time, including fewer samples in each window introduces risk of sacrificing control stability.

It is also important to note that the system is designed for therapeutic treatment and not as an alternative interface for a video gamer. This means that, while there might be faster ways

to interact with a game, the true goal is that the participant generates specific EMG signals resulting from prescribed muscle movements. During development, we noted that physical keys are automatically released after being struck whereas, in our application, inputs continue after the initial command at a rate of 6.25Hz. To prevent the occurrence of unwanted command repeats before the user has time to react to the initial input, we suppressed any repeated game input occurring at a latency shorter than 400ms. This approach is also motivated by the therapeutic goal, the interaction is designed to repeat movements, not to have a fast game play.

2.5 Implementation

To verify our approach and demonstrate our algorithmic framework, we implemented an application for therapeutic rehabilitation using 4 EMG sensors placed on the lower arm to play the popular game of Tetris. In this section we describe our acquisition setup, and realization in code implementation. To promote the accessibility of replication as to objective 3, we make use of widely available low-cost technology and public domain software libraries. We chose Python as our programming language due to its popularity and the availability of open-source games, machine learning libraries, and capacity to interface with EMG hardware.

2.5.1 EMG Acquisition Setup

We used a 4-channel acquisition setup with the TMSi SAGA high-density EMG device (TMSi Ltd. Oldenzaal, Netherlands). The device features on-board AD conversion, so

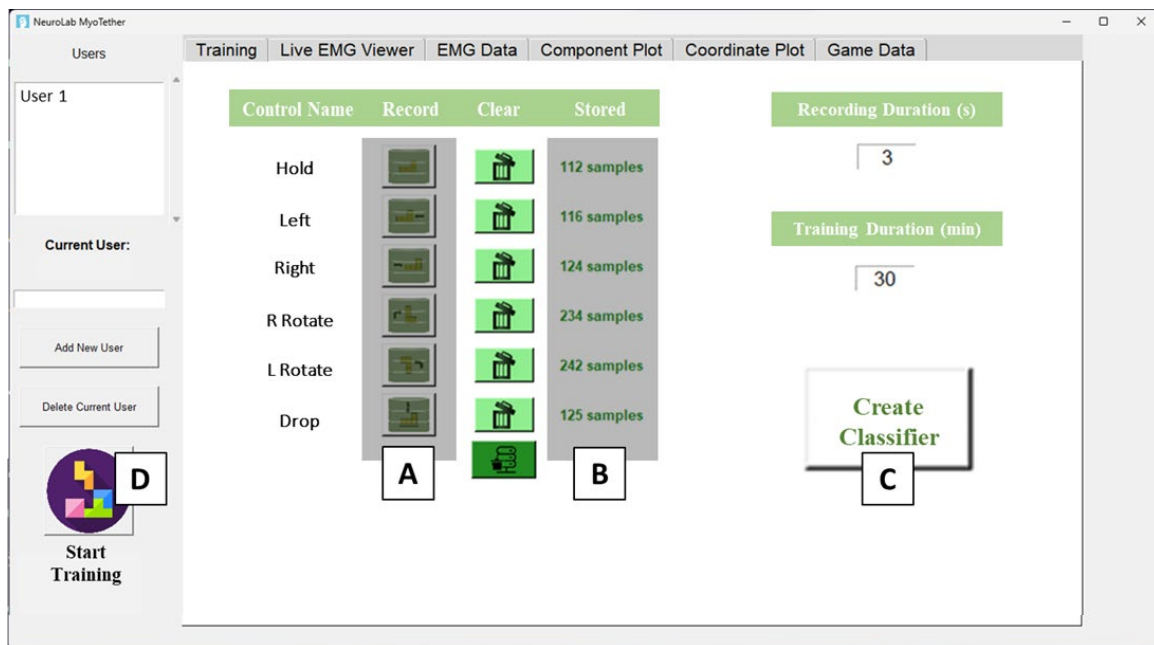


Figure 2.1: Graphical User Interface

The graphical user interface is designed to coordinate data collection (A) and storage (B), machine learning (C), functions that enable gameplay which is accessible via the “Start Training” button (D).

unfiltered, digitized EMG data is streamed directly to a PC through USB connection. The signal is recorded from pre-gelled Ag/AgCl adhesive EMG electrodes placed in a bipolar configuration over user-relevant muscles for each user. Study-specific sensor placements are described in Section 6, but this setup is generally designed to accommodate the sensor placement decisions of an expert therapist or researcher.

2.5.2 Realization in Code

We use the PyCharm integrated development environment (IDE) (JetBrains s.r.o) and Python’s basic library combined with various (open source) signal processing, machine learning and graphics libraries. In the following we provide the technical details. Digitized

EMG values are accessible during and after recording through a data queue, which is registered as a client of the TMSi application programming interface. Our simple graphical user interface (GUI) is created using Tkinter (Lundh 1999) to coordinate the recording, storage, and visualization of EMG data (Figure 2.1). Data storage and manipulation used NumPy (Harris et al. 2020), and visualization used Matplotlib (Hunter 2007). Band-pass filtering and feature extraction are performed using the Signal module of the SciPy library (Virtanen et al. 2020). For the LDA and GNB functions described in Section 3B2, the Scikit-learn library (version 1.2.2) (Pedregosa et al. 2011) is used. The classification outputs of the GNB module controls a videogame managed by PyGame (Shinners 2011) modules.

The GUI enables the user to record EMG data for each of six different movement tasks (Figure 2.1A). Upon recording, features are extracted from the data, and the resulting set of feature vector samples is labeled and stored (Figure 2.1B). The “Create Classifier” button (Figure 2.1C) performs LDA and fits the classifier model using the stored samples as prescribed in Section 4C. To achieve this functionality, we use the Scikit-learn packages for multi-class LDA, and GNB classification.

Specifically, we create an instance of the `LinearDiscriminantAnalysis` (Scikit-learn Developers 2023) object class, which we will refer to as the LDA object. Stored feature vectors and their labels are passed into the LDA object’s `fit` method, which performs the multiclass LDA. After fitting, the LDA object contains the matrix of eigenvectors A (see

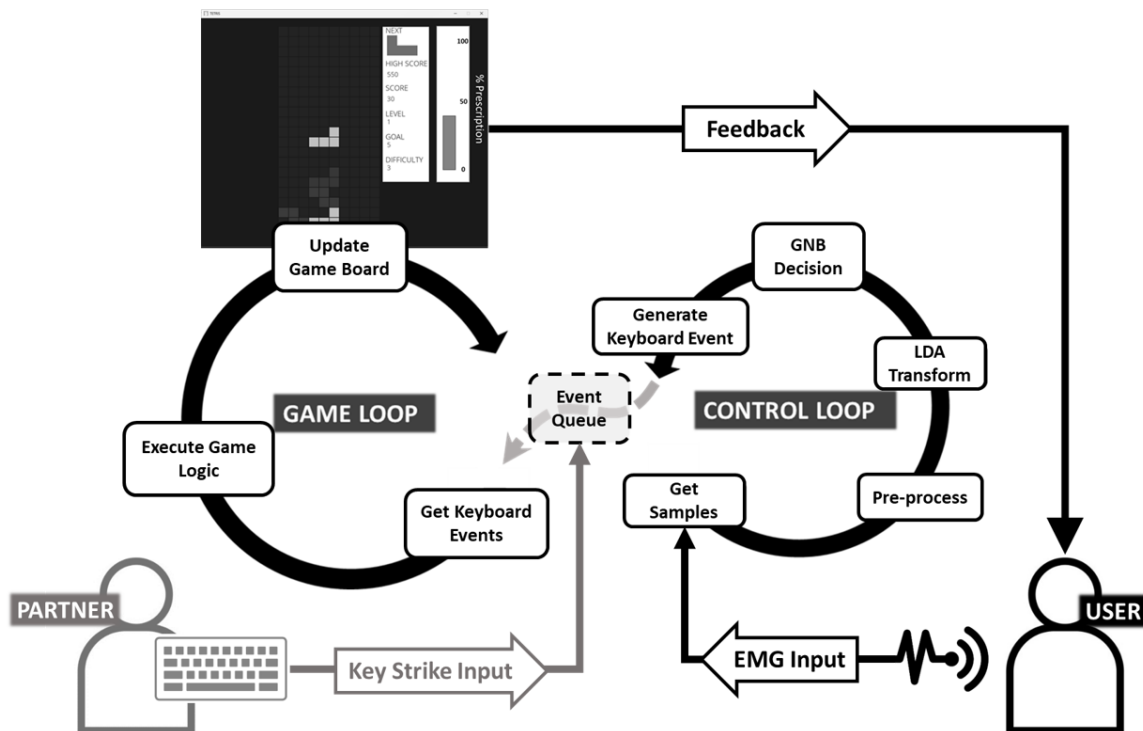


Figure 2.2: Game Control Schematic

A schematic game control procedure implemented Python code. The Control Loop samples data from the EMG device and performs operations to obtain movement classification decisions and generate corresponding keyboard events. Keyboard events are registered in the PyGame Event Queue, from which they are retrieved and handled by the pre-programmed PYTRIS Game Loop. The game loop executes the game logic and updates the game board, providing the user with feedback. The control scheme also accepts key strike inputs, allowing some game degrees of freedom to be controlled by a partner when necessary.

Section 2.4), which can transform new feature vectors in real-time when they are passed into the LDA object’s transform method. The procedure initiated by the “Create Classifier” button also creates an instance of the GaussianNB (Scikit-learn Developers) object class, which we will refer to as the GNB object. The GNB object creates a trained classifier when labelled feature vectors are passed into the fit method. The fitted GNB object takes transformed feature vectors into the predict_proba method during live gameplay and returns the likelihood of each possible movement task being performed. Once the LDA and GNB

objects are fitted, the user can open the game interface by pressing the “Start Training” button (Figure 2.1D).

We create the live videogame module by modifying an open-source Tetris game, called PYTRIS (Kim 2017). The object of the game is to control the position and orientation of falling geometric shapes (i.e., blocks) so that they stack in complete rows at the bottom of the game board. The original game is controlled by key strikes, so we mapped EMG signal classifications to virtual key strikes that correspond to the original controls.

In Figure 2.2, we show how EMG signal input controls the PYTRIS videogame. We use the pynput library (Palmer 2022) to create virtual keyboard events within a “control loop” (right) which are received by a “game loop” (left) by way of the PyGame event queue. Notably, the event queue may still receive input from real key presses. If there are too few sensors or the user’s impairment is too severe for reliable classification of six EMG patterns, the classifier can be trained on fewer movements and real keyboard events can be used to control the residual degrees of freedom. The key presses could be performed by the user, or by a partner in a collaborative gameplay scenario.

The unprocessed data that is sampled from the device in the control loop is also stored for future processing.

2.6 Validation in Healthy Volunteers

To validate our design approach, we assessed the system's classification accuracy and the stability of real-time control during PYTRIS gameplay. To generalize our findings to populations having bilateral motor deficits affecting the lower and upper limbs, we tested our approach in an individual with advanced multiple sclerosis (MS), in addition to healthy volunteers.

2.6.1 Participants

All participants were taking part in an ongoing investigation of individualized EMG biofeedback in individuals with multiple sclerosis. We conducted additional analyses on data that were collected during system calibration and intervention tailoring sessions for this study. All participants provided written informed consent to all procedures, which were approved by the Hamilton Integrated Research Ethics Board (HiREB project #16009).

We analyzed data from 5 healthy volunteers (3 males and 2 females, 25-29y) who are also members of our laboratory, and one 57-year-old female with a clinical diagnosis of primary progressive MS with a 28-year disease duration. All participants were right-handed.

The volunteer with MS scored 7.0 on the Kurtzke Expanded Disability Status Scale (EDSS), which was associated with limited walking ability, restriction to a wheelchair most of the day, and difficulty maintaining a standing posture for extended duration. Modified Ashworth Scale (MAS) scores indicated increased resistance to passive stretch in both left

and right knee flexor muscle groups with MAS scores of +1 and 1, respectively. Increased resistance was also present in both the dorsi-flexors and plantar-flexors at the right ankle with a score of 2 for both joint movement directions.

2.6.2 Movements and Sensors

Since many applications involve improving upper limb function, we used movements of the hand and forearm to validate our approach in healthy volunteers. Six movement tasks were: rest, wrist flexion and extension, hand supination, hand pronation, and finger abduction (splaying). The tasks corresponded to the game controls for: No Input, Left, Right, Rotate Right, Rotate Left, and Drop, respectively. To capture relevant muscle activities, we recorded signals from the right forearm over the Flexor Carpi Radialis (FCR), Pronator Teres (PrT), Extensor Digitorum Superficialis (EDS), and Anconeus (AN). The movements are shown in Figure 3.

To demonstrate the system's adaptability when providing deficit-specific feedback, for the volunteer with MS we tailored the training movements and corresponding muscle recording sites using specific training needs. The individual described difficulties maintaining balance while walking and poor postural stability when standing upright and completing tasks that involve reaching, grasping, and manipulating objects. We reasoned that this individual would benefit from exercises that involve coordinating intentional shifts in the center of mass with the execution of upper limb tasks while standing. Five movement tasks were used to control the gameplay including: neutral stance, shifting center of mass over

right foot, shifting center of mass over the left foot, right grip squeeze, and left grip squeeze.

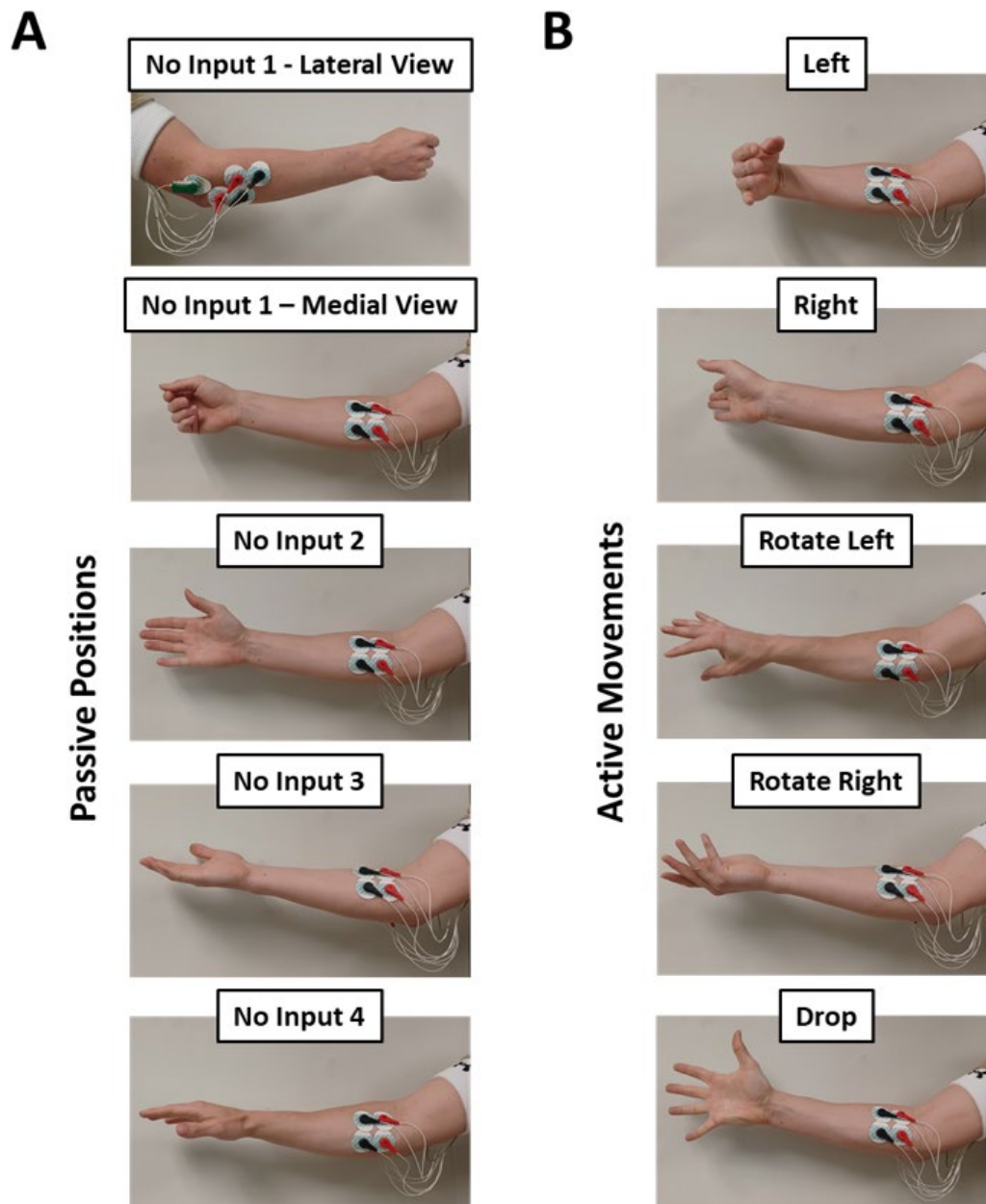


Figure 2.3: Calibration Movements and Positions

Panel A. Passive positions during which 2 seconds of data was recorded to train the No Input classification. No Input 1 is shown in both the medial and lateral view to make the electrode placement visible. Panel B. The active movements during which 8 seconds of data were recorded to train the Left, Right, Rotate Left, Rotate Right, and Drop classifications.

Grip squeeze movements were performed by applying force to silicone 9kg grip strength trainers (GoZone™). The tasks corresponded to the game controls for No Input, Left, Right, Rotate Right, and Drop, respectively. The Rotate Left control was omitted to simplify the game control scheme and support classifier performance. To train the Gaussian classifier, we recorded signals from the right and left Vastus Lateralis (VL) and left and right FCR muscles. To ensure safety during the exercise, the movements were performed with a support bar in front of the participant and a wheelchair positioned directly behind.

2.6.3 Calibration Procedure

For the healthy volunteers, eight seconds of data was recorded during each of the movement tasks. For the active movements (i.e., not rest), participants were instructed to rotate the hand clockwise or counterclockwise, flex or extend the wrist, or splay the fingers for the duration of the recording. In each case, the participant was instructed to perform the movement once, holding the end position and actively working against the limit of their range of motion until the recording was finished. The researcher began the recording after the onset of movement.

For the “rest” task, we segmented the recording into four 2-second intervals using different passive positions that we observed during pilot testing when users intended to invoke “No Input”. This was implemented since users were unable to reliably invoke “No Input” during gameplay if the hand was completely relaxed in a continuous 8-second calibration recording. Typically, the hand was held with the fingers slightly extended with the wrist neutral and forearm in supination or pronation depending on the most recent movement. Thus, the “No Input” data included two seconds in each of the following four poses: hand relaxed with the palm facing towards the midline, fingers extended and palm facing toward the midline, fingers extended and palm facing down, and fingers extended and the palm facing up (Figure 2.3A). In contrast to the active movements (shown in Figure 2.3B), we instructed the volunteers to maintain each position passively by avoiding movement during the recording. The EMG signal acquired from healthy participant 1 during each of the prescribed movements is shown in Figure 2.4A.

For the MS participant, 12 seconds of data were recorded for each of the 5 control movements. This larger sample size was required to support stable classification because both left and right knee extensors are active during rightward and leftward shifts of the torso. Depending on the anterior-posterior position of the center of mass during left and right shifts, different patterns of bilateral knee extensor activation may be observed. Thus, Right and Left calibration data were each collected in three separate 4-second intervals where the volunteer shifted her hip over the toe, over the mid-foot, or over the heel. The volunteer was instructed to stand in a neutral position with trunk centered between the feet

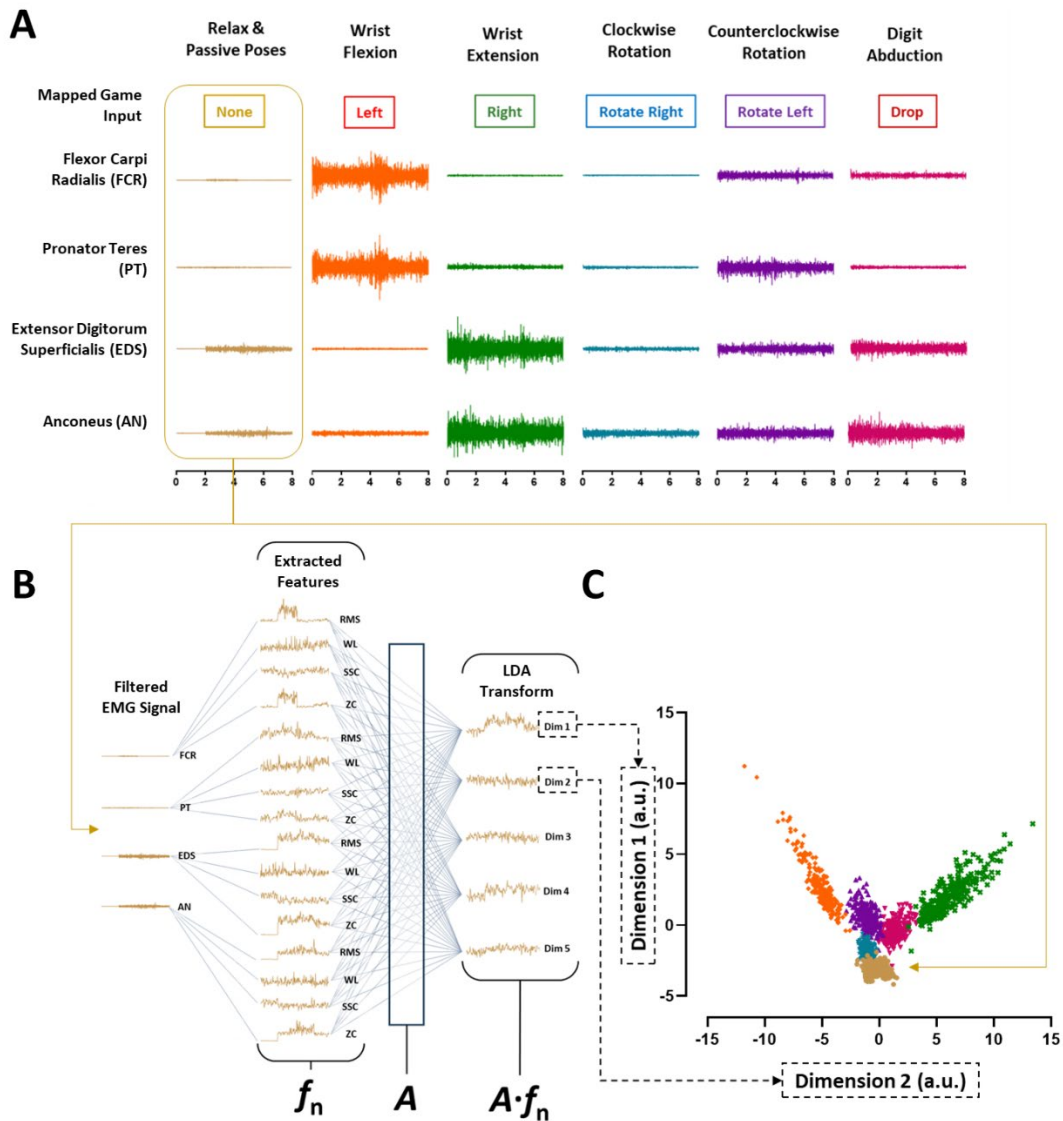


Figure 2.4: Calibration Processing Pipeline

Panel A. EMG data collected from muscles of the right forearm during chosen training movements in a representative healthy volunteer. The data is labelled according to the movement performed above each 8-second interval, and the colors further identify the 6 corresponding game control inputs. Panel B. The processing procedure applied to the filtered data acquired during calibration or live gameplay is illustrated. Four EMG signal features, including the root of the mean squared values (RMS), waveform length (WL), number of slope sign changes (SSC), and number of zero crossings (ZC), are extracted from each channel. The resulting 16-feature stream f_n is transformed by the eigenvector matrix A obtained by linear discriminant analysis (LDA) into the 5-dimensional space ($A \cdot f_n$). Panel C. The calibration data are represented in the two most prominent dimensions.

during the No Input recording, to squeeze the right grip trainer during the Rotate Right recording, and to squeeze the left grip trainer during the Drop recording. These three controls were collected in continuous 12-second intervals.

2.6.4 Performance Outcomes

To assess the performance of our classification method, we performed a 5-fold cross validation evaluating overall accuracy and the precision within each class. Accuracy is the percentage of all class predictions that are made correctly, and precision is the percent of assignments to each class that were made correctly (i.e. the true positive rate). This is a standard validation approach, but the validation sets are random subsets of the calibration data and do not necessarily capture novel patterns that arise spontaneously during unconstrained gameplay.

Therefore, we also recorded the portion of classifier decisions that agreed with the majority decision (i.e. in the 5 in 1 voting reduction) during gameplay. This was expressed as a value between 0.4 (2 of 5; the minimum for a majority decision to be made) and 1.0 (5 of 5; complete agreement) and called the “portion in agreement” (PIA). For the healthy controls, PIA was calculated over 10 minutes of continuous gameplay. The MS participant became too fatigued to continue after 4 minutes of gameplay, and so this shorter interval was used to compute the PIA.

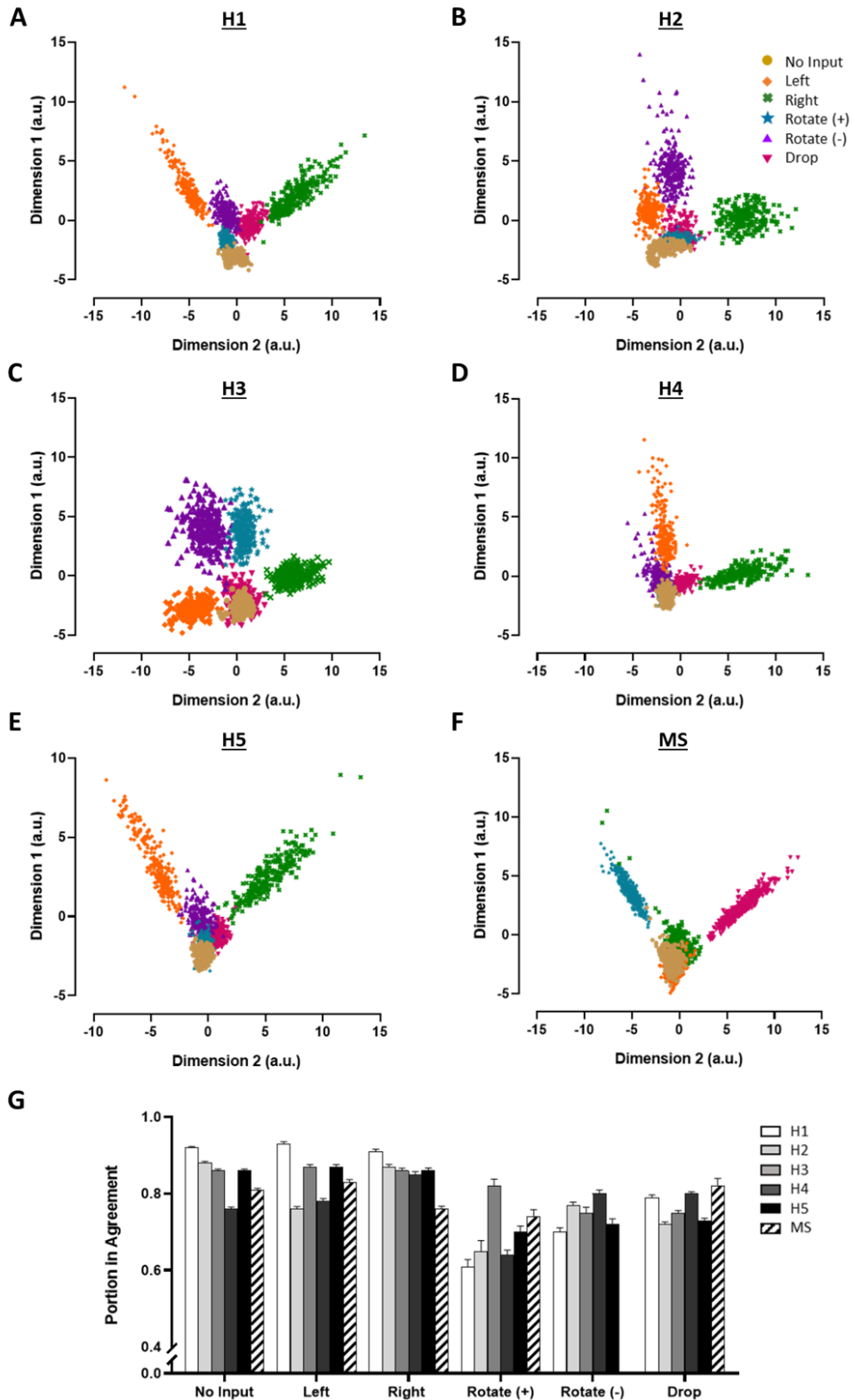


Figure 2.5: Calibration and Training Data

Panels A through F show the calibration data for each healthy volunteer and one volunteer with MS a coordinate space defined by the two most prominent dimensions of the LDA transform. The data is plotted in arbitrary units because each dimension is the linear combination of feature vector elements measured in different scales. Panel G shows the portion in agreement (PIA) during 10 minutes of gameplay for the healthy volunteers and 4 minutes of gameplay for the MS volunteer. The PIA is expressed as value that can range between 0.2 and 1, where 1 indicates 100% agreement (5 of 5 votes agree) and 0.4 indicates 40% agreement (2 of 5 votes agree). Error bars represent the standard error of the mean (SEM).

Table 2.1: Accuracy and Precision Metrics

Participant	Accuracy	Precision					
		No Input	Left	Right	Rotate Right	Rotate Left	Drop
H1	99.15 (0.40)	97.41 (2.04)	100.00 (0.00)	99.23 (1.05)	98.81 (1.78)	100.00 (0.00)	99.61 (0.40)
H2	93.56 (1.45)	92.63 (2.09)	99.22 (1.06)	99.62 (0.86)	80.47 (6.98)	98.48 (1.58)	93.98 (1.45)
H3	99.03 (0.46)	99.61 (0.88)	100.00 (0.00)	100.00 (0.00)	100.00 (0.00)	99.23 (1.05)	95.55 (2.09)
H4	93.54 (1.77)	94.55 (1.62)	93.89 (5.62)	98.11 (2.67)	87.88 (4.58)	95.47 (2.93)	92.48 (4.58)
H5	96.91 (0.71)	96.58 (2.80)	98.85 (1.70)	99.22 (1.75)	93.64 (3.45)	98.33 (1.75)	95.42 (3.45)
Avg	96.44 (2.78)	96.16 (2.68)	98.40 (2.57)	99.26 (0.71)	92.16 (8.11)	98.30 (1.72)	95.41 (2.78)
MS	91.59 (1.00)	80.47 (5.05)	89.60 (3.81)	89.90 (2.63)	98.54 (1.57)		100.00 (0.00)

Accuracy and precision metrics obtained from the 5-fold cross-validation procedure. Accuracy is the percent of correct class predictions when all control movements are considered together. Precision is the percentage of samples classified into each movement class correctly (i.e., true positives). For each volunteer, the parentheses contain the standard deviation of the accuracy and precision measures over 5 splits. The average and standard deviation of the metrics across the five healthy volunteers (H1-H5) is shown in bold.

2.6.5 Results

Figure 2.5 shows the 2 most prominent dimensions of the LDA transform for each of the volunteers in panel A through F. Visually, there is a shared pattern across the healthy

participants. The No Input class has the tightest clustering, and the Right and Left (wrist extension and flexion) have the greatest variance and the most separation from each other, and the rotation controls (Rotate Right and Rotate Left) exhibit poorer separation. In Figure 2.5F, the LDA transform for the MS volunteer shows the No Input, Left and Right controls are poorly separated compared to the Rotate Right and Drop movement patterns. It should be noted that poor separation in the two dimensions plotted in Figure 2.5 does not preclude good separation in the other dimensions which are not shown. For the healthy volunteers, 3 dimensions are not visually represented, and 2 dimensions are absent from the MS participant plot.

The classification accuracy and the precision for each movement class are reported in Table 2.1. Our Gaussian classification model is accurate with an average accuracy near of 96% for the healthy volunteers and 92% for the MS volunteer. For the healthy volunteers, the classifier performs best with the Left, Right, and Rotate Left classes having precision scores of 98%, 99% and 98%, respectively. For the MS volunteer, the performance was best for the Drop and Rotate Right classes with 100% and 99% precision, respectively. The poorest classification performance was demonstrated in the MS participant with precisions of 80%, 90% and 90% for No Input, Left, and Right.

2.7 Discussion

We identify user motivation, capacity to incorporate many sensors over distributed muscles, and accessibility and reproducibility as essential EMG biofeedback system qualities. We

also describe our development and preliminary testing of a system that realizes these qualities. The system uses simple machine learning with feature extraction and linear reduction classification that can integrate any number of sensors without constraining their placement. While our approach could be replicated in other languages, we implement our method in Python, which is the most widely used language. Further, our approach can be implemented with any off-the-shelf EMG system featuring a Python API, which is common for modern devices.

In a limited validation study, we found that the open-source packages available in Python provided the necessary functionality to create a stable system that demonstrated good classification performance. The poorest classification accuracy was 92%, which was observed for the individual with advanced MS, and this is on par with other published classification schemes (Khan et al. 2020). Of course, our application cannot be directly compared to any one example in the literature, because the sensor placements and movements were chosen to address the specific need of our volunteer, and not to replicate an existing paradigm.

We also assessed classification stability during gameplay using the portion of voters in agreement during the majority voting procedure (PIA). We found agreement between the precision scores obtained by cross-validation and PIA for some classes, but not others. The lowest precision scores and PIA values were both observed for Right Rotate, and both metrics were low for the Drop class as well. An association between precision and PIA is less clear for the other 4 classes, probably reflecting incongruences between the patterns of

activation elicited by cues during calibration and the user-initiated patterns observed during gameplay. Overall, no class demonstrated an average PIA less than 0.6 (3-of-5 agreement), and the mean value was 0.77 (4-of-5 agreement). We interpret these findings as suggestive of relatively stable classification during gameplay.

Importantly, cross-validation and stability values that we observed are not generalizable to all scenarios where our design may be implemented, as these could involve an infinite variety of sensor locations, movements, or even acquisition hardware. Rather, we show that it is feasible to obtain functional classification with our approach in the specific scenarios that we describe. Future studies will need to validate the adaptability of our approach more thoroughly in diverse application scenarios.

We did not address electroencephalography (EEG)-based brain-computer interfaces (EEG-BCI) although they have a related application and much of our discussion is also relevant to such systems (Hosseini et al. 2021). The potential of EEG-BCI in allowing users to interact with objects (via a computer) despite severe or complete paralysis is promising and exciting. However, the modality of EEG presents several complications that will hamper widespread adoption of EEG-BCI in the short-term. Electrode caps are time-consuming to prepare in a context where time is limited (i.e., ~1h physiotherapy treatments). The EEG signals are also recorded through many tissue layers and their quality is influenced by uncontrollable factors like user skin characteristics and hair. The signal is also highly sensitive to environmental noise and facial muscle activity. Overcoming these elements

requires training and technical expertise that is not yet widely available. A lack of competency is a translational barrier for EMG techniques in general (Campanini et al. 2020), but the EMG biofeedback approach that we propose is much less technically challenging. The electrical signal produced by superficial muscles is much larger in amplitude and therefore is robust to artifacts such as environmental noise, and sensors can be appropriately applied with the basic musculoskeletal anatomy knowledge common to most clinicians. The EMG signal collected during calibration is easy to interpret visually since the idea of a muscle being “on” or “off” is quite intuitive. In contrast, EEG traces represent weighted contributions from many neuronal generators and require considerable neuroscience expertise to interpret. The main implication of these contrasts is that independent troubleshooting is feasible for an EMG biofeedback system in most clinical contexts, but the same is probably not true for EEG-BCI. For these reasons, focusing efforts on the development of accessible EMG biofeedback systems will likely have a greater impact on rehabilitation outcomes.

Our approach provides an avenue for rehabilitation researchers to develop client-centered rehabilitation procedures, while also studying the rehabilitation process. The EMG data used for classification and game control is also saved for later review and analysis and can be compiled into databases that can be used to establish population norms and interpret changes in EMG signal patterns that may develop within a training session or over the course of a training intervention. Importantly, these benefits can only come about with broad clinical acceptance of EMG biofeedback technology. This work has proposed, and demonstrated the execution of, useful strategies towards this goal.

2.8 Conclusion

The usefulness of EMG biofeedback as a tool in neuro-rehabilitation settings is becoming clearer, but further progress is needed to push the technology into common use. We designed and tested an EMG biofeedback system prioritizing multi-sensor integration, user motivation and engagement, and researcher accessibility. The study provides a design template for researchers who wish to develop and evaluate a “gold-standard” EMG biofeedback method.

Chapter 3: Study 2

In Chapter 2, I describe the design and implementation of a classification-based multichannel EMG biofeedback system that can be applied in any of the use scenarios described in Chapter 1, Section 3. A key feature is the ability to tailor training movement paradigms the specific needs of a user, which is especially advantageous for patients with severe and heterogeneous patterns of motor impairment. Moreover, the classification-centered approach provides opportunity to closely monitor interactions between the user and the feedback algorithm to uncover useful information about the quality and dose of feedback training being delivered. In Chapter 2, a single session revealed that a standard sensor and movement scheme can be implemented effectively in healthy subjects. I also demonstrated the single-session effectiveness of a tailored scheme in one individual with multiple sclerosis. In Chapter 3, I create tailored sensor and movement schemes to the needs of participants with severe neuromuscular dysfunction resulting from MS and explore their feasibility over a multi-session intervention. The study explores important considerations for interpreting measurements derived from the classification record and identifies to facilitate their clinical utility.

Stability and Accuracy of Classification-Based EMG Biofeedback in Three Multiple Sclerosis Patients

Abstract

Electromyography (EMG)-based biofeedback can facilitate high volumes of volitional muscle activity (i.e., exercise) in individuals with severe motor impairments. Biofeedback

systems based on EMG classification can integrate activities from multiple sensors in a way that is flexible and scalable, allowing the selection and number of trained muscles to be tailored. The classification record can also provide insights about the quality of the biofeedback and training dose. We previously designed and tested a classification-based system within a single session. In this study, we explore the feasibility of a tailored 6-week intervention in 3 participants with advanced MS symptoms. Participants attended up to 3 sessions every week for 30 minutes of training. For two participants, the training was divided into two 15-minute blocks with separate tailored schemes. We thus attempted to implement five tailored classification-based EMG biofeedback interventions. The primary success criteria for implementation were: 1) creation of accurate classification models, and 2) participant ability to successfully interact with the biofeedback for the 15- or 30-minute training duration. Four of the five interventions were successful with typical classification accuracy above 95% and stable feedback control achieved during all training sessions. One intervention was not successful, having a median accuracy of 86% and failing to achieve meaningful feedback control in 3 of 7 sessions. This work is the first to demonstrate classification-based EMG biofeedback in MS patients with severe impairment. Future work should develop frameworks for efficient biofeedback personalization and determine normative values to enhance the interpretation of the classification record.

3.1 Introduction

Biofeedback therapies transform physiological or mechanical sensor data into engaging visual or auditory stimuli to facilitate therapeutic exercises in impaired populations

(Giggins et al. 2013). Biofeedback systems that use electromyographic (EMG) sensors transform the electrical potentials that determine whether muscles are active or at rest. These muscle potentials can be generated and controlled even by individuals with serious motor disorders that prevent them from engaging in traditional therapeutic exercises. Reduced range of motion, extreme weakness, poor coordination or dexterity, and inability to independently stand or ambulate do not prohibit participation in EMG biofeedback training.

Traditionally, EMG biofeedback is transformed using an “equation-based” approach. Values from EMG sensors are assigned to corresponding variables within a feedback control equation that continuously scales the position, size, or color of visual feedback objects (Davis and Lee 1980, Van Dijk et al. 2016, Prahm et al. 2018, Garcia-Hernandez et al. 2019, Cikajlo et al. 2021, Dost Sürücü and Tezen 2021, Enciso et al. 2021, Jian et al. 2021, Marin-pardo et al. 2021, Muguro et al. 2021). Equation-based biofeedback systems typically integrate one or two sensors that are placed at standardized recording sites making them simple and accessible, but also inflexible. Single-sensor systems can only train one muscle group at a time (Stepp et al. 2011, Garcia-Hernandez et al. 2019), and multi-sensor equation-based systems assume a fixed number of sensors and certain target muscles (Jian et al. 2021, Marin-pardo et al. 2021, Donnelly et al. 2023). Adjusting any of these parameters requires adjusting the equation. We have argued that “classification-based” EMG biofeedback methods are more impactful (Toepp et al. 2023). Classification-based methods combine values from any number of sensors into a single “feature vector” which

is classified by a machine-learning model. The assigned class corresponds to one of several discrete feedback outcomes, such as a controller command in a video game. For example, training may require users to generate muscle activity patterns that invoke certain class decisions with a predefined order and timing, similar to the popular “Guitar Hero” video game (Armiger and Vogelstein 2008, Oña et al. 2022).

Classification-based feedback does not require adherence to standard sensor locations and training tasks that involve certain muscles. Rather, the sensors must capture differences between the discrete muscle activity patterns being trained to support accurate EMG classification. Whether accurate classification can be reliably achieved is critical to classification-based EMG biofeedback’s feasibility, particularly in the face of serious neuromuscular impairment. The efficacy of EMG classification has been studied in individuals with cerebral palsy (CP) (MacIntosh et al. 2022), stroke (Lee et al. 2011b, Cesqui et al. 2013, Lu et al. 2019b, Song et al. 2022), and spinal cord injury (SCI) (Liu and Zhou 2013, Jordanic et al. 2016, Jordanić et al. 2016, Lu et al. 2019a, Jaja et al. 2021), and accuracy is found to vary considerably depending on the level of impairment. Accuracy was 37-83% in stroke patients when classifying movement in 4 directions during robotic arm training (Cesqui et al. 2013), and 34-97% for 6 hand gestures in stroke (Lee et al. 2011b, Lu et al. 2019b) and SCI (Lu et al. 2019a). Notably, these were standardized paradigms where a limited number of sensors (6 to 10) were placed consistently without consideration for individual impairments. In contrast, when studies used large arrays of tens or hundreds of sensors and weight each sensor according to its classification importance,

accuracy was consistently above 80% in stroke and SCI (Zhang and Zhou 2012, Liu and Zhou 2013, Jordanić et al. 2016). Large sensor arrays are not widely accessible, so identifying recording sites that support stable classification is an important activity and a significant contributor to feasibility.

Using an appropriate number of discrete training tasks is also significant. Studies in neurologically impaired individuals often test classification of as many forearm and hand muscle patterns as possible because the aim is to develop sophisticated control of robotic prosthetic devices (Zhang and Zhou 2012, Liu and Zhou 2013, Lu et al. 2019b, Song et al. 2022). However, biofeedback for therapeutic exercise need not involve more than a few carefully selected training movements. This is illustrated by Macintosh and colleagues, who achieved 86% accuracy during a 4-week training period in children with cerebral palsy using the Myo Armband with only 3 training movements (MacIntosh et al. 2021). These authors also identified a “primary target” gesture which was wrist extension with open fingers. This introduced the idea of combining one or two primary movements with less therapeutically relevant movements that are designed to support accurate EMG classification. For example, if the primary target is a gesture with the paretic hand, secondary training movements using the unaffected hand, or lower limbs present an easier classification challenge versus secondary movements being different movements of the impaired hand. This introduces yet another dimension of flexibility featured by classification-based EMG biofeedback.

Our recently published classification-based system supports the desirable features described above with just four EMG channels, which is a broadly accessible level of instrumentation (Toepp et al. 2023). In a small sample of healthy controls and one individual with primary progressive multiple sclerosis (MS) affecting the lower limbs, we observed good classification accuracy and stability during a single session. However, reproducing these findings in individuals with severe motor impairment over many training sessions is required to establish feasibility. It is essential to demonstrate the modality's robustness in the face of the muscle weakness, hypertonia, spasticity, and discoordination.

Individuals with multiple sclerosis (MS) expressing advanced motor symptoms are excellent test cases for classifier-based EMG biofeedback. While initial MS presentation varies, inflammatory damage eventually overwhelms the body's native repair mechanisms leading to progressive loss of motor function (Olek 2021). Progression of the disease coincides with reduction in physical activity, despite evidence for neuroprotective effects of exercise (Motl et al. 2005, 2017, Guo et al. 2020). In the later stages, MS patients exhibit challenging motor symptoms that prohibit traditional exercise, such that EMG biofeedback has potential to make significant impact by providing an accessible exercise modality.

In the present work, we examine the performance of our system in the context of a multi-week intervention targeting neuromuscular impairment in three individuals with advanced MS motor deficits. We created EMG biofeedback training schemes tailored to participant's symptoms and invited them to attend 18 training sessions within a 6-week study period. We

evaluated system performance during all sessions to demonstrate the feasibility of using classification-based EMG sensors to deliver tailored therapeutic exercise in a population with challenging neuromuscular impairments. We quantified the off-line accuracy and precision of the classification models and the on-line stability of patient interactions with the system during training. In addition, we used the classification record to determine the relative amount of time spent performing each training movement during a session and gain insight into the actual dose of biofeedback training delivered.

3.2 Methods

3.2.1 Participants

This report includes three cases from an ongoing investigation of tailored EMG biofeedback in multiple sclerosis (MS). The participants were recruited after being identified by their neurologist as experiencing significant muscle stiffness, weakness, hypertonia and/or spasticity not adequately addressed by the existing treatment course. Information about patient demographics, medications and history of MS can be found in Table 1. All participants were able to understand and follow instructions in English and did not have any visual impairment that could interfere with the interpretation of visual feedback. All participants provided written informed consent to all procedures, which were approved by the Hamilton Integrated Research Ethics Board (HiREB project #16009).

3.2.2 Classification-Based EMG Biofeedback

We previously described our classification-based EMG biofeedback approach in detail (Toepp et al. 2023). In this section we briefly describe our system's instrumentation, calibration, and training procedures. We also describe the process of tailoring the biofeedback based on needs specific to each case.

Instrumentation. EMG is recorded from pre-gelled Ag/AgCl adhesive electrodes placed in a bipolar configuration over muscles that were chosen specifically for each case. We use a 4-channel acquisition system (TMSi SAGA high-density EMG device, TMSi Ltd. Oldenzaal, Netherlands). The device features on-board AD conversion and streams digitized sensor samples directly to a PC through USB connection at a rate of 4 kHz.

Calibration. At the beginning of each training session, EMG data is recorded while the user performs each movement task and one task that involves maintaining a neutral (or resting) posture. The EMG pattern corresponding to the neutral posture will register a “No Input” command with the biofeedback system. Next, three to five movements are performed and used to register commands within a Tetris game during the training. Possible inputs to the training system include: No Input, Left, Right, Rotate (+), Rotate (-) and Drop. Rotate (+) and/or Rotate (-) may be assigned to keyboard arrows which are operated by a researcher to reduce the complexity of the EMG classification and improve the stability of the feedback stream.

EMG data collected during calibration are bandpass filtered between 20 and 400 Hz and four simple features are extracted from each channel using a 64ms window and 32ms hop: root mean square (RMS), waveform length (WL), number of zero crossings (ZC) and the number of slope sign changes (SSC). The result is a set of K 16-element feature vectors f for each training movement. The feature vectors are used for multi-class linear discriminant analysis²⁹ to create a matrix A that projects feature vectors into a de-correlated subspace by computing $A \cdot f_n$, where f_n is the n th feature vector in the calibration dataset K . A naïve Bayesian classification model³⁰ is then fitted using this transformed calibration data.

Game Control. New feature vectors are extracted from the filtered data stream during live training and projected into the classification subspace, each feature vector producing a classification decision indicating one of the training movements. The most frequent decision in each set of 5 classifications (i.e. the majority vote) registers a corresponding command (i.e., No Input, Left, Right, Rotate (+), Rotate (-), or Drop) with the biofeedback game interface.

Tailoring and Intervention Design. Case-specific sensor placements and training movements called “schemes” were developed during an initial tailoring session. Each participant described challenging movements and daily activities, and the Modified Ashworth Scale (MAS) was used to assess passive muscle stretch at the ankle, knee, wrist, and elbow. This information was taken together to create a profile of upper and lower-limb muscle impairment and to identify movements and sensor placements with potential benefit

to the individual. These scheme precursors were refined by successive rounds of calibration, testing (i.e., brief training trials), and adjustment, until acceptable feedback control was achieved. The threshold for acceptable control was participant success in controlling the Tetris blocks according to cues provided by a researcher.

After achieving acceptable control, individuals were invited to participate in three biofeedback training sessions every week for 6 weeks for a maximum of 18 sessions. The objective was to achieve 30 minutes of training during each session. The training schemes and the assessment evidence from which they were constructed are provided for each participant in the results.

3.2.3. Data Analysis

To assess the performance of the biofeedback system, we evaluated the classification model created during calibration using a fivefold cross validation. The evaluation measures overall accuracy, as well as the precision for each training movement (i.e., class). Accuracy is calculated as the percentage of all class predictions that are made correctly, while precision indicates the percentage of assignments that were made correctly for each class (i.e., the rate of true positives). Median accuracy and precision were taken across all the training sessions.

Since cross-validation is performed on random subsets of calibration data, an additional

measure is required to capture system stability in the face of spontaneous (potentially novel) muscle activation patterns during unconstrained gameplay. To evaluate control stability during training, we recorded the portion of classifier decisions agreeing with the majority decision (i.e., out of 5 votes). This was expressed as a value between 0.4 (2 of 5; the minimum for a majority decision to be made) and 1.0 (5 of 5; complete agreement) and called the “portion in agreement” (PIA). The average of the PIA value across all decisions registered as a game command within each training session was taken and then a grand average was calculated across all sessions for each training movement.

Table 3.1: Case Demographics

	Sex (M/F)	EDSS	Age (y)	Evolution (y)	Number of Sessions Completed	Drug Treatments
Case 1	F	7	57	28	18	Baclofen Gaba Penton
Case 2	F	8	49	23	7	Baclofen Escitalopram Oxalate Tizanidine Botox Injection (every 3 mo.)
Case 3	M	8	73	6	18	Naturopathic Remedies

The table provides each participant’s age, EDSS score, and duration of disease evolution, summarized drug treatment regimen and number of sessions completed during the 6-week trial. The EDSS scores can range from 0 to 10, with 10 indicating death due to MS. A score of 7.0 indicates heavy reliance on a wheelchair, and inability to walk more than 5 meters, even with aid. A score of 8.0 indicates complete loss of walking ability but retaining sufficient function in the upper limbs to perform many self-care functions. Evolution reflects the number of years since diagnosis as of the time of enrolment. The drug treatments were reported by the participants during the preliminary tailoring interview. EDSS – Kurtzke Expanded Disability Status Scale

The record of classification decisions also provides a convenient indicator of the relative proportion of training time spent producing the various discrete EMG patterns included in each training scheme. This proportion was calculated by dividing the number of registered classifications of each movement by the total number of classifications registered during the session. The portion assigned to each movement is therefore represented as a value between 0.0 and 1.0 where 1.0 denotes the entire training duration.

3.3 Results

3.3.1 Case 1

The participant is a 57-year-old right-handed female with a disease history of 28 years, score of 7.0 on the Kurtzke Expanded Disability Status Scale (EDSS). They had limited walking ability and were mostly restricted to a wheelchair. MAS indicated increased resistance to passive stretch in left and right knee flexor muscle groups with scores of +1 and 1, respectively. Increased resistance was also present in both the dorsi-flexors and plantar flexors at the right ankle with a score of 2 for both joint movement directions.

The individual reported poor balance while walking, standing, or reaching/manipulating objects. We designed a scheme to target coordination of intentional shifts in the center of mass while standing with upper limb tasks which we have previously described (Toepp et al. 2023). Since the primary target was balance, we assign the name “BAL” to this training scheme. The BAL training scheme, the classifier precision, the PIA, and the portion of training spent performing each movement are all provided in Figure 3.1A through 3.1D, respectively. The participant was able to attend all 18 sessions during the 6-week study period. The median calibration recording duration was 6 seconds across all training movements, stable feedback control was achieved during all sessions, and offline classification accuracy was 96% across sessions.

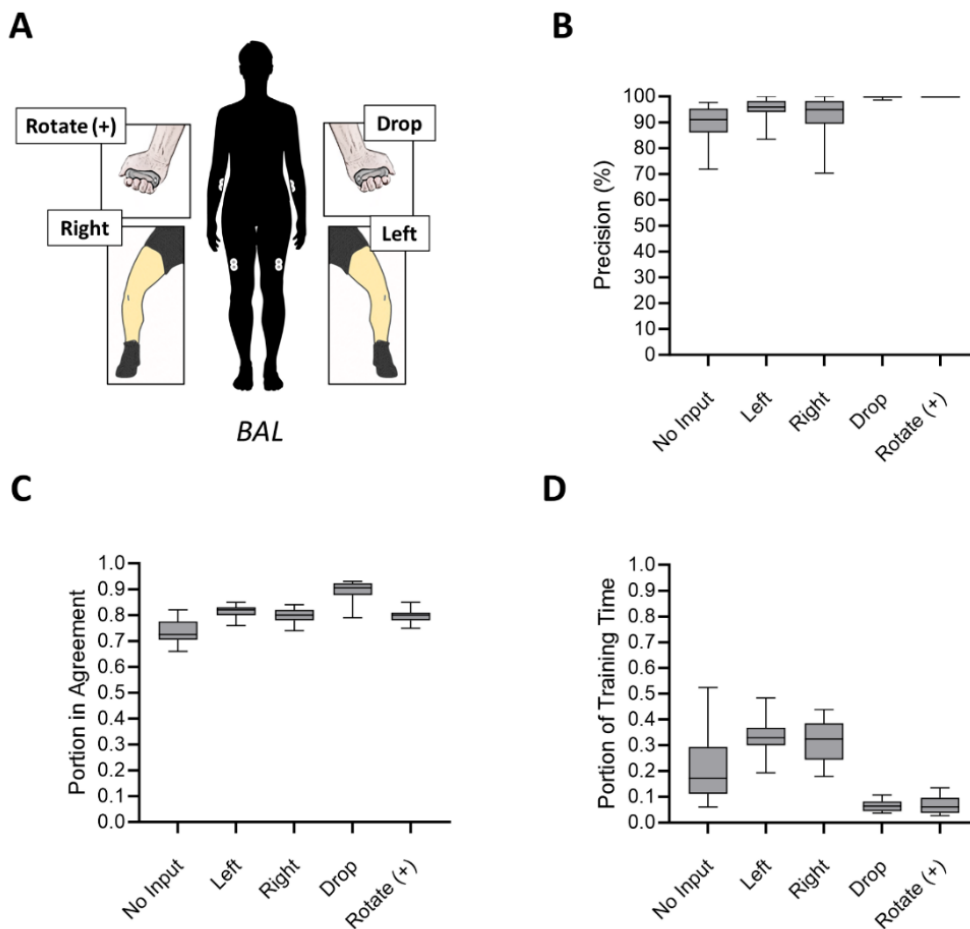


Figure 3.1: Case 1

The biofeedback training scheme and classification-derived metrics for Case 1. Panel A shows the BAL scheme wherein 5 movement tasks were used to control the gameplay: neutral stance, shift weight over the bent right knee, shift weight over the bent left knee, right grip squeeze, and left grip squeeze. Grip squeeze was performed by applying force to silicone 9 kg grip strength trainer (GoZone™). These movements corresponded to the game controls for No Input, Left, Right, Rotate (+), and Drop, respectively. The grip squeeze movements were detected by EMG sensors placed in a bipolar configuration over the corresponding FCR muscle. Shifts in weight over the left and right knee were detected by EMG sensors placed bilaterally over the VL muscle. Panel B shows the classification precision (true positive rate) for each training movement, Panel C shows the within-session mean PIA, and Panel D shows the portion of training time spent performing each movement. In Panels B-D, the box and whisker plots show the median, interquartile range (Q1-Q3), minimum and maximum values for each metric across all sessions. VL – vastus lateralis, FCR – flexor carpi radialis, BAL – balance

3.3.2 Case 2

The participant is a 47-year-old right-handed female with a 23-year disease history and a score of 8.0 on the Kurtzke Expanded Disability Status Scale (EDSS). They experienced severe weakness in both legs and hypertonia in the left knee extensors, ankle flexors and ankle extensors with MAS scores of 2 for each muscle group. The participant was restricted to a wheelchair during the training. The individual exhibited pronounced muscle impairment in the right upper limb, with hypertonia affecting the elbow (MAS score of 1+ in flexors and 3 in extensors) and wrist flexors (MAS score of 2).

During the initial tailoring session, the volunteer identified upper limb dysfunction as a high priority due to its association with loss of independence to perform common daily activities. They also identified loss of leg function as highly distressing with lower limb stiffness and spasms being a significant source of overall discomfort. We designed two biofeedback schemes, each with sensor placements and training movements to target either the upper or lower limb. Each scheme was used for half of the training duration (i.e., 15 minutes out of the 30-minute sessions). The upper limb scheme (UL) is shown in Figure 3.2A, and the lower limb scheme (LL) is shown in Figure 3.2B.

The participant was able to attend 7 of the 18 invited sessions during the 6-week study period. Attendance rate of less than 50% resulted from challenges with symptoms and transportation. The participant was able to achieve reliable game control with the UL scheme in all 7 sessions with a median calibration recording duration of 4 seconds per

movement, and median classification accuracy of 100%. For LL, reliable game control was not achieved for more than a few seconds during 3 of the 7 training sessions. The median off-line classification accuracy was 86%, and the calibration recording duration was 6 seconds for No Input, 5 seconds for Left and 4 seconds for both Right and Drop.

The precision values for each UL and LL scheme movement are shown in Figure 3.2C and 3.2D, PIA is shown in Figure 3.2E and 3.2F, and the portion of training spent performing each movement is provided in Figure 3.2F and 3.2G. Median PIA, accuracy, and precision values for LL in Figure 3.2D, 3.2F, and 3.2G represent 4 sessions of training, with completed durations of 14, 10, 4, and 15 minutes. In all cases where training was aborted before the 15-minute mark, the reason was loss of control stability.

3.3.3. Case 3

The participant is a 73-year-old right-handed male with recent MS diagnosis 6 years prior, and a score of 8.0 on the EDSS. Loss of lower limb function, especially on the right side rendered the participant restricted to a power wheelchair during the biofeedback training. MAS scores of 1 indicated the presence of increased tone in the right and left knee flexors, and the ankle flexors and extensors on the right side. Upper limb impairment was only present on the right side, with hypertonia affecting muscles across the elbow joint. The elbow flexors scored MAS 1+ and elbow extensors scored 2, corresponding with inability to volitionally extend the elbow beyond 120 degrees. The individual was also unable to open their right hand. A MAS score of 0 indicated normal tone in muscles crossing the wrist

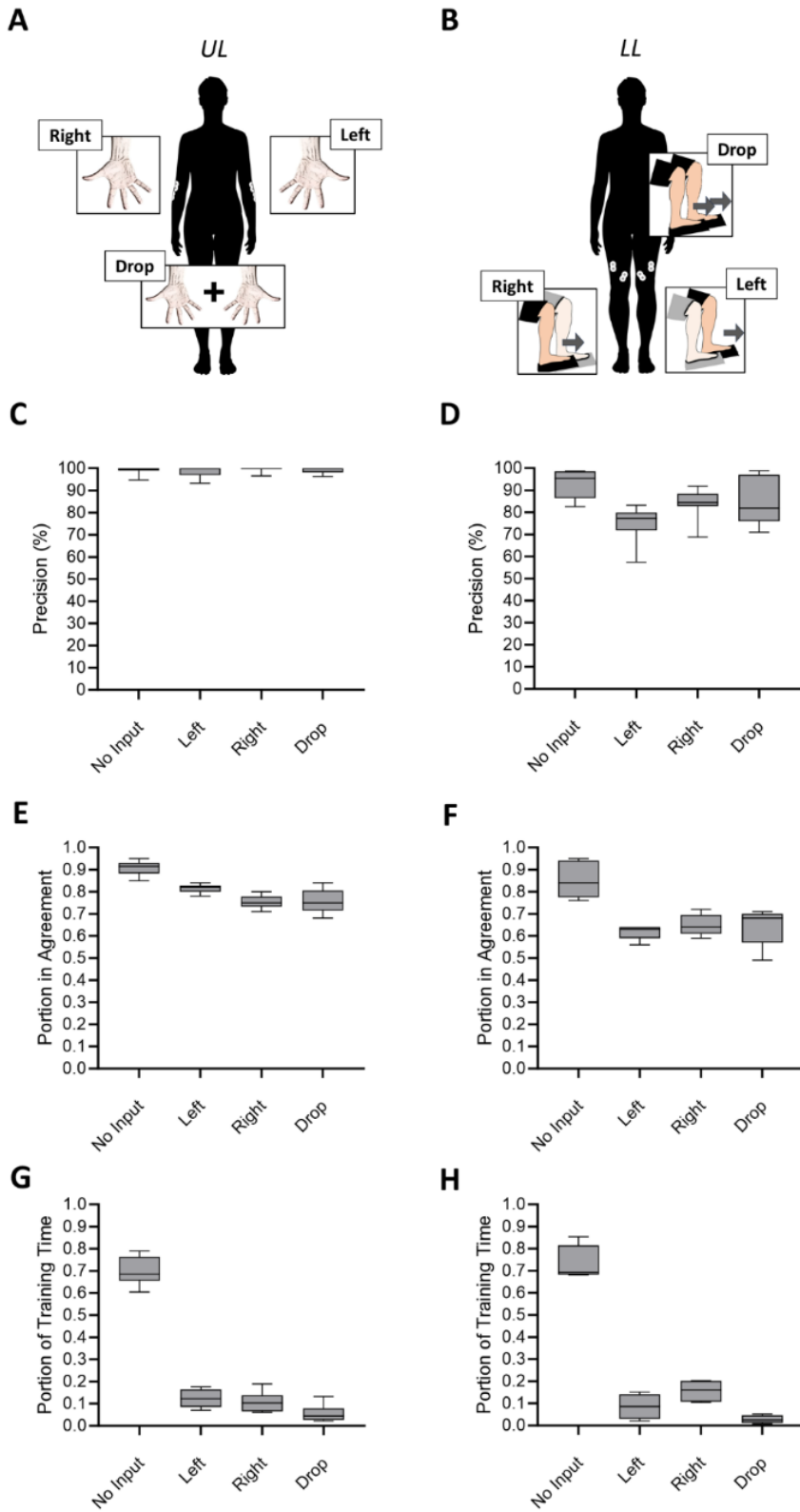


Figure 3.2: Case 2

The biofeedback training schemes, and classification-derived metrics are presented for Case 2. The UL and LL schemes are shown in Panels A and B, respectively. In the UL scheme, a pillow was placed on the participants lap to support the forearms during training. Right- and left-hand opening movements controlled Left and Right translation, and the Drop command was entered by performing both movements at the same time. Relaxing both Hands on the pillow resulted in No Input. These muscle activity patterns were captured by sensors placed bilaterally over the ECRL and EDS muscles. For the LL scheme, we placed the participants' feet on tilted platform in front of their braked wheelchair. The sensors were placed bilaterally over vastus lateralis (VL) and vastus medialis (VM) and the Left and Right commands were controlled by pushing against the platform with the corresponding foot as if trying push the chair backward. Simultaneously pushing with both feet resulted in the Drop command and relaxation was required to elicit No Input. For both schemes, we assigned Rotate (+) and Rotate (-) to the arrow keys on the computer keyboard which were operated by a researcher under the verbal direction of the participant. Panel C and D show the classification precision (true positive rate) for each training movement in UL and LL, respectively. Panel E and F show the within-session mean PIA for UL and LL. Panel G and H show the portion of training time spent performing each movement for UL and LL. In Panels C-H, the box and whisker plots show the median, interquartile range (Q1-Q3), minimum and maximum values for each metric across all sessions. ECRL – extensor carpi radialis longus, EDS – extensor digitorum superficialis, UL – upper limb, LL – lower limb

joint, suggesting that impaired hand opening reflects weakness in the digit extensor muscles rather than flexor tone.

The participant indicated that regaining function in the right arm and hand was most important to them. We therefore prioritized training that targets impairment at the elbow and in the hand. We could not achieve acceptable control when training both targets together, so we separately designed a scheme to target the hand (HA) and a scheme to target the elbow (EL), each to be performed for 15 minutes. The HA and EL schemes are illustrated in Figure 3.3A and 3.3B, respectively.

The participant was able to attend the 18 invited sessions during the 6-week study period. The median recording duration for the HA scheme during calibration was 4 seconds for all controls, and the resulting classification models exhibited 100% offline accuracy. Training was stopped after 4 minutes of training in one session due to a change in muscle tone that caused loss of effective biofeedback control. 15 minutes were completed in the remaining 17 sessions. The median recording duration during calibration for the EL scheme was 4 seconds for all controls, and median offline classification accuracy was 100%. Training was stopped after 3 minutes of one of the sessions due to a change in muscle tone that caused loss of effective game control. The complete 15 minutes of was performed in the remaining 17 sessions. The precision values for the HA and EL scheme movements are shown in Figure 3.3C and 3.3D, PIA for each scheme is shown in Figure 3.3E and 3.3F, and the portion of training spent performing each movement is provided in Figure 3.3F and 3.3G.

3.4 Discussion

Impactful physical therapy is challenging in progressive diseases like MS because motor deficits evolve over time. Because of its adaptability, classification-based EMG biofeedback may be an impactful therapeutic tool in these scenarios. We successfully created four tailored biofeedback training schemes for three individuals with advanced motor deficits due to MS. We also created one less successful training scheme that provided valuable insights with respect to the challenges that need to be addressed to bolster implementation in individuals with severe motor impairment.

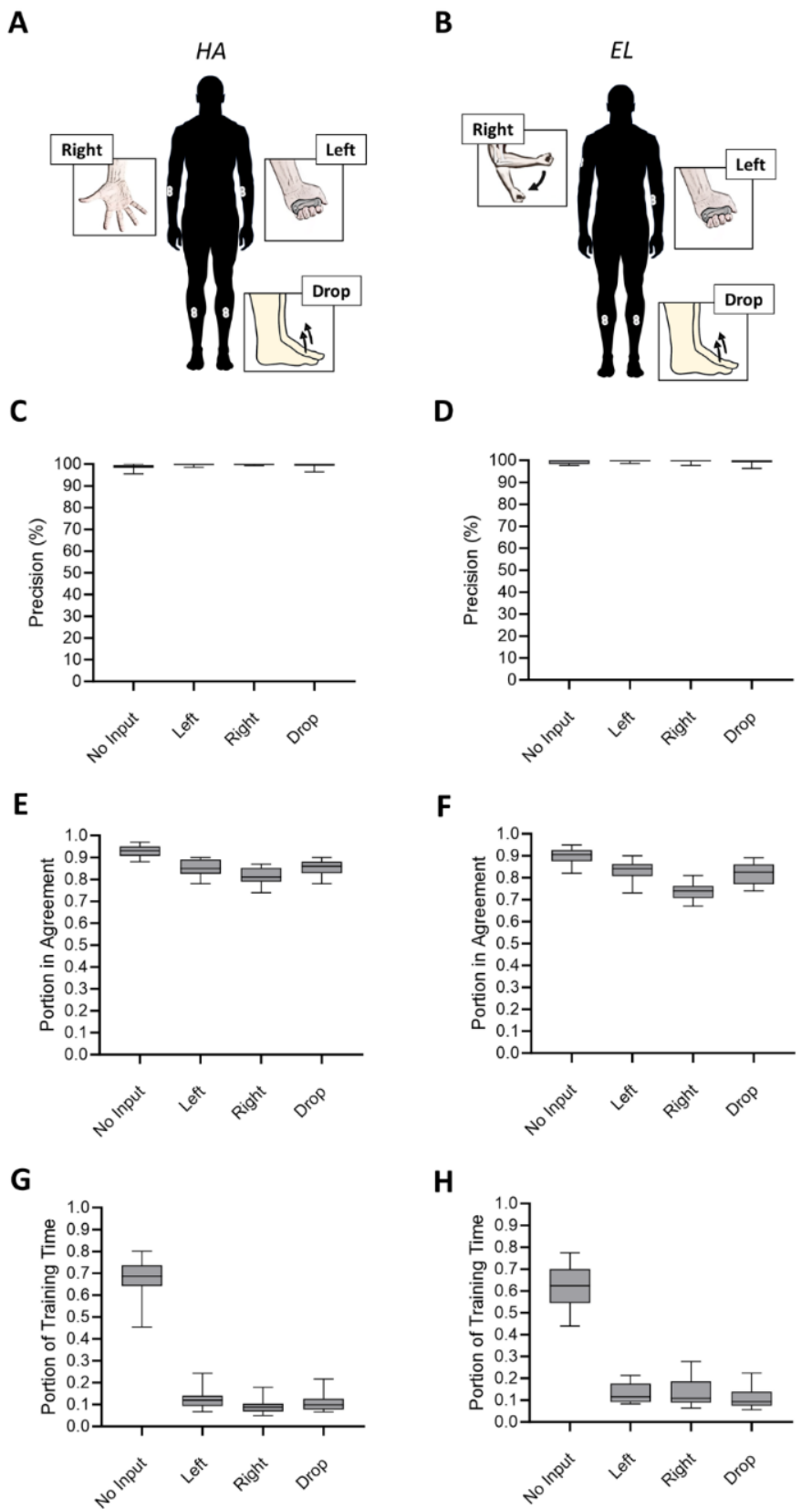


Figure 3.3: Case 3

The biofeedback training schemes, and classification-derived metrics are presented for Case 3. The HA and EL training schemes are shown in Panel A and B. We adopted a strategy wherein one sensor was placed over a scheme-specific target muscle. This sensor was placed over the EDS muscle for HA, and over the TB muscle for EL. Opening the hand and extending the elbow were both mapped to the Right game command within their respective training schemes. The remaining sensors were placed over three muscles which were kept consistent between the schemes. One of these sensors was placed over the left FCR muscle, and the remaining two sensors were placed over the left and right tibialis anterior (TA) muscles. The participant controlled the Left command by squeezing a grip strength trainer with the left hand. For the Drop command, the participant performed simultaneous dorsiflexion of the right and left ankles. The Rotate (+) and Rotate (-) commands were assigned to keyboard button presses. Panel C and D show the classification precision (true positive rate) for each training movement in HA and EL, respectively. Panel E and F show the within-session mean PIA. Panel G and H show the portion of training time spent performing each movement. In Panels C-H, the box and whisker plots show the median, interquartile range (Q1-Q3), minimum and maximum values for each metric across all sessions. FCR – flexor carpi radialis, EDS – extensor digitorum superficialis, TA – tibialis anterior, UL – upper limb, LL – lower limb

We consider the implementation of the BAL scheme in Case 1, the UL scheme in Case 2, and the HA and EL schemes in Case 3 to be successful because over 95% classification accuracy (Figure 4A) was reliably achieved and participants were usually able to complete the prescribed 15 or 30 minutes of training. Conversely, the LL scheme in Case 2 achieved only 86% accuracy, our minimum standard for game control stability was not achieved in three of the seven sessions, and the entire prescribed 15-minute training interval was completed on only one occasion. The off-line accuracy and precision, and the metrics derived from the on-line classification record are useful sources of insight into the determinants of success in classification-based EMG biofeedback implementation.

We chose to assess the portion in agreement (PIA) because it is easily accessible through the majority vote module in our control pipeline (Toepp et al. 2023) and it provides an

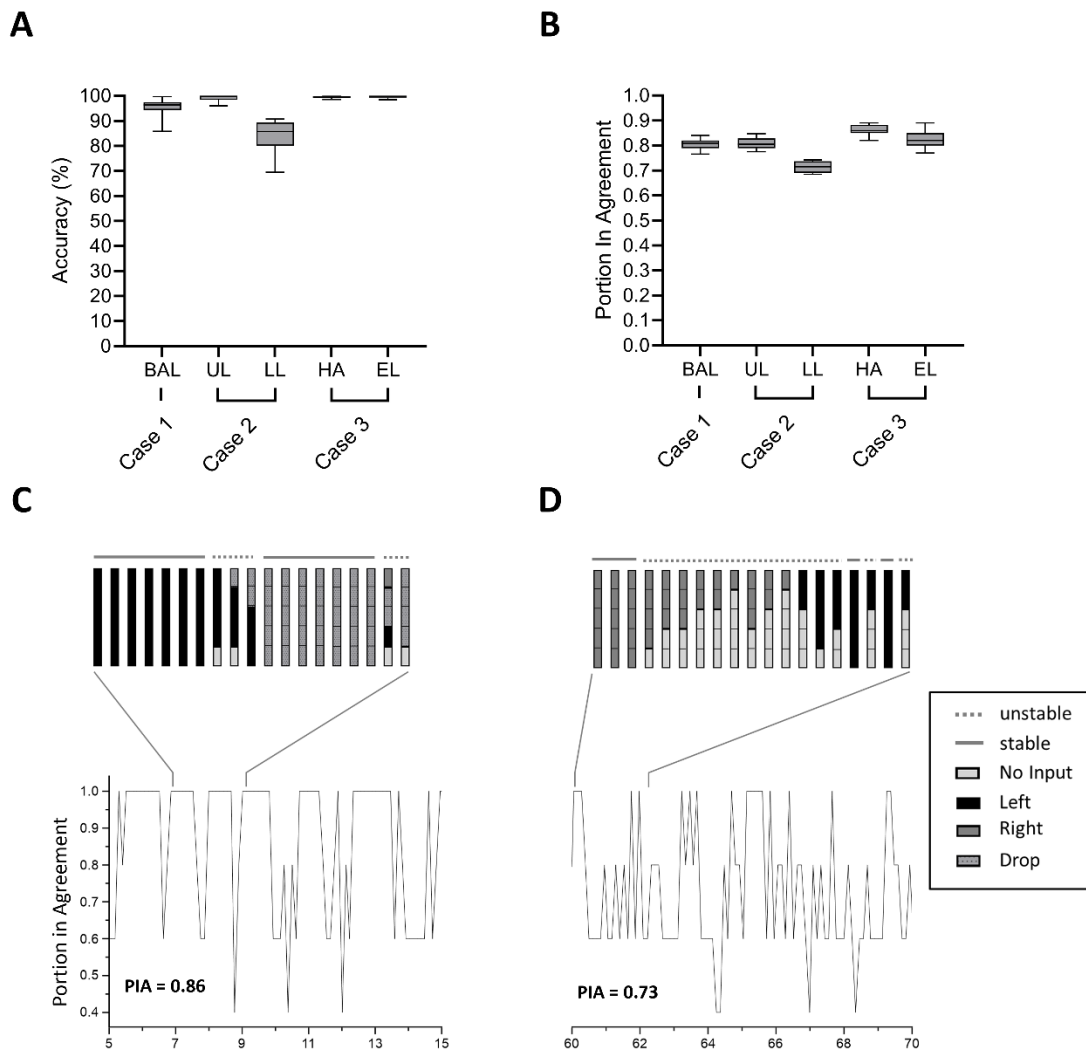


Figure 3.4: Accuracy and Portion in Agreement

Panels A and B show the median accuracy assessed during 5-fold cross validation and the PIA, respectively, across all sessions for each control scheme. Panels C and D illustrate the relation of PIA values during training to the majority vote record. Panel C shows the five-vote record for twenty consecutive control inputs (top) occurring within a ten-second interval of PIA values (bottom) that correspond to a relatively high average PIA. Panel D shows the voting record for twenty control inputs (top) within a ten second interval of PIA values (bottom) that produce a relatively low average PIA. Solid lines above the voting record entries indicate complete agreement among all 5 votes and thus, an interval of stable control. Broken lines indicate periods of less stable control where votes are split between two or more classes.

intuitive measure of the overall stability of interactions between the user and the system during a session. Figure 3.4C and 3.4D illustrate how PIA is derived from the majority vote record. A high average PIA (Figure 3.4C) is associated with long periods of stability where all five voters agree on one class (PIA of 1.0), interrupted by short unstable transition phases where some voters disagree ($0.4 < \text{PIA} < 0.8$). In cases of low PIA, the unstable transition phases are prolonged, and stable phases of complete voter agreement are shorter (Figure 3.4D).

To our knowledge, we are the first to use a measure of control stream stability to describe on-line classifier behavior. Transfer of a classifier's performance to an on-line context is usually assessed by measuring its accuracy against time-locked video record (Siu et al. 2016, MacIntosh et al. 2021, Han et al. 2022). These measurements evaluate classifier model robustness by using data intervals between discrete onset and offset events. In contrast, PIA captures an intuitive and meaningful characteristic of classification, its stability, in a continuous manner without the need for multiple modalities to detect movement onset and offset.

Several factors likely determine the control stability. First, we observed that low average PIA values (Figure 3.4B) usually coincided with low off-line classification accuracy. The lowest accuracy among all schemes was demonstrated by LL in Case 2 at 86%, and this coincided with the lowest PIA at 0.72 (Figure 3.4B). Conversely, all other (successful) schemes exhibited off-line accuracy above 95% and PIA values above 0.8. It is likely that

the effectiveness of the initial calibration directly impacts control stability, and therefore interpretations about the meaning of PIA with respect to the user's motor behavior should be avoided unless off-line accuracy is near 100% and is thus unlikely to be a major contributor.

UL, HA, and EL demonstrated 100% median precision across all controls, but the median PIA ranged from 0.74 (Right in the EL scheme) to 0.93 (No Input in the HA scheme), suggesting influences outside of the classifier efficacy. One such influence may be changes in EMG movement signatures from baseline because of fatigue or accumulating effects of movement-related neuromuscular dysfunction. Abnormal muscle stretch reflexes and soft tissue changes can cause spasticity (Trompetto et al. 2014), which can alter the EMG patterns produced when same movement is repeated many times (Marinelli et al. 2017, Trompetto et al. 2019, Puce et al. 2021). In progressive MS, the ability to sustain voluntary activation is also compromised (Wolkorte et al. 2016), so movement attempts may become more transient as the training session continues. These factors may contribute to the range of PIA values observed among schemes exhibiting near-perfect off-line accuracy.

The context in which a movement is used to control the game may also be important. Movements that are performed in a more sustained or continuous manner during training, such as holding a posture or joint position, are likely to result in longer periods of stable classification and higher PIA. For example, the No Input control (neutral posture) prevents the Tetris block from moving, and the highest median PIA was observed for this control when classifier accuracy was not a factor (i.e., in UL, HA, and EL). In contrast, the Rotate

and Drop commands are each entered to cause more transient events, i.e., rotating the block by 90 degrees, or dropping the block to the bottom of the board.

Normative values for specific control schemes in healthy users would facilitate interpretation of PAI in terms motor impairment. The impetus to expend resources to create such normative databases will require evidence of the training scheme's therapeutic impact and its utility in a broad patient population. While exercise therapy is established as an effective means to address spasticity and fatigue in MS (Donzé and Massot 2021), EMG biofeedback interventions vary considerably in the dose of exercise that they deliver a single session. Only one study has assessed the impact classification-based EMG biofeedback training in MS (Oña et al. 2022). The intervention involved training hand gestures for 12-20 minutes twice every week for 8 weeks. These authors reported improvements in upper limb function, but the frequency and duration of training movements within the training intervals was not reported. This is not surprising because recording such details in real-time would be daunting in a minimally structured game-based exercise scenario. It is, however, possible to use the classification record to measure the portion of the training time spent producing each training movement to obtain a more precise indication of the training dose.

In our study, 30 minutes of training was prescribed in each case with that duration being comprised of two 15-minute training blocks using different schemes in cases 2 and 3. Approximately 20% of the BAL training (Figure 3.1D) was comprised of No Input, and

that portion was at least 60% for the other training schemes (Figure 3.2G, 3.2H, 3.3G and 3.3H). Therefore 24 minutes of exercise were administered per 30-minute interval in Case 1 and only 12 minutes (i.e., less than half of that in Case 1) in Cases 2 and 3. The actual training dose also varied for movements that represented primary therapeutic targets. Right hand opening in the HA scheme and right elbow extension in the EL schemes both accounted for only ~10% of the training interval in their respective schemes (Figure 3.4D and 3.4E) equating to ~3 minutes in every 30 minutes of training. In contrast, the main therapeutic component of the BAL scheme, which were shifts of weight over the left and right knee, accounted for approximately 60% of the training duration and ~18 in every 30 training minutes. Future research will need to determine the implications of dose when exercise therapy is administered via classification-based EMG biofeedback. Fortunately, the exercise dose can be easily and automatically monitored by this modality's classification mechanism.

3.5 Conclusion

In three case studies, we demonstrated the feasibility of creating and implementing tailored classification-based EMG biofeedback interventions in individuals with advanced MS symptoms. We showed that accurate classification and stable game control can be achieved in the presence of significant neuromuscular dysfunction and that the dose of therapeutic exercise delivered could be easily monitored and interpreted. This work provides a foundation for future investigations to uncover the clinical impact of classification-based EMG biofeedback training.

Chapter 4: Study 3

In the previous chapters, I demonstrated the implementation of an optimized surface EMG biofeedback method that uses a classification-based approach enabling automated assessment through simple analysis of the classification record. The surface EMG trace that is acquired during training may also present an opportunity to gain insight into neuromotor processes without requiring significant additional acquisition time or expertise. In Chapter 4, I develop a simple acquisition protocol that can generate analogous EMG data to that produced in a variety of biofeedback and other contexts. I then demonstrate the inter-rater and inter-session reliability of analyses performed using a simple cursor placement application. Finally, I propose a simple statistical format through which the findings can be leveraged to aid interpretation of surface EMG collected in similar contexts.

Accessible Motor Assessment with Surface EMG: Key Parameters and Reliability

Abstract

Despite the evident value of surface electromyography (EMG) in neurorehabilitation, its clinical use is limited. Researchers have developed many sophisticated EMG methods to test scientific hypotheses and address technical issues. However, there is a lack of simple and easily reproduced (i.e., clinician-accessible) procedures with available reference literature to support interpretation. To make EMG assessments accessible and interpretable for clinicians, we propose a template for surface EMG acquisition and data analysis using stereotyped upper and lower-limb movements and manual cursor placements. We apply our

template by creating a simple protocol for measuring the root mean square (RMS) and mean frequency (MNF) of the EMG signal in active muscles during hand opening (HOP), wrist extension and flexion (WEF), and elbow flexion (EF). In 36 healthy males and females, we assess interclass correlations (ICCs) to evaluate the relative inter-rater reliability of manual cursor placements, and the relative inter-session reliability of the MNF and RMS values. We also assess smallest detectable change (SDC) between assessments as a function of the number of contributing measurements (i.e., repetitions). Manual cursor placement exhibited excellent inter-rater reliability ($ICC > 0.9$) and inter-session reliability of MNF and RMS feature measurements was good ($0.75 > ICC > 0.9$) or excellent. As expected, SDCs decreased as movement repetitions increased. We demonstrate a clinician-accessible template for reliable EMG assessment, and an intuitive approach to interpreting changes in the obtained measurements. Designing protocols explicitly for broad use by clinicians will be necessary to advance clinical acceptance and integration of the modality into practice.

4.1 Introduction

Surface electromyography (EMG) can provide insights into the state of movement control in healthy and neurologically impaired individuals (Nelson-Wong et al. 2009, Reiman et al. 2012, Babyar et al. 2022, Maura et al. 2023). For example, EMG studies reveal residual motor transmission, reflecting intact motor axons across the injured segments, in more than 60% of patients diagnosed with “complete” spinal cord injury (SCI) (Mckay et al. 2004, Heald et al. 2017). Surface EMG may thus help to predict the likelihood of recovery in the absence of visible or palpable signs of motor output (Calancie et al. 2004, Pilkar et al.

2020). Some EMG signal features are also sensitive to fatigue and may facilitate exercise or functional electrical stimulation (FES) by optimizing intervention intensity and duration. For instance, fatigue-related changes in root mean square (RMS) and median frequency are blunted with muscle-strengthening interventions (Oliveira and Gonçalves 2009), and may be useful in scenarios like multiple sclerosis where fatigue-related EMG changes are more pronounced and associated with impaired function (Eken et al. 2020).

Despite the apparent value of surface EMG in neurorehabilitation, it has not been broadly adopted in clinical practice. Several detailed tutorials, reviews, and editorials have identified barriers to clinical translation (Campanini et al. 2020, 2022, Merletti et al. 2021, 2023), often citing the challenge of interpreting EMG data. Indeed, the practical value of any assessment tool depends on the ease with which a clinician can draw valid conclusions from values that it provides. In the case of EMG, it may be unclear whether differences in the timing or amplitude of signals are caused by physiological change or measurement error, making the use of EMG unappealing (Hug 2011). Moreover, interpreting changes within an individual over time is especially important in populations such as stroke where variation in lesion size, location, and time since injury prevent group-level data from producing insights about the expected impact of damage on EMG signal parameters (Li et al. 2014, Angelova et al. 2018). The expected signal characteristics during movement in healthy individuals, and the expected error in individual surface EMG measurements is thus essential for interpretation. This information is required to identify and track injury-related EMG signatures over time to elucidate prognostic or prescriptive insights.

The current literature regarding inter-session differences in EMG measurements mostly concerns isometric or isokinetic movements constrained by custom-built limb positioning apparatuses (Lee et al. 2011a, Carius et al. 2015). These devices are generally not commercially available and are therefore difficult to reproduce. Between-session reliability of EMG measures during less-constrained dynamic movements such as running, squats, push-ups, chest press, or arm raises has been studied in various postures and sometimes while holding weights (de Araújo et al. 2009, Smoliga et al. 2010, Sorbie et al. 2018). In these studies, data are normalized to the maximum voluntary isometric contraction (MVIC) to reduce intra-subject variability and facilitate interpretation across studies. However, isometric reference tasks may be less appropriate for dynamic movements (Allison et al. 1993, Balshaw and Hunter 2012, Guerrero-Henriquez et al. 2022), and maximal efforts are sensitive to prior training and motivation (Soderberg and Knutson 2000), central lesions, or pain (Allison et al. 1998).

Moreover, measuring MVIC reliably requires careful positioning and cuing to ensure consistency between assessment days, assessors, or measurement settings. Varying diligence among clinicians in controlling factors that may impact an MVIC represents a potential added source of measurement error. For this reason, EMG measurements with as few modifiable elements as possible may be required to ensure that protocols can be faithfully reproduced in diverse clinical settings. Indeed, the vast body of published EMG

literature features varied approaches to similar questions and many dauntingly complex procedures are developed to address specific technical issues or test specific hypotheses.

A dedicated approach that addresses the specific challenge of making EMG assessments accessible and interpretable for clinicians is warranted. In the present work, we propose a clinician-friendly template for surface EMG assessment protocols using stereotyped upper and lower-limb movements without limb-positioning devices or maximal normalization tasks. We provide an example of a use case for the template to create and implement a simple protocol for evaluating hand, wrist, and elbow movements. We evaluate the relative inter-rater and inter-session reliability of our method in a healthy sample and demonstrate how clinicians can leverage their own accumulated databases to evaluate absolute reliability and support valid interpretation. The simplicity of our approach supports broad use and rapid accumulation of data to establish the meaningful change thresholds and normative ranges needed for easy interpretation by clinicians. Moreover, this method is designed especially for physiotherapists, physiatrists, and other allied rehabilitation practitioners who may not be neuroscientists *per se* but would nonetheless benefit from surface EMG insights regarding the structure of motor output.

4.2 Methods

4.2.1 Assessment Protocol Template

A single continuous recording is acquired in two phases as illustrated in Figure 4.1. The first phase establishes a baseline EMG pattern wherein the individual holds a “neutral” joint

position or posture. This reference interval facilitates visual cursor placements by providing a reference against which an assessor can compare changes in the signal that result from cued movements (see *Analysis*). We refer to this phase as the baseline (BL) phase.

After the BL phase, several repetitions of the investigated movement are captured in the movement (MOV) phase. The tempo t of the movement repetitions during the MOV phase are cued by a metronome which is played from the beginning of the BL phase and throughout the entire testing interval. The metronome frequency is chosen according to the desired movement velocity. The individual is instructed to begin their movements on the n^{th} metronome beat which marks the beginning of the MOV phase. The n^{th} beat should follow 4-5 seconds of neutral posture (BL) to ensure a sufficient “rest” period enabling easy visual interpretation of the EMG trace in the MOV phase.

There are two types of cue response. First, each subsequent metronome beat may cue alternation between movement A and its opposite movement B (e.g., joint flexion then extension). This pattern may be investigated if antagonist-agonist co-activation or if both concentric and eccentric phases of agonist muscle contraction are of interest. The second type of cue response pattern may be used if volitional activation of a muscle during only one phase (concentric or eccentric) is of interest. In this case, responses alternate between movement and relaxation to the neutral position.

The length of the MOV interval may be tailored to the purpose of the assessment. If fatigue

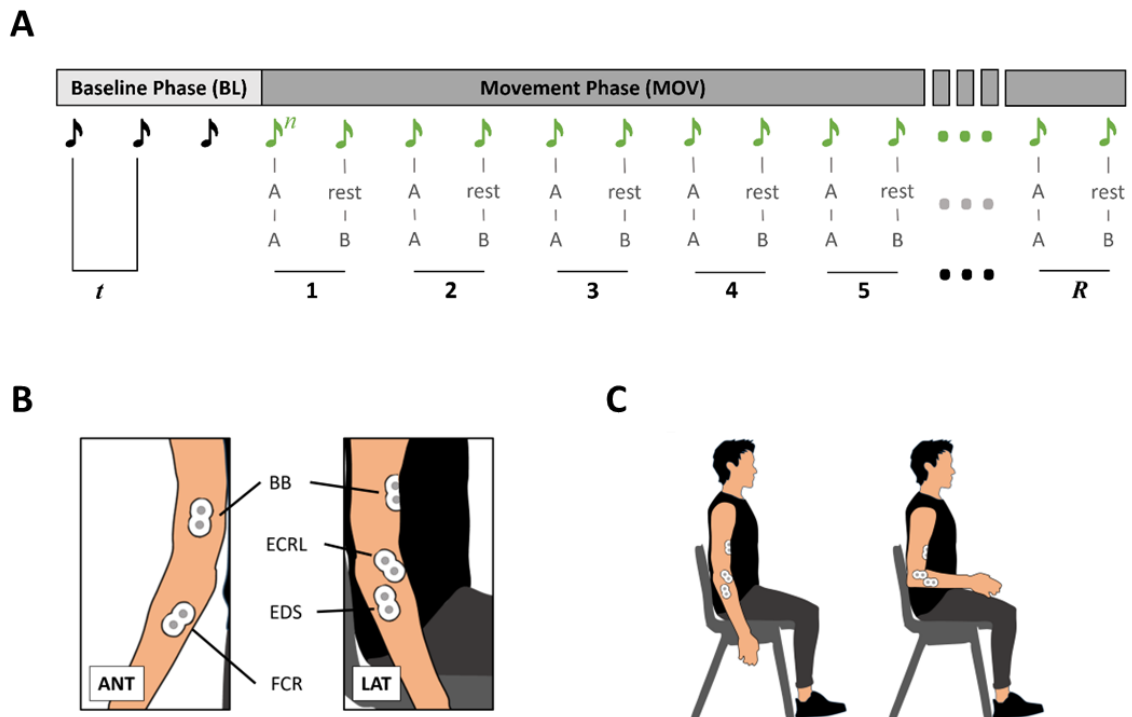


Figure 4.1 Acquisition Protocol Template, Sensor Placement and Positioning

Panel A shows a schematic of the key parameters of the proposed assessment template. Baseline (BL) and Movement (MOV) phases at the top of the figure. Metronome beats are represented by note icons with inter-beat interval (t) indicated by their spacing. The first beat of the MOV phase (n) cues the first of R movement repetition cycles, each including two metronome beat responses. Depending on the purpose of the investigation cycles include either alternation between movement A and rest, or movement A and movement B. Panel B shows the electrode placements and Panel C shows the participant posture during the BL phase in the present study. Panel B shows the anterior (ANT) and lateral (LAT) view of the electrode placement for biceps brachii (BB), extensor carpi radialis longus (ECRL), extensor digitorum superficialis (EDS), and flexor carpi radialis (FCR). Panel C shows starting posture with the right arm relaxed by the participants side for the elbow flexion (EF) assessment (left) and the elbow held at approximately 90 degrees for the wrist extension flexion (WEF) and hand open (HOP) assessment. Electrode leads are not depicted.

is the measure of interest, the MOV interval may be extended to allow a large volume of work. Conversely, evaluations of co-contraction or the detection and quantification of residual neuromuscular function may be achieved with a shorter MOV interval. Thus, in addition to specifying sensor placement, a protocol using the present template must specify:

1) BL “neutral” posture, 2) cue response type, 3) metronome frequency in beats per minute (bpm), and 4) movement instructions to be provided to the assessed individual.

4.2.2 Upper-Limb Movements in Healthy Males and Females

Upper limb function is severely impaired with peripheral central lesions resulting from traumatic injury (e.g., nerve laceration, head, or spinal trauma), ischemic events, or neurodegenerative diseases. Assessments of residual neuromuscular function with surface EMG could supplement clinical evaluations, especially in cases where visible movement is minimal or hard to interpret. To demonstrate an application of our assessment protocol template, we acquired and analyzed EMG signals in muscles of the right upper limb during three simple movement assessments on a sample of healthy volunteers. We repeated the assessment on two separate days and two assessors independently placed event cursors to demonstrate the inter-session and inter-rater reliability of the method, respectively.

Participants. Included participants were required to be within the range of 18 to 40 years old, had not suffered a fracture or other upper-limb injury affecting the neuromuscular system in the prior 12 months, and had no stable or unstable medical condition that could conceivably impact motor function. Thirty-six participants were recruited in and around Hamilton, Ontario, Canada. The mean age was 23.6 ± 4.9 y with an equal number of males and females ($n = 18$), and most participants (~86%) were right-handed.

Movements and Positioning. Three different movement assessments were performed: 1) Elbow Flexion (EF), 2) Wrist Extension and Flexion (WEF), and 3) Hand Opening (HOP). For all assessments, the participant was seated upright in a standard chair with no armrests. In all assessments, the left arm (not assessed) was relaxed at the participant's side with the palm facing medially. A metronome with an inter-beat interval (t) of 1.2s (50bpm) was used for all assessments such that each subsequent movement cycle was separated by approximately 2.4 seconds ($t \times 2$). Participants were instructed to start moving on the 4th beat to commence the MOV phase. The entire recording interval was 45 seconds, allowing all participants to complete at least 15 repetitions after the onset of the MOV phase. Sensor placement and participant posture during BL are illustrated in Figure 1B and 1C, respectively.

Elbow Flexion – During the BL phase for the EF assessment, the right upper limb was held in a neutral or “rest” posture and relaxed at the participant's side with the palm facing medially. The EF movement involved flexing the elbow to ~45 degrees, and then returning it to the starting position on the subsequent metronome beat. The movement was modelled for the participant before the assessment.

Wrist Extension & Flexion – During the BL phase for the WEF assessment, the right elbow was flexed to ~90 degrees (without shoulder abduction) with the palm facing medially, the wrist in a neutral position (not flexed or extended) and the digits relaxed. The WEF movement involved moving the wrist first into extension then flexion on the subsequent

beat. To isolate muscle activation related to wrist control, the participants were instructed to avoid actively moving the fingers during the movements. Rather they were instructed to allow the digits move naturally.

Hand Opening – During the BL phase for the HOP assessment, the right elbow was flexed to ~90 degrees (without shoulder abduction) with the palm facing medially, the wrist in a neutral position (not flexed or extended) and the hand relaxed. For the HOP movement, participants were instructed to open the hand as wide as possible, and then close it again on the subsequent beat.

Electromyography. EMG was recorded from biceps brachii (BB) for EF, extensor carpi radialis longus (ECRL) and flexor carpi radialis (FCR) for WEF, and extensor digitorum superficialis (EDS) for HOP. Sensor placement was performed according to SENIAM guidelines (Hermens et al. 2000) using surface electrodes (9 mm diameter Ag–AgCl) (Figure 1B). At all sites, the skin was lightly abraded and cleaned with isopropyl alcohol. For BB, sensors were placed one third of the distance along a line connecting the middle of the antecubital fossa and the acromion process at the shoulder. ECRL was palpated to identify the most prominent part of the muscle belly during active wrist extension with the elbow in 90 degrees of flexion. Sensors were placed on FCR by measuring one third of the distance from the medial epicondyle of the humerus to the styloid process of the radius and palpating to find the longitudinal borders of the muscle. EDS sensors were placed one fourth of the distance between the lateral epicondyle of the humerus and the styloid process

of the ulna after palpating to find the longitudinal borders of the muscle. The inter-electrode distance was 20mm for all muscles. Recordings were amplified by 1000 (Intronix Technologies Corporation Model 2024F, Bolton, Ontario, Canada) and sampled at 4 kHz (Power1401, Cambridge Electronics Design, Cambridge, UK), then subjected offline to a digital band-pass filter (2nd order Butterworth) with low and high cutoffs at 20Hz and 500Hz, respectively.

Cursor Placements. The acquired surface EMG signal is band pass filtered and displayed so that an assessor can place event cursors at the onset of surface EMG responses associated with cued movements. While algorithms exist that use peak detection and thresholds to place cursors automatically, the outputs of these algorithms will invariably require visual validation. Manual placement of cursors by a clinical assessor with knowledge of metronome frequency, BL phase length, and the movements involved is an accessible alternative.

To facilitate accurate cursor placement, smoothed amplitude and frequency time series can be provided along with the un-smoothed and un-rectified band-pass filtered EMG signal. We produced a simple model for a cursor placement program with these elements using MATLAB (MathWorks, Natick, United States) and it is shown in Figure 4.2 with data from a BB recording during an elbow flexion assessment. The assessor places cursors at the visually identified onset of activity for each muscle response in the band pass filtered trace (Figure 4.2A), while using associated rises in smoothed RMS and mean frequency (MNF)

time series (Figures 4.2B & 4.2C) for validation in cases where signal to noise ratio is low or there is spurious activity.

EMG Measurements. Assessor A (ST) and Assessor B (RR) placed the first cursor in each recording by visually identifying the onset of the first “significant” pulse of activity following the quiet interval denoting the BL phase. Cursors for subsequent repetitions were placed by identifying regular bursts of activity at intervals approximating twice the metronome interval. This corresponds to the same movement repeated every second metronome beat, since the movements of interest are interleaved with an opposing movement (WEF) or a return to a neutral position (EF and HOP). EMG measurements were computed within the 1.2s window following each cursor placed in the agonist EMG trace using the *rms*, and *meanfreq* MATLAB functions. Given a vector of EMG samples x , $rms(x)$ calculates the RMS according to equation 1:

$$RMS = \sqrt{\frac{1}{N} \sum_{i=1}^N x_i^2} \quad (1)$$

where x_i are the band-pass filtered EMG signal samples, and N is the number of samples in the window considered (1.2s x 4000Hz = 4800 samples). MNF was calculated by equation 2:

$$MNF = \frac{\sum_{i=1}^M f_i P_i}{\sum_{i=1}^M P_i} \quad (2)$$

Where P_i is the i^{th} frequency in the power spectrum and M is the highest harmonic included.

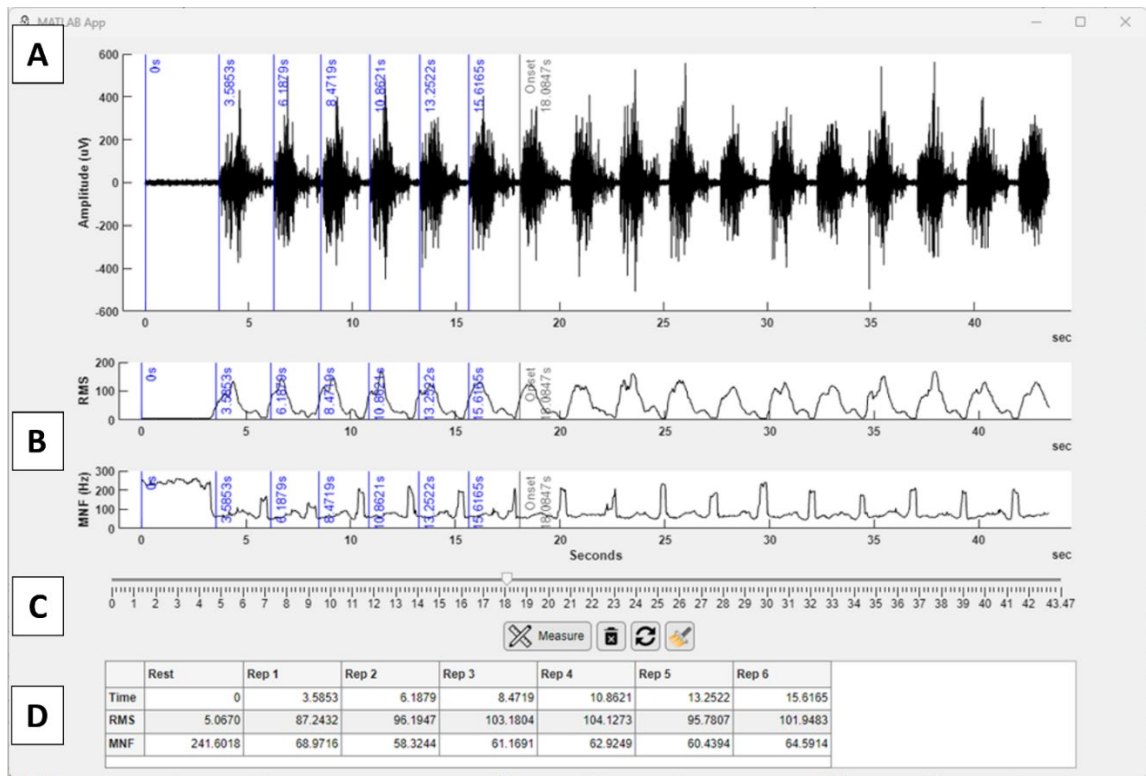


Figure 4.2: Cursor Placement Application

Our simple cursor placement user interface with the band-pass filtered EMG signal (A) displayed along with smoothed RMS and MNF traces (B) to facilitate accurate cursor placement. A slider widget (C) allows the user to place cursors and calculate signal features, which are displayed with their corresponding cursor times 1(D).

The first repetition after the BL period does not reflect the same movement speed or preparatory state as the subsequent repetitions and was thus removed from all analyses. Statistical analyses were performed on the mean of the 14 repetition measurements following the first (discarded) repetition. In addition, test-retest reliability (SDC) was computed for the rolling average from repetitions 2-15 (see *Statistical Analyses*) to demonstrate the expected benefit of adding repetitions.

Statistical Analyses. Relative inter-session and inter-rater reliability were assessed using two-way random effects model, ICC (2, k), as EMG data are acquired and analyzed by researchers (ST and RR) assumed to represent a population of well-trained assessors (Weir 2005). Previously established guidelines for interpreting the ICC were used with coefficients below 0.5 indicting low reliability, 0.5-0.75 indicating moderate reliability, 0.75-0.9 indicating strong reliability, and >0.9 indicating excellent reliability (Portney and Watkins 2009, Koo and Li 2016).

The SDC was calculated at the individual level by multiplying the standard error of measurement (SEM) by the root of 2 and then by the *z*-score for the associated confidence level (Schambra et al. 2015). The impact of adding movement repetitions was investigated by calculating the SDC of the RMS and MNF mean from 1 to 14 repetitions.

Since the confidence level provides an intuitive interpretation, we calculated SDCs using the *z*-scores associated with 85% ($z=1.440$), 90% ($z=1.645$) and 95% ($z=1.960$) confidence levels. In addition, we computed the SEM from the standard deviation of deltas expressed as a percent of the baseline value which indicates the smallest *relative* change that can be considered “real” with each level of confidence. All statistics were performed using SPSS statistical software.

4.3 Results

4.2.1 Inter-Rater Reliability

The deviation between cursors placed by assessors A and B are shown in Figure 4.3 with their mean and 95% confidence interval. The mean deviation tended to be positive, reflecting a tendency of assessor B to place cursors slightly later than assessor A. The mean deviation was 15ms (-93ms to 123ms) for BB during EF, 51ms (-147ms to 249ms) for ECRL, and 37ms (-144ms to +219ms) in FCR during WEF, and 26ms (-92ms to 144ms) in EDS during HOP. Corresponding interclass correlations are shown in Table 4.1 for cursor time and the resulting 14-repetition average RMS and MNF values. The ICC (2, 35) was either 1.0 or very near 1.0, indicating excellent inter-rater reliability for windowing based on manual cursor placement.

4.2.2 Inter-Session Reliability

The between sessions interclass correlation coefficients for the 14-repetition average of the RMS and MNF feature values are presented with 95% confidence intervals in Table 4.1. Both RMS and MNF demonstrated good-to-excellent reliability in ECRL with wrist extension (i.e., during the WEF assessment) and in EDS during HOP. In BB during EF, RMS also demonstrated good-to-excellent reliability while MNF demonstrated moderate-to-excellent reliability. In the FCR during wrist flexion (i.e., during the WEF assessment), MNF demonstrated good-to-excellent reliability while the 95% confidence interval for RMS indicated moderate-to-excellent reliability.

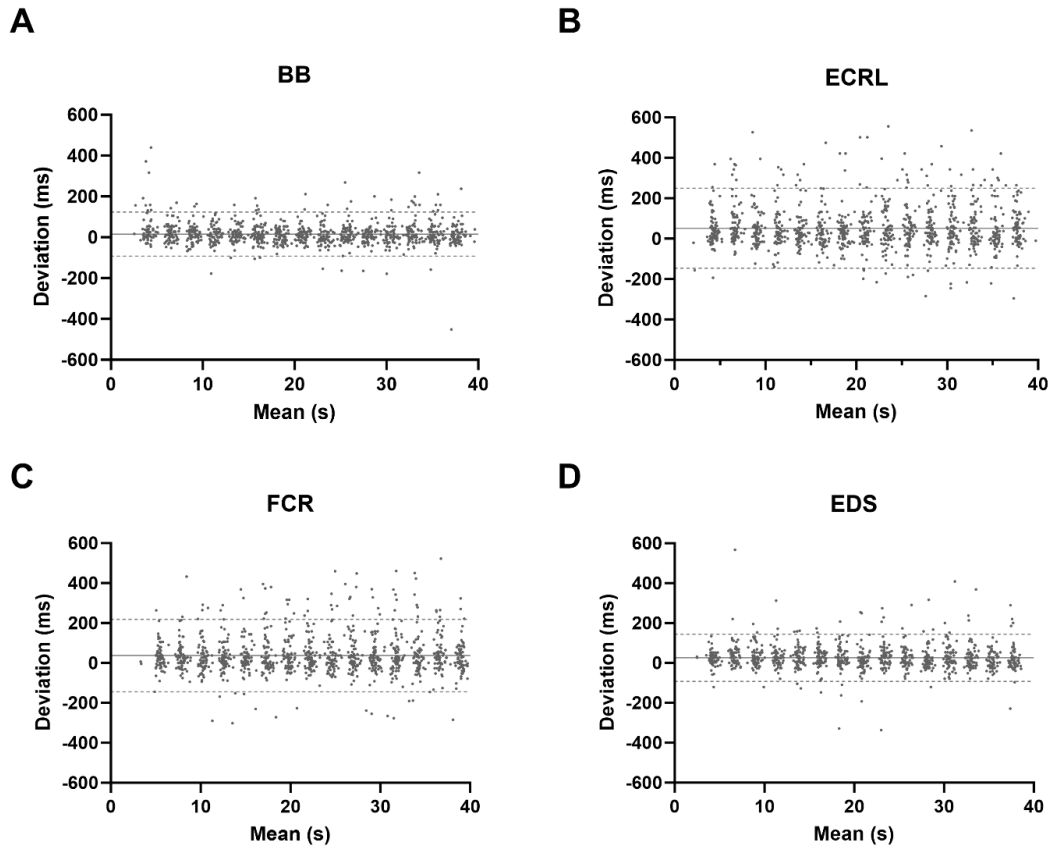


Figure 4.3: Inter-Rater Cursor Placements

Bland-Altman plots showing the deviation of cursor times in milliseconds between raters ST and RR with the mean and 95% CI of the deviations indicated by the solid and broken horizontal lines, respectively. Panel A shows cursor placement deviations between the assessors for the biceps brachii (BB) during elbow flexion. Panel B shows deviations for extensor carpi radialis longus (ECRL) during wrist extension. Panel C shows deviations for flexor carpi radialis (FCR) during wrist flexion. Panel D shows deviations for extensor digitorum superficialis (EDS) during hand opening. Deviations are calculated by subtracting the cursor time for assessor A from that of assessor B (i.e., $dev = B - A$)

The relative SDC of the RMS value is shown in Figure 4.4A to 4.4D for 1 to 14 repetitions at each of three confidence levels (SDC_{85} , SDC_{90} and SDC_{95}). The lowest SDC_{95} observed was 51% for BB during EF, 90% for ECRL during wrist extension, 37% for FCR during wrist flexion, and 18% for EDS during HOP. For all assessments, the SDC decreased with

the addition of repetitions. For BB, the SDC_{95} was reduced by 21% for the 14-repetition average relative to a single repetition. Similarly, 14 repetitions lowered SDC_{95} by 118% for ECRL, 66% for FCR, and 15% for EDS compared to that of a single RMS value. Notably, the SDC values for BB and EDS reached their floor after 5 and 7 repetitions, respectively, while ECRL and FCR continue to decline as repetitions are added.

The SDC of the MNF value in Hz is shown in Figure 4.4E to 4.4H for 1 to 14 repetitions at the three assessed confidence levels. The lowest SDC_{95} observed was 8Hz for BB during EF, 14Hz for ECRL during wrist extension, 20Hz for FCR during wrist flexion, and 15Hz for EDS during HOP. As with RMS, the SDC for all assessed movements decreased as repetitions were added. Fourteen repetitions lowered the SDC_{95} by 3Hz for BB, 4Hz for ECRL, 5Hz for FCR, and 4Hz for EDS. The SDC values for BB and EDS reach a floor after fewer than 14 repetitions (at 8 and 3 repetitions, respectively), while ECRL and FCR continue to decline as repetitions are added.

4.4 Discussion

This work aimed to demonstrate a practical and interpretable surface EMG assessment template and thereby increase the utility of surface EMG in clinical settings. In our application, we found that manual placement of cursors in the filtered EMG signal by two different assessors is reliable, and that relative reliability between assessments on different days was good or excellent for both RMS and MNF. We also calculated an intuitive measure of absolute reliability, the SDC, which is applicable in rehabilitation where changes in

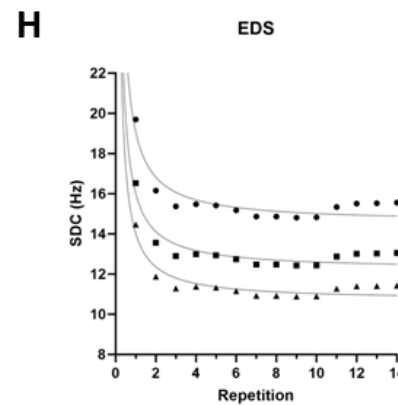
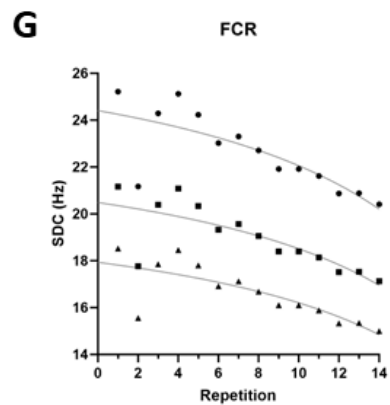
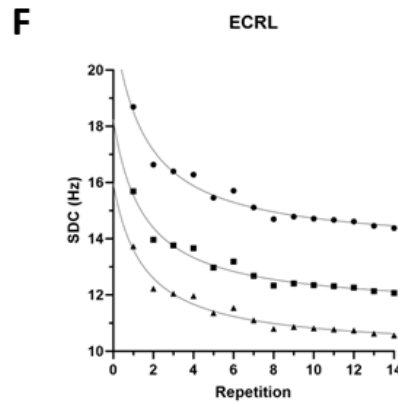
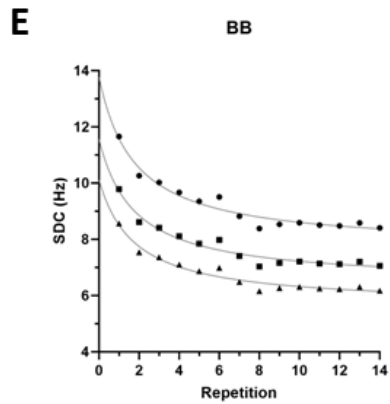
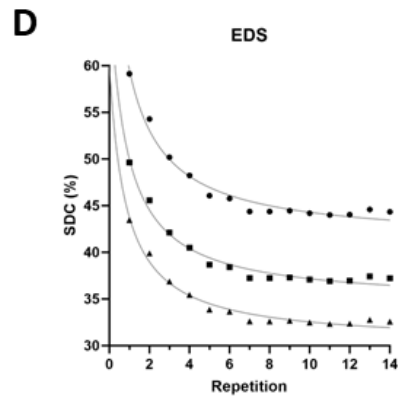
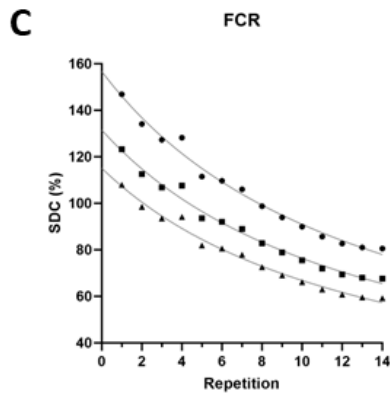
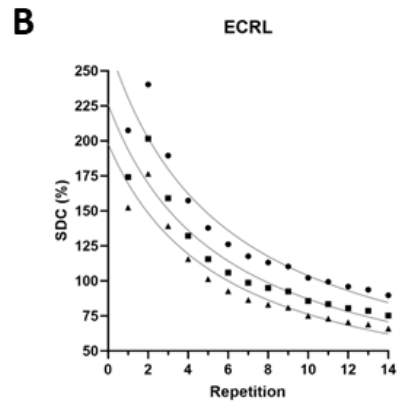
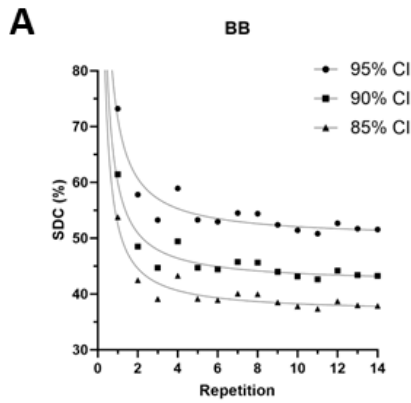


Figure 4.4: Smallest Detectible Change

The smallest detectible change (SDC) for RMS expressed as a percentage of the first session measurement, and for MNF in absolute units (Hz). The top four panels show RMS SDCs for elbow flexion in biceps brachii (A), wrist extension in extensor carpi radialis longus (B) wrist flexion in flexor carpi radialis (C), and hand opening in extensor digitorum superficialis (D). The bottom 4 panels show MNF SDCs for elbow flexion in biceps brachii (E), wrist extension in extensor carpi radialis longus (F) wrist flexion in flexor carpi radialis (G), and hand opening in extensor digitorum superficialis (H). The SDCs are calculated at 95%, 90%, and 85% confidence levels when 1 to 14 repetitions are averaged, and a fitted standard curve are shown to facilitate visual interpretation.

motor function over time are of interest.

The strong reliability of visual cursor placement between our assessors is notable in showing that individuals with an understanding of the acquisition template (i.e., the movement instructions and tempo) can generate reproducible signal measurements. While automated methods are a topic of active research due to their promise of more objective and reproducible measurements (Tenan et al. 2017, Crotty et al. 2021, Kowalski et al. 2021), visual onset detection is traditionally considered the ‘gold standard’ method (Van Boxtel et al. 1993, Hodges 1996, Staude et al. 2001, Allison 2003). As the sophistication of algorithms advances, automated onset detection will likely produce more reliable outputs in more and more contexts. However, the variety of existing approaches and the requirement to tune the algorithms to each specific dataset adds considerable complexity to the process. On the other hand, the visual pattern recognition capacity of the human brain is more than sufficient to identify activity onset in most cases. Moreover, the visual detection does not require ‘tuning’ beyond ensuring that the assessor is aware of contextual information about the muscles and movements that generated the activity. We believe visual cursor placement is an appropriate standard for analysis of surface EMG in clinical practice

Table 4.1: Relative Reliability of Features and Cursor Placements

	Elbow Flexion (BB)		Wrist Extension (ECRL)		Wrist Flexion (FCR)		Hand Opening (EDS)		
	ICC	Lower	Upper	ICC	Lower	Upper	ICC	Lower	Upper
			<i>95% CI</i>		<i>95% CI</i>				<i>95% CI</i>
Inter-rater									
Cursor Time	1.00	1.00	1.00	1.00	1.00	1.00	1.00	1.00	1.00
RMS	1.00	1.00	1.00	1.00	1.00	1.00	1.00	1.00	1.00
MNF	1.00	1.00	1.00	1.00	1.00	1.00	1.00	1.00	1.00
Inter-session									
RMS	0.88	0.77	0.94	0.90	0.81	0.95	0.83	0.65	0.91
MNF	0.86	0.73	0.93	0.90	0.80	0.95	0.91	0.83	0.96

Inter-rater and inter-session interclass correlations (ICC) are shown with 95% confidence intervals. ICCs for individual cursor placements are provided for Cursor Time, and the ICCs for the 14-repetition average of the root-mean square (RMS) and mean frequency (MNF) were calculated for each movement and corresponding muscle.

due to the practicality of its implementation and acceptable reliability.

In the present study, we report inter-class correlations indicating good or excellent inter-session reliability. However, these values provide little aid to clinicians in interpreting feature values themselves. We therefore provided a more explicit interpretation aid by calculating the smallest detectible change at different confidence levels (i.e., SDC₈₅, SDC₉₀, and SDC₉₅) and for different numbers of repetitions (1 to 14). Assessing the SDC at different confidence levels allows users to operationalize degrees of confidence in observed changes rather than accepting or rejecting the change outright. The proximity of the observed change to two adjacent confidence boundaries (e.g., SDC₉₅ versus SDC₉₀) could also inform changes in the number of repetitions to increase confidence in the assessment outcome. Of course, the confidence level should not be conflated with the size or importance of the change. Studies should establish clinically meaningful difference thresholds so the assessment parameters can be optimized for their detection with the desired degree of confidence.

Clinically meaningful change thresholds have not been determined for EMG features in any specific clinical population. However, SDC values may be useful when EMG features are used to monitor activity in specific muscles during prescribed movements within a rehabilitation program. The most prominent examples are interventions that use surface EMG signal as training feedback (EMG biofeedback) (Toepp et al. 2023) or to trigger functional electrical stimulation (FES) (Feldner et al. 2019). In these cases, the EMG signal

is the primary target of the treatment so the threshold at which EMG features can be said to have changed ‘significantly’ is immensely important.

Our protocol template is designed to efficiently assess minimally constrained dynamic movements and can be performed directly prior to or following an FES or EMG Biofeedback session, consuming very little additional time. Rehabilitation professionals tend to see surface EMG as a treatment tool (Feldner et al. 2019, Campanini et al. 2020, Merletti et al. 2023), likely as a function of spending the majority of their time planning and delivering interventions. Making it easy for clinicians to integrate data collection into their treatment programs by simplifying acquisition and providing reference resources like SDC values to aid interpretation will significantly improve the appeal of surface EMG.

We chose to calculate the RMS SDC values relative to the prior (i.e., the first) measurement to provide a more generalizable statistic than the absolute (μV) values. Features that capture EMG signal amplitude (e.g., RMS) are more sensitive to electrode size, spacing, location, and amplifier gain than spectral features (Castroflorio et al. 2005), and the amplitude-force relationship is affected by electrode placement over the muscle belly (Ahamed et al. 2014). In lieu of universal standardization of acquisition hardware, materials, and sensor placement procedures, we believe that representing statistics like SDCs in relative terms provides a more broadly accessible interpretation for amplitude-based features like RMS. The degree to which our relative values can be reproduced by others will be the ultimate test of this hypothesis.

From Figure 4.4, it is apparent that the SDC values can be reduced by increasing the number of repetitions and that the number of repetitions required to maximize the sensitivity varies between features and movement assessments. In our example, we observed that EF and HOP (A and D) were minimized with fewer than 14 repetitions for both RMS and MNF, while WEF assessments (B and C) tended to continue a downward slope and may benefit from additional repetitions. While we assessed inter-rater reliability of cursor placements, acquisition was performed by only one researcher (ST) in this study. As such, it will be informative for future work to describe inter-rater reliability capturing the consistency between assessors in various aspects of data collection (e.g., skin preparation, electrode placement, movement instruction, etc.).

Our findings also reflect the choice of specific parameter values within our template. We chose a tempo of 50bpm, which corresponds to certain movement speed. Higher or lower movement tempos may cue different contraction velocities. Faster contractions correspond with higher amplitude values (Miller et al. 2012) while spectral features are generally higher during dynamic than static contractions but do not vary significantly with changes in velocity (Shankar et al. 1989, Miller et al. 2012). For frequency measures, it should be noted that differences between static and dynamic contractions disappear at low contraction speeds (Christensen et al. 1995). These factors could conceivably have an impact on the expected values and reliability of measures collected at different metronome tempos. Participants were instructed to start on the 4th beat and to move to the beat of the metronome

and we chose an analysis interval of 1.2 seconds to match the inter-tone interval. Because the movements were dynamic and not physically constrained, they were not isokinetic, and it is likely that a portion at the end of the analysis interval reflects an isometric hold while the participant waits for the next beat. Therefore, it may be informative to investigate narrower windows starting at varying latencies from the onset of activity. A similar approach was taken by Angelova and colleagues (Angelova et al. 2018) who analyzed 0.3407s intervals of signal during a single dynamic elbow flexion movement using movement onset identified in a video recording. In the current context, segmentation could be similarly achieved using cursors placed within the signal trace.

We assessed inter-session reliability for up to 14 repetitions. For some movements (WEF), it appears that more repetitions are required to minimize the SDC thresholds. We also made specific choices in spectral processing prior to cursor placement and feature calculation. We chose a high pass cutoff of 20 Hz which is recommended for attenuating movement artifact (De Luca et al. 2010). Our choice of a 500Hz low pass cutoff is recommended because measurable muscle-related signals are only detectible below this boundary (McManus et al. 2020). However, cutoffs as low as 350Hz are considered acceptable since the portion of muscle-related EMG energy at higher frequencies is very low (Merletti and Muceli 2019). Whether a different low pass cutoff meaningfully impacts the reliability of assessments following the proposed template is an interesting topic for future work.

In the present study we demonstrate a practical and interpretable approach to surface EMG assessment that is designed to increase the accessibility of surface EMG to clinical

practitioners. We show that reliable EMG feature measurements can be obtained without the use of burdensome maximal effort tasks or limb-positioning devices and that visual cursor placement is sufficient for reliable feature analysis between assessors. This is an early but necessary step in developing a dedicated surface EMG assessment approach for broad clinician use.

Chapter 5: Conclusions and Impact

This thesis advanced the translation of surface EMG methods to clinical application through several meaningful contributions. First, review of clinician surveys and interviews revealed that prominent clinical figures (predominantly physiotherapists) encounter surface EMG mostly in the context of EMG biofeedback, which they frequently report using and believing in its benefits. Approaching EMG biofeedback as an important tool within translational strategies is a significant contribution to the current discussion. Leading translation advocates see perceptions of surface EMG primarily as a therapeutic tool as a barrier, obscuring its many useful assessment applications (Campanini et al. 2020, Merletti et al. 2023). This thesis puts forth a different perspective wherein a popular therapeutic application (EMG biofeedback) is a potential avenue to introduce clinicians to simple surface EMG assessments.

In Chapters 2 and 3, the thesis makes strides toward the creation of a gold standard for EMG biofeedback systems. At present, EMG biofeedback systems are heterogenous in their design, making consensus regarding their efficacy in clinical scenarios difficult to reach. The developed biofeedback system is tailorable with respect to muscles and movements targeted, and its design facilitates the monitoring of the training dose and various characteristics of user-feedback interactions. The system is also created with off-the-shelf hardware and open-source software so others can easily reproduce it. Facilitating adoption of a standard system across clinical studies of EMG biofeedback will facilitate a more coherent body of literature on the topic and clarify arguments for adoption based on

scientific evidence. In addition to the development of the system itself, the thesis demonstrates the feasibility of its implementation in healthy and impaired individuals, and across multiple training sessions. It sets the stage for clinical researchers to design and test biofeedback training schemes that address specific motor impairments.

This thesis also argues that feedback based on discrete classification is more stable, flexible, and comprehensive than continuous scaling (i.e. equation-based feedback). However, it should be noted that these two types of biofeedback need not be mutually exclusive, and adding continuous biofeedback elements could be helpful in many situations. While adding multiple scaled EMG channel representations to a training game may not be feasible without overwhelming user, back-end applications can effectively do so for the operating clinician. Access to individual sensor channels data could allow a therapist to confirm that targeted muscles are engaged during training. If control stability is lost, identifying the sensor channel(s) where aberrant EMG activity is occurring could allow the therapist to pause training and administer targeted stretches or massage, or wait for activity to return to normal. While the system that I developed does not integrate scaled EMG channel representations, such a modification would add an element of sophisticated exercise monitoring.

The clinical exposure of simple surface EMG assessments could be increased through the adoption of EMG biofeedback if efforts are made to develop accessible complementary methods. Chapter 4 presents a simple protocol with metronome-cued dynamic contractions,

no movement-constraining hardware, and no normalization methods. These features make acquisition simple and easy to adapt to different movements of interest. The data generated is also analogous to that produced during biofeedback training using the system described in Chapter 1 and 2 in that the data are not normalized to a maximal effort the contractions are not isometric or isokinetic. Therefore, the thesis provides a reasonable estimate of the relative inter-rater and inter-session reliability of feature measurements collected during biofeedback training. I also provide estimates of absolute reliability in the form of smallest detectable change between sessions, and the association between this value and the number of repetitions for which data is acquired. The smallest detectable change is an intuitive aid for interpreting changes in muscle activation that occur over the course of an intervention and will be essential to the leveraging of surface EMG data from biofeedback sessions.

This thesis does have some notable limitations. Testing of the developed biofeedback system was restricted to healthy individuals or MS patients. Generalization of findings described in Chapter 2 and 3 to applications in other populations is therefore uncertain. However, the MS participants did exhibit relatively high levels of disability (EDSS scores of 7 or 8), suggesting the biofeedback is likely feasible populations with less severe impairment. Because each training scheme was tailored to an individual participant, it would also have been beneficial to include age- and sex-matched controls for each case in Study 2. Finally, Study 3 included only healthy young participants. Implementation of the described acquisition and analysis procedure may be more challenging in older individuals

or those with neurological impairments, and the reported reliability statistics are not necessarily generalizable.

Future research should apply this EMG biofeedback approach in various therapeutic contexts, including recovery from stroke or spinal injury, re- or pre-habilitation of knee or hip arthroplasty, balance training in at-risk populations, and many others. Smallest detectible change in simple surface EMG measurements, such as RMS or MNF should be quantified with respect to signals collected during training to facilitate the utility of EMG biofeedback as a dual-purpose modality (i.e., assessment and therapy). Perhaps most importantly, the initial version of the surface EMG biofeedback system that was developed in this thesis, should be refined with feedback from physiotherapists and other rehabilitation professionals who are its intended end-users.

In conclusion, this thesis provides essential foundations for the translation of surface EMG methods into clinical practice. In the pursuit of an informed translational strategy, an improved surface EMG technique was developed to maximize its therapeutic impact, and an accessible complementary assessment method was demonstrated. This thesis therefore takes important steps to promote the clinical adoption of surface EMG methods to the benefit of clinicians and their patients.

References

Abdullahi A, Truijen S, Saeys W. Neurobiology of Recovery of Motor Function after Stroke: The Central Nervous System Biomarker Effects of Constraint-Induced Movement Therapy. *Neural Plast.* (2020); **2020**

Ahamed NU, Sundaraj K, Alqahtani M, *et al.* EMG-force relationship during static contraction: Effects on sensor placement locations on biceps brachii muscle. *Technol. Heal. Care* (2014); **22**: 505–513.

Allison GT. Trunk muscle onset detection technique for EMG signals with ECG artefact. *J. Electromyogr. Kinesiol.* (2003); **13**: 209–216.

Allison GT, Godfrey P, Robinson G. EMG signal amplitude assessment during abdominal bracing and hollowing. *J. Electromyogr. Kinesiol.* (1998); **8**: 51–57.

Allison GT, Marshall RN, Singer KP. EMG signal amplitude normalization technique in stretch-shortening cycle movements. *J. Electromyogr. Kinesiol.* (1993); **3**: 236–244.

Anam K, Al-Jumaily A. A novel extreme learning machine for dimensionality reduction on finger movement classification using sEMG. In: *Int. IEEE/EMBS Conf. Neural Eng. NER* (2015); pp. 824–827. IEEE.

Anam K, Al-Jumaily A. Evaluation of extreme learning machine for classification of individual and combined finger movements using electromyography on amputees and non-amputees. *Neural Networks* (2017); **85**: 51–68. Elsevier Ltd.

Angelova S, Ribagin S, Raikova R, *et al.* Power frequency spectrum analysis of surface EMG signals of upper limb muscles during elbow flexion – A comparison between healthy subjects and stroke survivors. *J. Electromyogr. Kinesiol.* (2018); **38**: 7–16. Elsevier.

Anwer S, Equebal A, Nezamuddin M, *et al.* Effect of gender on strength gains after isometric exercise coupled with electromyographic biofeedback in knee osteoarthritis: A preliminary study. *Ann. Phys. Rehabil. Med.* (2013); **56**: 434–442.

Anwer S, Quddus N, Miraj M, *et al.* Effectiveness of electromyographic biofeedback training on quadriceps muscle strength in osteoarthritis of knee. *Hong Kong Physiother. J.* (2011); **29**: 86–93. Elsevier.

de Araújo RC, Tucci HT, de Andrade R, *et al.* Reliability of electromyographic amplitude values of the upper limb muscles during closed kinetic chain exercises with stable and unstable surfaces. *J. Electromyogr. Kinesiol.* (2009); **19**: 685–694.

Armatas CA, Summers JJ, Bradshaw JL. Mirror Movements in Normal Adult Subjects. *J. Clin. Exp. Neuropsychol.* (1994); **16**: 405–413.

Armiger RS, Vogelstein RJ. Air-Guitar Hero: A real-time video game interface for training and evaluation of dexterous upper-extremity neuroprosthetic control algorithms. *2008 IEEE-BIOCAS Biomed. Circuits Syst. Conf. BIOCAS 2008* (2008);121–124.

Avanzino L, Bassolino M, Pozzo T, *et al.* Use-dependent hemispheric balance. *J.*

Neurosci. (2011); **31**: 3423–3428.

Babyar SR, Holland TJ, Rothbart D, *et al.* Electromyographic Analyses of Trunk Musculature after Stroke: An Integrative Review. *Top. Stroke Rehabil.* (2022); **29**: 366–381. Taylor & Francis.

Baeza-Barragán MR, Labajos Manzanares MT, Vergara CR, *et al.* The use of virtual reality technologies in the treatment of duchenne muscular dystrophy: Systematic review. *JMIR mHealth uHealth* (2020); **8**: 1–12.

Balas EA, Boren SA. Managing Clinical Knowledge for Health Care Improvement. *Yearb. Med. Inform.* (2000); **09**: 65–70.

Balas EA, Chapman WW. Road map for diffusion of innovation in health care. *Health Aff.* (2018); **37**: 198–204.

Balbinot G, Joner Wiest M, Li G, *et al.* The use of surface EMG in neurorehabilitation following traumatic spinal cord injury: A scoping review. *Clin. Neurophysiol.* (2022); **138**: 61–73.

Balshaw TG, Hunter AM. Evaluation of electromyography normalisation methods for the back squat. *J. Electromyogr. Kinesiol.* (2012); **22**: 308–319. Elsevier Ltd.

Barbarotto R, Laiacona M, Frosio R, *et al.* A normative study on visual reaction times and two Stroop colour-word tests. *Neurol. Sci.* (1998); **19**: 161–170.

Basmajian J V. Control of individual motor units: a guide and preliminary reading for

prospective subjects in single motor unit training experiments. *Am. J. Phys. Med.* (1973); **52**: 257–260.

Basmajian J V. Biofeedback in rehabilitation: A review of principles and practices. *Arch. Phys. Med. Rehabil.* 1981 pp. 469–475. American Congress of Rehabilitation Medicine, [Chicago] :

Batzianoulis I, Krausz NE, Simon AM, *et al.* Decoding the grasping intention from electromyography during reaching motions. *J. Neuroeng. Rehabil.* (2018); **15**: 1–13. *Journal of NeuroEngineering and Rehabilitation.*

Bedi K. pong-python. 2016

Beer RF, Ellis MD, Holubar BG, *et al.* Impact of gravity loading on post-stroke reaching and its relationship to weakness. *Muscle and Nerve* (2007); **36**: 242–250.

Van den Berghe G, Wouters P, Weekers F, *et al.* Intensive Insulin Therapy in Critically Ill Patients. *N. Engl. J. Med.* (2001); **345**: 1359–1367.

Besomi M, Hodges PW, Clancy EA, *et al.* Consensus for experimental design in electromyography (CEDE) project: Amplitude normalization matrix. *J. Electromyogr. Kinesiol.* (2020); **53**: 102438. Elsevier.

Besomi M, Hodges PW, Van Dieën J, *et al.* Consensus for experimental design in electromyography (CEDE) project: Electrode selection matrix. *J. Electromyogr. Kinesiol.* (2019); **48**: 128–144. Elsevier.

Billings SA, Lee KL. Nonlinear Fisher discriminant analysis using a minimum squared error cost function and the orthogonal least squares algorithm. *Neural Networks* (2002); **15**: 263–270.

Biswas RD. Snake Eater. 2021

Bizzi E, Cheung VCK, D'Avella A, *et al.* Combining modules for movement. *Brain Res. Rev.* 2008 pp. 125–133.

Van Boxtel GJM, Geraats LHD, Van Den Berg-Lenssen MMC, *et al.* Detection of EMG onset in ERP research. *Psychophysiology* (1993); **30**: 405–412.

Braun T, Rieckmann A, Weber F, *et al.* Current use of measurement instruments by physiotherapists working in Germany: A cross-sectional online survey. *BMC Health Serv. Res.* (2018); **18**: 1–16. BMC Health Services Research.

Calancie B, Molano MR, Broton JG. Abductor hallucis for monitoring lower-limb recovery after spinal cord injury in man. *Spinal Cord* (2004); **42**: 573–580.

Campanini I, Disselhorst-Klug C, Rymer WZ, *et al.* Surface EMG in Clinical Assessment and Neurorehabilitation: Barriers Limiting Its Use. *Front. Neurol.* (2020); **11**: 135–163.

Campanini I, Merlo A, Disselhorst-Klug C, *et al.* Fundamental Concepts of Bipolar and High-Density Surface EMG Understanding and Teaching for Clinical, Occupational, and Sport Applications: Origin, Detection, and Main Errors. *Sensors* (2022); **22**

- Cappellini G, Sylos-Labini F, Assenza C, *et al.* Clinical Relevance of State-of-the-Art Analysis of Surface Electromyography in Cerebral Palsy. *Front. Neurol.* (2020); **11**: 1–17.
- Carius D, Kugler P, Kuhwald HM, *et al.* Absolute and relative intrasession reliability of surface EMG variables for voluntary precise forearm movements. *J. Electromyogr. Kinesiol.* (2015); **25**: 860–869.
- Carr JH, Mungovan SF, Shepherd RB, *et al.* Physiotherapy in stroke rehabilitation: Bases for australian physiotherapists' choice of treatment. *Physiother. Theory Pract.* (1994); **10**: 201–209.
- De Carvalho M, Ryczkowski A, Andersen P, *et al.* International Survey of ALS Experts about Critical Questions for Assessing Patients with ALS. *Amyotroph. Lateral Scler. Front. Degener.* (2017); **18**: 505–510.
- Castroflorio T, Farina D, Bottin A, *et al.* Surface EMG of jaw elevator muscles: Effect of electrode location and inter-electrode distance. *J. Oral Rehabil.* (2005); **32**: 411–417.
- Celik I, Sahin I, Aydin M. Reliability and Validity Study of the Mobile Learning Adoption Scale Developed Based on the Diffusion of Innovations Theory. *Int. J. Educ. Math.* (2014); **2**: 300–316.
- Cesqui B, Tropea P, Micera S, *et al.* EMG-based pattern recognition approach in post stroke robot-aided rehabilitation: A feasibility study. *J. Neuroeng. Rehabil.* (2013); **10**: 1. Journal of NeuroEngineering and Rehabilitation.

Chen YT, Li S, Magat E, *et al.* Motor overflow and spasticity in chronic stroke share a common pathophysiological process: Analysis of within-limb and between-limb EMG-EMG coherence. *Front. Neurol.* (2018); **9**: 795.

Cheung VCK, Turolla A, Agostini M, *et al.* Muscle synergy patterns as physiological markers of motor cortical damage. *Proc. Natl. Acad. Sci. U. S. A.* (2012); **109**: 14652–14656. National Academy of Sciences.

Chipchase LS, Williams MT, Robertson VJ. A national study of the availability and use of electrophysical agents by Australian physiotherapists. *Physiother. Theory Pract.* (2009); **25**: 279–296.

Christensen H, Søgaard K, Jensen BR, *et al.* Intramuscular and surface EMG power spectrum from dynamic and static contractions. *J. Electromyogr. Kinesiol.* (1995); **5**: 27–36.

Chu JU, Moon I, Mun MS. A supervised feature projection for real-time multifunction myoelectric hand control. *Annu. Int. Conf. IEEE Eng. Med. Biol. - Proc.* (2006); 2417–2420.

Cikajlo I, Zadavec M, Matjačić Z, *et al.* High-density electromyography biofeedback during robotic wrist exercises for reducing co-activation of antagonist muscles: a case report. *Int. J. Rehabil. Res.* (2021); **44**: 92–97.

Clark DJ, Ting LH, Zajac FE, *et al.* Merging of healthy motor modules predicts reduced locomotor performance and muscle coordination complexity post-stroke. *J.*

Neurophysiol. (2010); **103**: 844–857.

Cleland BT, Madhavan S. Motor overflow in the lower limb after stroke: Insights into mechanisms. *Eur. J. Neurosci.* (2022); **56**: 4455–4468.

Cofré Lizama LE, Khan F, Lee PVS, *et al.* The use of laboratory gait analysis for understanding gait deterioration in people with multiple sclerosis. *Mult. Scler.* (2016); **22**: 1768–1776.

Cordo P, Wolf S, Lou JS, *et al.* Treatment of severe hand impairment following stroke by combining assisted movement, muscle vibration, and biofeedback. *J. Neurol. Phys. Ther.* (2013); **37**: 194–203.

Côté-Allard U, Fall CL, Drouin A, *et al.* Deep Learning for Electromyographic Hand Gesture Signal Classification Using Transfer Learning. *IEEE Trans. Neural Syst. Rehabil. Eng.* (2019); **27**: 760–771.

Cram JR. The history of surface electromyography. *Appl. Psychophysiol. Biofeedback.* 2003 pp. 81–91.

Crotty ED, Furlong LAM, Hayes K, *et al.* Onset detection in surface electromyographic signals across isometric explosive and ramped contractions: A comparison of computer-based methods. *Physiol. Meas.* (2021); **42**: 35010. IOP Publishing.

D’Avella A, Portone A, Fernandez L, *et al.* Control of fast-reaching movements by muscle synergy combinations. *J. Neurosci.* (2006); **26**: 7791–7810.

Davis AE, Lee RG. EMG Biofeedback in Patients with Motor Disorders: An Aid for Coordinating Activity in Antagonistic Muscle Groups. *Can. J. Neurol. Sci. / J. Can. des Sci. Neurol.* (1980); **7**: 199–206.

Van Dijk L, Van Der Sluis CK, Van Dijk HW, *et al.* Learning an EMG controlled game: Task-specific adaptations and transfer. *PLoS One* (2016); **11**

Domingos P, Pazzani M. Beyond Independence: Conditions for the Optimality of the Simple Bayesian Classifier. *Mach. Learn.* (1996);105–112.

Donnelly MR, Phanord CS, Marin-Pardo O, *et al.* Acceptability of a Telerehabilitation Biofeedback System Among Stroke Survivors: A Qualitative Analysis. *OTJR Occup. Particip. Heal.* (2023);

Donzé C, Massot C. Rehabilitation in multiple sclerosis in 2021. Press. Medicale. 2021. Elsevier Masson s.r.l.

Dost Sürücü G, Tezen Ö. The effect of EMG biofeedback on lower extremity functions in hemiplegic patients. *Acta Neurol. Belg.* (2021); **121**: 113–118.

Van Eerd D, Munhall C, Irvin E, *et al.* Effectiveness of workplace interventions in the prevention of upper extremity musculoskeletal disorders and symptoms: An update of the evidence. *Occup. Environ. Med.* 2016 pp. 62–70.

Ehrenborg C, Archenholtz B. Is surface EMG biofeedback an effective training method for persons with neck and shoulder complaints after whiplash-associated disorders concerning activities of daily living and pain-a randomized controlled trial. *Clin.*

Rehabil. (2010); **24**: 715–726.

Eken MM, Richards R, Beckerman H, *et al.* Quantifying muscle fatigue during walking in people with multiple sclerosis. *Clin. Biomech.* (2020); **72**: 94–101. Elsevier.

Enciso J, Variya D, Sunthonlap J, *et al.* Electromyography-driven exergaming in wheelchairs on a mobile platform: Bench and pilot testing of the WOW-mobile fitness system. *JMIR Rehabil. Assist. Technol.* (2021); **8**

Englehart K, Hudgins B. A Robust, Real-Time Control Scheme for Multifunction Myoelectric Control. *IEEE Trans. Biomed. Eng.* (2003); **50**: 848–854.

Feldner HA, Howell D, Kelly VE, *et al.* “Look, Your Muscles Are Firing!”: A Qualitative Study of Clinician Perspectives on the Use of Surface Electromyography in Neurorehabilitation. *Arch. Phys. Med. Rehabil.* (2019); **100**: 663–675.

Fling BW, Seidler RD. Task-dependent effects of interhemispheric inhibition on motor control. *Behav. Brain Res.* (2012); **226**: 211–217.

Gallina A, Disselhorst-Klug C, Farina D, *et al.* Consensus for experimental design in electromyography (CEDE) project: High-density surface electromyography matrix. *J. Electromyogr. Kinesiol.* (2022); **64**

Garcia-Hernandez N, Garza-Martinez K, Parra-Vega V, *et al.* Development of an EMG-based exergaming system for isometric muscle training and its effectiveness to enhance motivation, performance and muscle strength. *Int. J. Hum. Comput. Stud.* (2019); **124**: 44–55.

Giggins OM, Persson UMC, Caulfield B. Biofeedback in rehabilitation. *J. Neuroeng. Rehabil.* (2013); **10**: 1. Journal of NeuroEngineering and Rehabilitation.

Glanz M, Klawansky S, Chalmers T. Biofeedback therapy in stroke rehabilitation: A review. *J. R. Soc. Med.* (1997); **90**: 33–39.

Gleadhill C, Bolsewicz K, Davidson SRE, *et al.* Physiotherapists' opinions, barriers, and enablers to providing evidence-based care: a mixed-methods study. *BMC Health Serv. Res.* (2022); **22**: 1–16. BioMed Central.

Goffredo M, Infarinato F, Pournajaf S, *et al.* Barriers to sEMG assessment during overground robot-assisted gait training in subacute stroke patients. *Front. Neurol.* (2020); **11**: 1–8.

Grimshaw JM, Eccles MP, Lavis JN, *et al.* Knowledge translation of research findings. *Implement. Sci.* (2012); **7**: 1. BioMed Central Ltd.

Guerrero-Henriquez J, Tapia C, Vargas-Matamala M. Variability in Normalization Methods of Surface Electromyography Signals in Eccentric Hamstring Contraction. *J. Sport Rehabil.* (2022); **31**: 1083–1088.

Guo LY, Lozinski B, Yong VW. Exercise in multiple sclerosis and its models: Focus on the central nervous system outcomes. *J. Neurosci. Res.* 2020 pp. 509–523.

Hadjiosif AM, Branscheidt M, Anaya MA, *et al.* Dissociation between abnormal motor synergies and impaired reaching dexterity after stroke. *J. Neurophysiol.* (2022); **127**: 856–868. American Physiological Society.

Han M, Zandigohar M, Günay SY, *et al.* Inference of Upcoming Human Grasp Using EMG During Reach-to-Grasp Movement. *Front. Neurosci.* (2022); **16**: 1–14.

Harris CR, Millman KJ, van der Walt SJ, *et al.* Array programming with NumPy. *Nature.* 2020 pp. 357–362.

Hartmann D, Strauhal MJ, Nelson CA. Treatment of women in the United States with localized, provoked vulvodynia: practice survey of women’s health physical therapists. *J. Reprod. Med.* (2007); **52**: 48–52.

Heald E, Hart R, Kilgore K, *et al.* Characterization of Volitional Electromyographic Signals in the Lower Extremity after Motor Complete Spinal Cord Injury. *Neurorehabil. Neural Repair* (2017); **31**: 583–591.

Heimly V, Grimsmo A, Faxvaag A. Diffusion of Electronic Health Records and electronic communication in Norway. *Appl. Clin. Inform.* (2011); **2**: 355–364.

Herbert RD, Sherrington C, Maher C, *et al.* Evidence-based practice -- imperfect but necessary. *Physiother. Theory Pract.* (2001); **17**: 201–211.

Hermens HJ, Freriks B, Disselhorst-Klug C, *et al.* Development of recommendations for SEMG sensors and sensor placement procedures. *J. Electromyogr. Kinesiol.* (2000); **10**: 361–374.

Hodges P. A comparison of computer-based methods for the determination of onset of muscle contraction using electromyography. *Electroencephalogr. Clin. Neurophysiol.* (1996); **101**: 511–519.

Hodges PW. Editorial: Consensus for Experimental Design in Electromyography (CEDE) project. *J. Electromyogr. Kinesiol.* (2020); **50**: 102343. Elsevier.

Holtermann A, Mork PJ, Andersen LL, *et al.* The use of EMG biofeedback for learning of selective activation of intra-muscular parts within the serratus anterior muscle. A novel approach for rehabilitation of scapular muscle imbalance. *J. Electromyogr. Kinesiol.* (2010); **20**: 359–365.

Holtermann A, Roeleveld K. EMG amplitude distribution changes over the upper trapezius muscle are similar in sustained and ramp contractions. *Acta Physiol.* (2006); **186**: 159–168.

Hosseini MP, Hosseini A, Ahi K. A Review on Machine Learning for EEG Signal Processing in Bioengineering. *IEEE Rev. Biomed. Eng.* (2021); **14**: 204–218. IEEE.

Hübers A, Orekhov Y, Ziemann U. Interhemispheric motor inhibition: Its role in controlling electromyographic mirror activity. *Eur. J. Neurosci.* (2008); **28**: 364–371.

Hug F. Can muscle coordination be precisely studied by surface electromyography? *J. Electromyogr. Kinesiol.* (2011); **21**: 1–12.

Hunter JD. Matplotlib: A 2D Graphics Environment. *Comput. Sci. Eng.* (2007); **9**: 90–95.

Ison M, Artemiadis P. The role of muscle synergies in myoelectric control: Trends and challenges for simultaneous multifunction control. *J. Neural Eng.* 2014

Israely S, Leisman G, Carmeli E. Neuromuscular synergies in motor control in normal and poststroke individuals. *Rev. Neurosci.* (2018); **29**: 593–612.

Jaja R, Badhiwala J, Guest J, *et al.* Trajectory-Based Classification of Recovery in Sensorimotor Complete Traumatic Cervical Spinal Cord Injury Blessing N. (2021);

Jian C, Deng L, Liu H, *et al.* Modulating and restoring inter-muscular coordination in stroke patients using two-dimensional myoelectric computer interface: a cross-sectional and longitudinal study. *J. Neural Eng.* (2021); **18**. IOP Publishing.

Johnsen B, Fuglsang-Frederiksen A, Vingtoft S, *et al.* Differences in the handling of the EMG examination at seven European laboratories. *Electroencephalogr. Clin. Neurophysiol. Evoked Potentials* (1994); **93**: 155–158.

Jordanic M, Rojas-Martínez M, Mañanas MA, *et al.* Spatial distribution of HD-EMG improves identification of task and force in patients with incomplete spinal cord injury. *J. Neuroeng. Rehabil.* (2016); **13**: 1–11. Journal of NeuroEngineering and Rehabilitation.

Jordanić M, Rojas-Martínez M, Mañanas MA, *et al.* Prediction of isometric motor tasks and effort levels based on high-density EMG in patients with incomplete spinal cord injury. *J. Neural Eng.* (2016); **13**

Karandreas N, Papadopoulou M, Kokotis P, *et al.* Impaired interhemispheric inhibition in amyotrophic lateral sclerosis. *Amyotroph. Lateral Scler.* (2007); **8**: 112–118.

Kavanagh BP, Nurok M. Standardized intensive care: Protocol misalignment and impact

misattribution. *Am. J. Respir. Crit. Care Med.* (2016); **193**: 17–22.

Khan SM, Khan AA, Farooq O. Selection of features and classifiers for EMG-EEG-Based upper limb assistive devices - A review. *IEEE Rev. Biomed. Eng.* 2020 pp. 248–260.

Kim I. PYTRIS. 2017

Kim KS, Choi HH, Moon CS, *et al.* Comparison of k-nearest neighbor, quadratic discriminant and linear discriminant analysis in classification of electromyogram signals based on the wrist-motion directions. *Curr. Appl. Phys.* (2011); **11**: 740–745. Elsevier B.V.

Kim Y, Kim WS, Shim JK, *et al.* Difference of motor overflow depending on the impaired or unimpaired hand in stroke patients. *Hum. Mov. Sci.* (2015); **39**: 154–162.

Klein CS, Li S, Hu X, *et al.* Editorial: Electromyography (EMG) Techniques for the Assessment and Rehabilitation of Motor Impairment Following Stroke. *Front. Neurol.* (2018); **9**: 1–3.

Koo TK, Li MY. Cracking the Code: Providing Insight Into the Fundamentals of Research and Evidence-Based Practice A Guideline of Selecting and Reporting Intraclass Correlation Coefficients for Reliability Research. *J. Chiropr. Med.* (2016); **15**: 155–163.

Kowalski E, Catelli DS, Lamontagne M. Comparing the accuracy of visual and

computerized onset detection methods on simulated electromyography signals with varying signal-to-noise ratios. *J. Funct. Morphol. Kinesiol.* (2021); **6**

Kumar A, Munirji L, Nayif S, *et al.* Motor Performance and Skill Acquisition in Oral Motor Training With Exergames: A Pilot Study. *Front. Aging Neurosci.* (2022); **14**

Lee D, Bae Y. Interactive Videogame Improved Rehabilitation Motivation and Walking Speed in Chronic Stroke Patients: A Dual-Center Controlled Trial. *Games Health J.* (2022); **11**: 268–274.

Lee J, Jung MY, Kim SH. Reliability of spike and turn variables of surface EMG during isometric voluntary contractions of the biceps brachii muscle. *J. Electromyogr. Kinesiol.* (2011a); **21**: 119–127.

Lee SW, Wilson KM, Lock BA, *et al.* Subject-specific myoelectric pattern classification of functional hand movements for stroke survivors. *IEEE Trans. Neural Syst. Rehabil. Eng.* (2011b); **19**: 558–566. IEEE.

Li Pi Shan R, Nicolle M, Chan M, *et al.* Electrodiagnostic Testing and Treatment for Carpal Tunnel Syndrome in Canada. *Can. J. Neurol. Sci.* (2015); **43**: 178–182.

Li X, Shin H, Zhou P, *et al.* Power spectral analysis of surface electromyography (EMG) at matched contraction levels of the first dorsal interosseous muscle in stroke survivors. *Clin. Neurophysiol.* (2014); **125**: 988–994. International Federation of Clinical Neurophysiology.

Liu J, Zhou P. A novel myoelectric pattern recognition strategy for hand function

restoration after incomplete cervical spinal cord injury. *IEEE Trans. Neural Syst. Rehabil. Eng.* (2013); **21**: 96–103.

Liu Y, Lao J, Gao K, *et al.* Outcome of nerve transfers for traumatic complete brachial plexus avulsion: Results of 28 patients by DASH and NRS questionnaires. *J. Hand Surg. Eur. Vol.* (2012); **37**: 413–421.

Lu EC, Wang RH, Hebert D, *et al.* The development of an upper limb stroke rehabilitation robot: Identification of clinical practices and design requirements through a survey of therapists. *Disabil. Rehabil. Assist. Technol.* (2011); **6**: 420–431.

Lu Z, Stampas A, Francisco GE, *et al.* Offline and online myoelectric pattern recognition analysis and real-time control of a robotic hand after spinal cord injury. *J. Neural Eng.* (2019a); **16**: ab0cf0. IOP Publishing.

Lu Z, Tong KY, Zhang X, *et al.* Myoelectric pattern recognition for controlling a robotic hand: A feasibility study in stroke. *IEEE Trans. Biomed. Eng.* (2019b); **66**: 365–372. IEEE.

De Luca CJ, Donald Gilmore L, Kuznetsov M, *et al.* Filtering the surface EMG signal: Movement artifact and baseline noise contamination. *J. Biomech.* (2010); **43**: 1573–1579. Elsevier Ltd.

Lúcio A, D’Ancona CAL, Perissinotto MC, *et al.* Pelvic floor muscle training with and without electrical stimulation in the treatment of lower urinary tract symptoms in women with multiple sclerosis. *J. Wound, Ostomy Cont. Nurs.* (2016); **43**: 414–419.

Lundh. An introduction to tkinter. URL www.pythonware.com/library/tkinter/introduction/index.htm. 1999

MacIntosh A, Desailly E, Vignais N, *et al.* A biofeedback-enhanced therapeutic exercise video game intervention for young people with cerebral palsy: A randomized single-case experimental design feasibility study. *PLoS One* (2020); **15**

MacIntosh A, Vignais N, Desailly E, *et al.* A Classification and Calibration Procedure for Gesture Specific Home-Based Therapy Exercise in Young People with Cerebral Palsy. *IEEE Trans. Neural Syst. Rehabil. Eng.* (2021); **29**: 144–155.

MacIntosh A, Vignais N, Vigneron V, *et al.* The design and evaluation of electromyography and inertial biofeedback in hand motor therapy gaming. *Assist. Technol.* (2022); **34**: 213–221.

Mackey A, Stinear C, Stott S, *et al.* Upper limb function and cortical organization in youth with unilateral cerebral palsy. *Front. Neurol.* (2014); **5 JUL**: 1–9.

Maggio MG, Latella D, Maresca G, *et al.* Virtual reality and cognitive rehabilitation in people with stroke: An overview. *J. Neurosci. Nurs.* (2019a); **51**: 101–105.

Maggio MG, Russo M, Cuzzola MF, *et al.* Virtual reality in multiple sclerosis rehabilitation: A review on cognitive and motor outcomes. *J. Clin. Neurosci.* (2019b); **65**: 106–111. Elsevier Ltd.

Mahalanobis P. On the generalized distance in statistics. *Gen. distance Stat.* (1936); **2**: 49–55. Proceedings of the National Institute of Sciences of India.

Manca A, Cereatti A, Bar-On L, *et al.* A Survey on the Use and Barriers of Surface Electromyography in Neurorehabilitation. *Front. Neurol.* (2020); **11**: 573616.

Manzur-Valdivia H, Alvarez-Ruf J. Surface Electromyography in Clinical Practice. A Perspective From a Developing Country. *Front. Neurol.* (2020); **11**: 1–6.

Marin-Pardo O, Laine CM, Rennie M, *et al.* A virtual reality muscle–computer interface for neurorehabilitation in chronic stroke: A pilot study. *Sensors (Switzerland)* (2020); **20**: 1–21.

Marin-pardo O, Phanord C, Donnelly MR, *et al.* Development of a low-cost, modular muscle–computer interface for at-home telerehabilitation for chronic stroke. *Sensors* (2021); **21**: 1–15.

Marinelli L, Currà A, Trompetto C, *et al.* Spasticity and spastic dystonia: the two faces of velocity-dependent hypertonia. *J. Electromyogr. Kinesiol.* (2017); **37**: 84–89. Elsevier.

Maura RM, Rueda Parra S, Stevens RE, *et al.* Literature review of stroke assessment for upper-extremity physical function via EEG, EMG, kinematic, and kinetic measurements and their reliability. *J. Neuroeng. Rehabil.* 2023. BioMed Central.

Mayston MJ, Harrison LM, Stephens JA. A neurophysiological study of mirror movements in adults and children. *Ann. Neurol.* (1999); **45**: 583–594.

McClurg D, Ashe RG, Lowe-Strong AS. Neuromuscular electrical stimulation and the treatment of lower urinary tract dysfunction in multiple sclerosis - A double blind,

placebo controlled, randomised clinical trial. *Neurourol. Urodyn.* (2008); **27**: 231–237.

McClurg D, Ashe RG, Marshall K, *et al.* Comparison of pelvic floor muscle training, electromyography biofeedback, and neuromuscular electrical stimulation for bladder dysfunction in people with multiple sclerosis: A randomized pilot study. *Neurourol. Urodyn.* (2006); **25**: 337–348.

Mckay WB, Lim HK, Priebe MM, *et al.* Clinical Neurophysiological Assessment of Residual Motor Control in Post-Spinal Cord Injury Paralysis. *Neurorehabil. Neural Repair* (2004); **18**: 144–153.

McManus L, Lowery M, Merletti R, *et al.* Consensus for experimental design in electromyography (CEDE) project: Terminology matrix. *J. Electromyogr. Kinesiol.* (2021); **59**

McManus L, De Vito G, Lowery MM. Analysis and Biophysics of Surface EMG for Physiotherapists and Kinesiologists: Toward a Common Language With Rehabilitation Engineers. *Front. Neurol.* (2020); **11**: 576729.

Merletti R, Campanini I, Rymer WZ, *et al.* Editorial: Surface Electromyography: Barriers Limiting Widespread Use of sEMG in Clinical Assessment and Neurorehabilitation. *Front. Neurol.* (2021); **12**: 10–13.

Merletti R, Cerone GL. Tutorial. Surface EMG detection, conditioning and pre-processing: Best practices. *J. Electromyogr. Kinesiol.* (2020); **54**: 102440. Elsevier.

Merletti R, Muceli S. Tutorial. Surface EMG detection in space and time: Best practices.

J. Electromyogr. Kinesiol. (2019); **49**. Elsevier Ltd.

Merletti R, Temporiti F, Gatti R, *et al.* Translation of surface electromyography to clinical and motor rehabilitation applications: The need for new clinical figures.

Transl. Neurosci. 2023

Miller J, Croce R, Smith W, *et al.* Contraction intensity and velocity on vastus lateralis semg power spectrum and amplitude. *Percept. Mot. Skills* (2012); **114**: 847–856.

Mims HW. Electromyography in Clinical Practice. South. Med. J. 1956 pp. 804–807.

Motl RW, McAuley E, Snook EM. Physical activity and multiple sclerosis: A meta-analysis. *Mult. Scler.* (2005); **11**: 459–463.

Motl RW, Sandroff BM, Kwakkel G, *et al.* Exercise in patients with multiple sclerosis.

Lancet Neurol. (2017); **16**: 848–856. Elsevier Ltd.

Muguro JK, Laksono PW, Rahmaniar W, *et al.* Development of Surface EMG Game

Control Interface for Persons with Upper Limb Functional Impairments. *Signals* (2021); **2**: 834–851.

Muguro JK, Sasaki M, Matsushita K, *et al.* Development of neck surface

electromyography gaming control interface for application in tetraplegic patients' entertainment. In: *AIP Conf. Proc.* (2020); p. 30039.

Munoz-Novoa M, Kristoffersen MB, Sunnerhagen KS, *et al.* Upper Limb Stroke

Rehabilitation Using Surface Electromyography: A Systematic Review and Meta-Analysis. *Front. Hum. Neurosci.* (2022); **16**

Nejad MG, Sherrell DL, Babakus E. Influentials and influence mechanisms in new product diffusion: An integrative review. *J. Mark. Theory Pract.* (2014); **22**: 185–208.

Nelson-Wong EA, Howarth SAM, Winter DA, *et al.* Application of autocorrelation and cross-correlation analyses in human movement and rehabilitation research. *J. Orthop. Sports Phys. Ther.* (2009); **39**: 287–295.

NICE-SUGAR Study Investigators, Finfer S, Chittock DR, *et al.* Intensive versus conventional glucose control in critically ill patients. *N. Engl. J. Med.* (2009); **360**: 1283–97.

Nilsson LM, Nordholm LA. Physical therapy in stroke rehabilitation: Bases for swedish physiotherapists' choice of treatment. *Physiother. Theory Pract.* (1992); **8**: 49–55.

Novikov Z, Singer SJ, Milstein A. Innovation Diffusion Across 13 Specialties and Associated Clinician Characteristics. In: *Adv. Health Care Manag.* (2024); pp. 97–115.

Okamura A, Guidetti BC, Caselli R, *et al.* HOW DO BOARD-CERTIFIED HAND SURGEONS MANAGE CARPAL TUNNEL SYNDROME? A NATIONAL SURVEY. *Acta Ortop. Bras.* (2018); **26**: 48–53.

Olek MJ. Multiple Sclerosis. *Ann. Intern. Med.* (2021); **174**: ITC81–ITC96.

Oliveira A de SC, Gonçalves M. EMG amplitude and frequency parameters of muscular activity: Effect of resistance training based on electromyographic fatigue threshold. *J. Electromyogr. Kinesiol.* (2009); **19**: 295–303.

Oña ED, Marcos-Antón S, Copaci DS, *et al.* Effects of EMG-Controlled Video Games on the Upper Limb Functionality in Patients with Multiple Sclerosis: A Feasibility Study and Development Description. *Comput. Intell. Neurosci.* (2022); **2022**

Paci M, Faedda G, Ugolini A, *et al.* Barriers to evidence-based practice implementation in physiotherapy: A systematic review and meta-analysis. *Int. J. Qual. Heal. Care* (2021); **33**: 1–13.

Pai G, Talmon R, Bronstein A, *et al.* DIMAL: Deep isometric manifold learning using sparse geodesic sampling. *Proc. - 2019 IEEE Winter Conf. Appl. Comput. Vision, WACV 2019* (2019);819–828. IEEE.

Palmer M. pynput. 2022

Pantano P, Mainero C, Domenico Iannetti G, *et al.* Contribution of corticospinal tract damage to cortical motor reorganization after a single clinical attack of multiple sclerosis. *Neuroimage* (2002); **17**: 1837–1843.

Pedregosa F, Varoquaux G, Gramfort A, *et al.* Scikit-learn: Machine learning in Python. *J. Mach. Learn.* (2011); **12**: 2825–2830.

Peters B, Giuffre JL. Canadian Trends in Carpal Tunnel Surgery. *J. Hand Surg. Am.* (2018); **43**: 1035.e1-1035.e8. Elsevier Inc.

- Peters DM, McPherson AK, Fletcher B, *et al.* Counting repetitions: An observational study of video game play in people with chronic poststroke hemiparesis. *J. Neurol. Phys. Ther.* (2013); **37**: 105–111.
- Picelli A, Baricich A, Cisari C, *et al.* The Italian real-life post-stroke spasticity survey: unmet needs in the management of spasticity with botulinum toxin type A. *Funct. Neurol.* (2017); **32**: 89–96.
- Pilkar R, Momeni K, Ramanujam A, *et al.* Use of Surface EMG in Clinical Rehabilitation of Individuals With SCI: Barriers and Future Considerations. *Front. Neurol.* (2020); **11**: 1–6.
- Portney LG, Watkins MP. *Foundations of Clinical Research: Applications to Practice.* 2nd ed. 2009. Pearson Education, Inc., New Jersey.
- Prahm C, Kayali F, Sturma A, *et al.* PlayBionic: Game-Based Interventions to Encourage Patient Engagement and Performance in Prosthetic Motor Rehabilitation. *PM R.* 2018 pp. 1252–1260.
- Puce L, Currà A, Marinelli L, *et al.* Spasticity, spastic dystonia, and static stretch reflex in hypertonic muscles of patients with multiple sclerosis. *Clin. Neurophysiol. Pract.* (2021); **6**: 194–202.
- Pulliam CL. Electromyographic-based neural network control of transhumeral prostheses. *J. Rehabil. Res. Dev.* (2011); **48**: 1–16.
- Purushothaman G, Vikas R. Identification of a feature selection based pattern recognition

scheme for finger movement recognition from multichannel EMG signals. *Australas. Phys. Eng. Sci. Med.* (2018); **41**: 549–559.

Reiman MP, Bolgla LA, Loudon JK. A literature review of studies evaluating gluteus maximus and gluteus medius activation during rehabilitation exercises. *Physiother. Theory Pract.* (2012); **28**: 257–268.

Reis ZSN, Maia TA, Marcolino MS, *et al.* Is There Evidence of Cost Benefits of Electronic Medical Records, Standards, or Interoperability in Hospital Information Systems? Overview of Systematic Reviews. *JMIR Med. Informatics* (2017); **5**: e26.

Rogers EM. *Diffusion of Innovations*. 5th ed. New York Free Press. 2003. Simon and Schuster, New York.

Saul LK, Roweis ST. Think globally, fit locally: unsupervised learning of low dimensional manifolds. *J. Mach. Learn. Res.* (2003); **4**: 119–155.

Schambra HM, Ogden RT, Martínez-Hernández IE, *et al.* The reliability of repeated TMS measures in older adults and in patients with subacute and chronic stroke. *Front. Cell. Neurosci.* (2015); **9**: 335.

Schuler T, Brütsch K, Müller R, *et al.* Virtual realities as motivational tools for robotic assisted gait training in children: A surface electromyography study. *NeuroRehabilitation* (2011); **28**: 401–411.

Scikit-learn Developers. `sklearn.naive_bayes.GaussianNB`.

Scikit-learn Developers. sklearn.discriminant_analysis.LinearDiscriminantAnalysis. 2023

Scurlock-Evans L, Upton P, Upton D. Evidence-Based Practice in physiotherapy: A systematic review of barriers, enablers and interventions. *Physiother. (United Kingdom)* (2014); **100**: 208–219. The Chartered Society of Physiotherapy.

Shankar S, Gander RE, Brandell BR. Changes in the myoelectric signal (MES) power spectra during dynamic contractions. *Electroencephalogr. Clin. Neurophysiol.* (1989); **73**: 142–150.

Sharma S. Space Invaders. 2021

Sharp BE, Miller SA. Potential for Integrating Diffusion of Innovation Principles into Life Cycle Assessment of Emerging Technologies. *Environ. Sci. Technol.* (2016); **50**: 2771–2781.

Shinners P. PyGame - Python Game Development. 2011

Simon-Martinez C, Decraene L, Zielinski I, *et al.* The impact of brain lesion characteristics and the corticospinal tract wiring on mirror movements in unilateral cerebral palsy. *Sci. Rep.* (2022); **12**: 16301.

Singh R. Botulinum toxin use in rehabilitation clinics: A survey to highlight differences and similarities. *Int. J. Rehabil. Res.* (2017); **40**: 370–373.

Siu HC, Shah JA, Stirling LA. Classification of anticipatory signals for grasp and release from surface electromyography. *Sensors (Switzerland)* (2016); **16**: 1–18.

Smoliga JM, Myers JB, Redfern MS, *et al.* Reliability and precision of EMG in leg, torso, and arm muscles during running. *J. Electromyogr. Kinesiol.* (2010); **20**: e1–e9.

van Snippenburg W, Kröner A, Flim M, *et al.* Awareness and Management of Dysphagia in Dutch Intensive Care Units: A Nationwide Survey. *Dysphagia* (2019); **34**: 220–228.

Snörljung Å, Mattsson K, Gustafsson LK. The diverging perception among physiotherapists of how to work with the concept of evidence: A phenomenographic analysis. *J. Eval. Clin. Pract.* (2014); **20**: 759–766.

Soderberg GL, Knutson LM. A guide for use and interpretation of kinesiologic electromyographic data. *Phys. Ther.* (2000); **80**: 485–498.

Song X, van de Ven SS, Chen S, *et al.* Proposal of a Wearable Multimodal Sensing-Based Serious Games Approach for Hand Movement Training After Stroke. *Front. Physiol.* (2022); **13**: 1–15.

Sorbie GG, Williams MJ, Boyle DW, *et al.* Intra-session and inter-day reliability of the Myon 320 electromyography system during sub-maximal contractions. *Front. Physiol.* (2018); **9**: 309.

Stauder G, Flachenecker C, Daumer M, *et al.* Onset Detection in Surface Electromyographic Signals : *J. Appl. Signal Process.* (2001); **2**: 67–81.

Stapp CE, Britton D, Chang C, *et al.* Feasibility of game-based electromyographic biofeedback for dysphagia rehabilitation. *2011 5th Int. IEEE/EMBS Conf. Neural*

Eng. NER 2011 (2011);233–236. IEEE.

Sturma A, Hrubby LA, Prahm C, *et al.* Rehabilitation of upper extremity nerve injuries using surface EMG biofeedback: Protocols for clinical application. *Front. Neurosci.* (2018); **12**

Takechi U, Matsunaga K, Nakanishi R, *et al.* Longitudinal changes of motor cortical excitability and transcallosal inhibition after subcortical stroke. *Clin. Neurophysiol.* (2014); **125**: 2055–2069.

Tated N. Pacman-Game. 2019

Tenan MS, Tweedell AJ, Haynes CA. Iterative assessment of statistically-oriented and standard algorithms for determining muscle onset with intramuscular electromyography. *J. Appl. Biomech.* (2017); **33**: 464–468.

Ternes AM, Fielding J, Addamo PK, *et al.* Concurrent motor and cognitive function in multiple sclerosis: A motor overflow and motor stability study. *Cogn. Behav. Neurol.* (2014); **27**: 68–76.

Thiamchoo N, Phukpattaranont P. Evaluation of feature projection techniques in object grasp classification using electromyogram signals from different limb positions. *PeerJ Comput. Sci.* (2022); **8**: 1–24.

Toepp SL, Mohrenschildt M v., Nelson AJ. An EMG-Based Biofeedback System for Tailored Interventions Involving Distributed Muscles. *IEEE Sens. J.* (2023); **23**: 28095–28109.

Trompetto C, Marinelli L, Mori L, *et al.* Pathophysiology of spasticity: Implications for neurorehabilitation. *Biomed Res. Int.* 2014

Trompetto C, Marinelli L, Puce L, *et al.* “Spastic dystonia” or “Inability to voluntary silence EMG activity”? Time for clarifying the nomenclature. *Clin. Neurophysiol.* (2019); **130**: 1076–1077.

Del Vecchio A, Holobar A, Falla D, *et al.* Tutorial: Analysis of motor unit discharge characteristics from high-density surface EMG signals. *J. Electromyogr. Kinesiol.* (2020); **53**

Virtanen P, Gommers R, Oliphant TE, *et al.* Author Correction: SciPy 1.0: fundamental algorithms for scientific computing in Python. *Nat. Methods* (2020); **17**: 352–352.

Wagner B, Steiner M, Huber DFX, *et al.* The effect of biofeedback interventions on pain, overall symptoms, quality of life and physiological parameters in patients with pelvic pain: A systematic review. *Wien. Klin. Wochenschr.* 2022 pp. 11–48.

Weir JP. Quantifying test-retest reliability using the intraclass correlation coefficient and the SEM. *J. Strength Cond. Res.* 2005 pp. 231–240.

Wold S, Esbensen K, Geladi P. Chimometrics and intelligent laboratory systems. In: *IEEE Conf. Emerg. Technol. Fact. Autom. Efta* (1987); pp. 704–706.

Wolkorte R, Heersema DJ, Zijdewind I. Reduced voluntary activation during brief and sustained contractions of a hand muscle in secondary-progressive multiple sclerosis patients. *Neurorehabil. Neural Repair* (2016); **30**: 307–316.

Yahya A, Malarkey AR, Eschbaugh RL, *et al.* Trends in the surgical treatment for cubital tunnel syndrome: A survey of members of the american society for surgery of the hand. *Hand* (2018); **13**: 516–521.

Yoo JW, Lee DR, Sim YJ, *et al.* Effects of innovative virtual reality game and EMG biofeedback on neuromotor control in cerebral palsy. *Biomed. Mater. Eng.* (2014); **24**: 3613–3618.

Yu H, Yang J. A direct LDA algorithm for high-dimensional data — with application to face recognition. *Pattern Recognit.* (2001); **34**: 2067–2070.

Zhang X, Zhou P. High-Density Myoelectric Pattern Recognition Toward Improved Stroke Rehabilitation. *IEEE Trans. Biomed. Eng.* (2012); **59**